# Role of nitrification, denitrification, and nitrous oxide ($N_2O$) production in aquatic nitrogen cycling

Dissertation zur Erlangung des Doktorgrades

an der Fakultät für Mathematik, Informatik und Naturwissenschaften

Fachbereich Geowissenschaften

der Universität Hamburg

Vorgelegt von

Lisa Brase

geboren in München

Hamburg

2017

Tag der Disputation: 11. Juli 2017

Folgende Gutachter empfehlen die Annahme der Dissertation:

Dr. Kirstin Dähnke

und

Prof. Dr. Kay-Christian Emeis

## Zusammenfassung

Der Anstieg von reaktivem Stickstoff durch anthropogene Nährstoffeinträge in aquatischen Ökosystemen ist ein weitverbreitetes Problem, welches zu erheblichen Veränderungen innerhalb des Stickstoffkreislaufes führen kann und damit zu einer allgemeinen Zunahme der Eutrophierung in Gewässern. Stickstoffumsetzende Prozesse wie Nitrifizierung und Denitrifizierung können durch zunehmende Einträge reaktiven Stickstoffs nicht nur verstärkt werden, sondern tragen auch zu einer Intensivierung der Produktion des klimarelevanten Treibhausgases $N_2O$ (Distickstoffmonoxid) bei.

In dieser Dissertation werden die Auswirkungen der durch den Menschen verursachten Veränderung des Stickstoffkreislaufes auf den reaktiven Stickstoff in der Wassersäule, auf die verschiedenen $N_2O$ bildenden Prozesse Nitrifizierung und Denitrifizierung, sowie auf $N_2O$ selbst untersucht. Die folgende Arbeit zeigt am Beispiel eines kleinen Flusses unter Zuhilfenahme von Nitratisotopensignaturen, dass selbst eine Intensivierung der stickstoffumwandelnden Prozesse dem zunehmenden Nährstoffeintrag nicht entgegen wirken kann. Des Weiteren wird mittels hochauflösender $N_2O$-Messungen im Elbeästuar aufgeführt, dass diese Intensivierung von Nitrifizierung und Denitrifizierung einen erheblichen Beitrag zur $N_2O$-Produktion und den daraus resultierenden Emissionen leistet.

Im ersten Abschnitt dieser Arbeit (Kapitel 2) wird untersucht, wie sich ein zunehmender Gradient an stickstoffeintragenden, anthropogenen Einflüssen auf die internen nährstoffumsetzenden Prozesse, sprich Nitrataufbau und -abbau, in einem kleinen Fluss auswirkt. Hierbei zeigt sich, dass der interne Nitrataufbau mittels Nitrifizierung mit steigendem anthropogenem Nitrateintrag nur noch eine untergeordnete Rolle spielt, wenn gleich sich auch die interne Nitratproduktion erhöht. Ebenso führt der erhöhte Nährstoffeintrag, unabhängig von der Jahreszeit, zu einem verstärkten Nitratabbau im Flusssediment. Allerdings ist der anfänglich proportionale Anstieg des Nitratabbaus mit steigendem Stickstoffeintrag begrenzt und kann daher dem externen Nitrateintrag nicht entgegenwirken.

Nebst ihrer Wirkung auf die reaktive Stickstoffbilanz (oder deren Fehlen auf diese) setzen beide Prozesse, Nitrifizierung und Denitrifizierung, auch signifikante Mengen an $N_2O$

frei. Diese Prozesse wurden bereits individuell im Elbeästuar untersucht, aber ihr ganzheitlicher Effekt auf die $N_2O$-Produktion im gegenwärtigen Ästuar ist unklar.

Im Rahmen von Transektmessungen konnte die Hamburger Hafenregion als Abschnitt mit der höchsten $N_2O$-Produktion identifiziert werden, wie in Kapitel 3 gezeigt wird. Hier spielt vor allem die Entstehung des $N_2O$ durch Nitrifizierung eine tragende Rolle, aber im sauerstoffärmsten Bereich des Hafens trägt auch Denitrifizierung einen Teil zur $N_2O$-Konzentration bei. Betrachtet man den gesamten Frischwasserbereich im Elbeästuar, gibt es allerdings im Vergleich zu $N_2O$ Messungen der 80er-Jahre einen Wandel von Denitrifizierung zu Nitrifizierung als Hauptquelle. Auffallend ist, dass seit Ende der 80er-Jahre ein stetiger Nährstoffrückgang im Elbeästuar verzeichnet wird, die gemessene $N_2O$-Sättigung aber im Vergleich zu Messungen Mitte der 90er-Jahre keinen Rückgang der Werte zeigt.

Da der Hamburger Hafen als eine Region mit der höchsten $N_2O$-Produktion identifiziert werden konnte, wurden in Kapitel 4 $N_2O$-Dynamiken im Gezeitenverlauf untersucht. Stationäre $N_2O$-Messungen im Hamburger Hafen zeigen mit Rückgang des Hochwassers eine allgemeine Zunahme der $N_2O$-Konzentration und, wie bereits in den Transektmessungen aufgezeigt, basiert diese $N_2O$-Produktion in dieser sauerstoffarmen Region überwiegend auf Insitu-Produktion, sprich eine $N_2O$-Produktion durch Nitrifizierung und Denitrifizierung. Abiotische Einflüsse, wie eine erhöhte Remineralisierung, eine allgemeine Abnahme der Sauerstoffkonzentration und ein geringerer Abfluss, können hierbei die interne $N_2O$-Produktion intensivieren indem sie den Stickstoffumsatz fördern. Zusätzlich konnte ein geringerer Eintrag von allochthonem $N_2O$ aus den angrenzenden Hafenbecken und/oder Uferzonen aufgezeigt werden und ist daher als kleinere $N_2O$-Quelle zu berücksichtigen. Diese Untersuchungen bestätigen eine sehr hohe $N_2O$-Produktion durch biologische Prozesse im Hamburger Hafen, was diese Region als konstante Quelle für $N_2O$-Emissionen charakterisiert.

## Abstract

The increase of reactive nitrogen due to anthropogenic nutrient inputs is a widespread problem in the aquatic environment which can lead to significant alterations of the nitrogen cycle and thus to a general increase in eutrophication. Processes of N-turnover, such as nitrification and denitrification, can be influenced by an increased level of reactive nitrogen and contribute to an intensified production of the climate-relevant greenhouse gas $N_2O$ (nitrous oxide).

This thesis demonstrates human-driven accelerations of the nitrogen cycle and their effect on water column reactive N internal processing and on $N_2O$ production. In a small river, it is demonstrated that even an intensification of internal N-turnover processes cannot counteract additional nutrient inputs. Furthermore, by using high-resolution measurements of $N_2O$, it is shown that such enhancement of nitrification and denitrification contributes to substantial $N_2O$ production and resulting emissions.

The first part of this thesis (chapter 2) describes the influences of an anthropogenic gradient on internal nutrient cycling processes, i.e. nitrate production and consumption, in a small river. It is shown that contribution of nitrate due to nitrification decreases with increasing eutrophication, although sedimentary nitrate production is enhanced and contributes to nitrate concentration in the river. Similarly, additional nutrient increase leads to an increased nitrate consumption rate in the river sediment, regardless of seasonality. Although nitrate removal always exceeded internal nitrate production, the filter capacity of the sediment is limited and overwhelmed by surplus N inputs.

Besides their impact on the water column nitrate inventory (or the lack thereof), nitrification and denitrification are significant sources of nitrous oxide ($N_2O$). Both processes have been investigated individually in the Elbe estuary, but their integrated effect on $N_2O$ concentration in the contemporary estuary is unclear.

By using transect measurements, the Hamburg port region was identified as a hot-spot of biological $N_2O$ production, as demonstrated in chapter 3. This is mainly due to nitrification, but also denitrification can contribute to additional $N_2O$ in the area of lowest measured oxygen values. Relating to the entire Elbe estuary freshwater area, and contrary to measurements in the late 80s, internal $N_2O$ processes appear to have changed from denitrification to nitrification as the main $N_2O$ contributing source. It is notable, that $N_2O$

saturation did not decrease since the middle of the 90s, even though a continuous nutrient decrease occurred since the late 80s.

Since the port of Hamburg was identified as the area with highest $N_2O$ production, $N_2O$ dynamics in this area are examined in chapter 4 by stationary measurements in a tide controlled context. Stationary measurements showed an increase of $N_2O$ concentration with ebb tides and, as already concluded from transect measurements, $N_2O$ production in this low oxygen area is mainly attributed to in-situ production, i.e. by means of nitrification and denitrification. An increased remineralization and abiotic factors, such as a decrease in oxygen concentration and a lower discharge can further lead to an intensified internal $N_2O$ production by fueling nitrogen turnover processes. In addition, a small contribution of allochthonous $N_2O$ can be allocated to $N_2O$ derived from harbor basins and/or riparian zones and thus is a minor $N_2O$ source. The research conducted within the present thesis confirms the port of Hamburg as a hot-spot of biological $N_2O$ production and as a constant net source of $N_2O$ emissions to the atmosphere.

## Table of contents

# 1. Introduction

## 1.1. The nitrogen cycle in aquatic environments and its production of $N_2O$

Despite comprising the majority of the earth's atmosphere (78%), nitrogen is a limiting nutrient for biological use, i.e. primary production. It is a component in all amino acids, a part of proteins and present in the bases that make up nucleic acids, such as DNA and RNA. Thus, nitrogen is essential for many biological processes.

It is present in a variety of chemical forms where inorganic nitrogen includes ammonium ($NH_4^+$), nitrate ($NO_3^-$), nitrite ($NO_2^-$), nitrous oxide ($N_2O$), nitric oxide (NO), and inorganic dinitrogen ($N_2$).

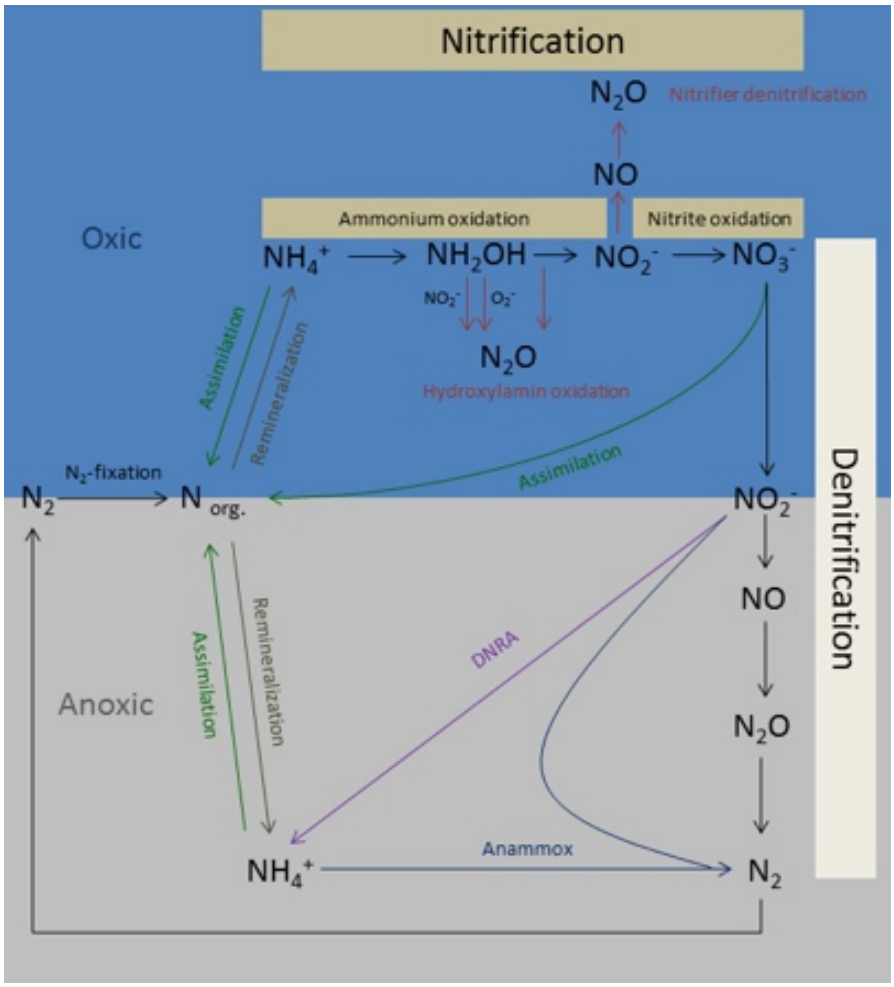


Figure 1.1: Simplified scheme of the N-cycle, processes of nitrogen turnover in an oxic and anoxic environment with a focus on nitrification and denitrification and their production of $N_2O$. (modified after Francis et al., 2007)

In the aquatic environment, sources and sinks of nitrogen are well known and highly dependent on redox conditions. Except for a few microorganisms, $N_2$ cannot be used as a source of nitrogen and thus biota needs reactive forms of nitrogen as a supply for their requirement of protein synthesis. Whether the different inorganic nitrogen forms are oxidized or reduced by microbial organisms depends on the specification of the microbes, i.e. if they are aerobic or anaerobic. This means that the prevailing form of nitrogen is mainly controlled by oxygen concentration in the environment.

Within the different sources and sinks of nitrogen, two main pathways are important in the oxic and anoxic environment, nitrification and denitrification, respectively.

Besides nitrification being known as a nitrogen source and denitrification representing a sink, both processes also contribute to $N_2O$ production (Figure 1.1) – a gaseous nitrogen compound representing an important greenhouse gas (GHG) in the atmosphere. Due to its major sink, the destruction in the stratosphere by photolysis of almost 90% of $N_2O$ ($N_2O + h\nu \rightarrow N_2 + O^*$), the remaining $N_2O$ (6%) can react with O* to produce $NO_x$, and thus also represents a major sink for ozone (Crutzen, 1970; WMO, 2014). Hence, $N_2O$ is important as a greenhouse gas with a large global warming potential and as an ozone-depleting substance. Its radiative efficiency per molecule within a time horizon of 100 years is 298 times higher than radiative efficiency of carbon dioxide (Ramaswamy et al., 2001). Due to its chemical inertness, $N_2O$ has a long atmospheric residence time of 114 years (EPA, 2010). At this point in time the influence of $N_2O$ on the anthropogenic greenhouse effect is estimated at 6.2% with an average atmospheric concentration of 319 – 322 ppb and a continuous increase of 0.25% ± 0.05% per year over the last decades (EPA, 2010; IPCC, 2013, see Fig. 1.2).

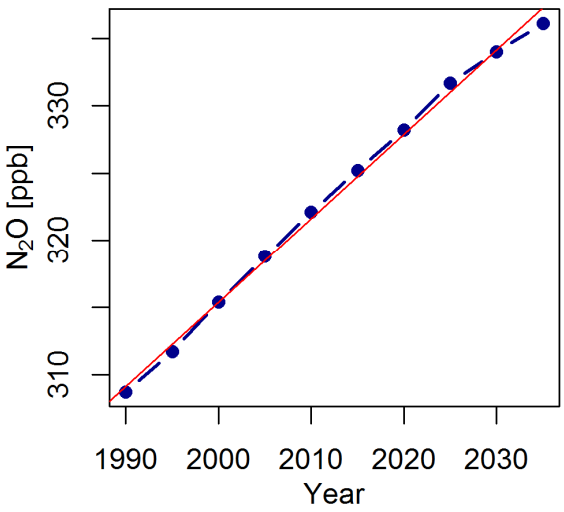


Figure 1.2: Continuous increase of atmospheric $N_2O$ mole fraction (annual means), the red line shows an increase of ~0.8 ppb $N_2O$ per year. (IPCC, 2013) No smoothing is applied. The projections have been harmonized to start from the same value in 1990. (Meinshausen et al., 2011)

### 1.1.1. **Nitrification & Denitrification - and $N_2O$ production**

***Nitrification***

Nitrification is an autotrophic aerobic microbial process and describes the production of nitrate ($NO_3^-$) by the oxidation of ammonium ($NH_4^+$) via two steps (simplified, Figure 1.1):

1) ammonium is oxidized to nitrite: $NH_4^+ + 1.5\ O_2 \rightarrow NO_2^- + H_2O + 2H^+$
2) nitrite is oxidized to nitrate: $NO_2^- + 0.5\ O_2 \rightarrow NO_3^-$

Step 1 can be performed by two groups of organisms, archaea and bacteria, while step 2 is mainly done by bacteria. Furthermore, nitrification leads to a significant consumption of oxygen, while simultaneously $N_2O$ increases with decreasing oxygen amount (Goreau et al., 1980).

Besides the production of nitrite, during the first step of nitrification, $N_2O$ is produced as a side product from intermediates of biological hydroxylamine oxidation (e.g. HNO, $N_2O_2H_2$), while hydroxylamine ($NH_2OH$) itself acts as an intermediate during this pathway (Poughon et al., 2001; Ritchie and Nicholas, 1972; Stüven et al., 1992).

Another $N_2O$ producing pathway of nitrification is nitrifier denitrification where the oxidation of $NH_4^+$ to $NO_2^-$ is followed directly by the reduction of $NO_2^-$ to $N_2O$ (Wrage et al., 2001).

***Denitrification***

Denitrification is the stepwise heterotrophic dissimilatory reduction of nitrate ($NO_3^-$) to molecular nitrogen ($N_2$) under anaerobic conditions (Figure 1.1).

Bacteria use organic compounds for energy and carbon yield, where the nitrogen oxides ($NO_3^-$, $NO_2^-$) act as the terminal electron acceptors for the oxidation of organic matter and gaseous nitrogen is produced (Payne, 1973).

Since denitrification is also dependent on the amount of carbon in organic matter, which is oxidized to carbon dioxide ($CO_2$), the total denitrification equation can be expressed as (Richards, 1965):

$$(CH_2O)_{106}(NH_3)_{16}H_3PO_4 + 94.4\ HNO_3 + 4.89\ H^+ \rightarrow 106\ CO_2 + 55.2\ N_2 + 177\ H_2O + H_3OPO_4$$

In this pathway, $N_2O$ acts as an intermediate which can be either released or reduced in low-oxygen/anoxic environments (Codispoti and Christensen, 1985). During denitrification different enzymes are needed for each step of reduction (Hochstein and Tomlinson, 1988) and thus $N_2O$ production increased due to an imbalance of nitrogen-reducing enzymes, e.g. due to oxygen inhibition (Knowles, 1982; Lu and Chandran, 2010), nitrite accumulation (Von Schulthess et al., 1994) or due to a limitation of biodegradable organic compounds (Itokawa et al., 2001). Additionally, if sufficient $NO_3^-$ is abundant in the soil, $NO_3^-$ is preferred as an electron acceptor instead of $N_2O$ (Schlegel, 1992).

### 1.1.2. **Ancillary processes of the N-cycle**

***Assimilation***

During nitrogen assimilation, dissolved inorganic forms of nitrogen (DIN), e.g. $NH_4^+$ or $NO_3^-$ are taken up by organisms. This process is often associated to photoautotrophs, i.e. phytoplankton, in conjunction with photosynthesis and thus primary productivity and heterotrophic bacteria.

In contrast to $NH_4^+$ which is a reduced nitrogen form, the assimilation of nitrate has to involve two steps of reduction in the cell (to $NH_4^+$ via $NO_2^-$) before it can be converted into biomass. Thus, mostly assimilation of $NH_4^+$ is preferred in heterotrophic bacteria (Kirchman, 1994) and different phytoplankton groups.

Besides denitrification, assimilation also represents an important sink of fixed nitrogen.

***Nitrogen-fixation ($N_2$-fixation)***

Biological nitrogen fixation describes the conversion of atmospheric nitrogen into ammonia ($NH_3$), where diazotrophs (e.g. cyanobacteria, green sulfur bacteria) are able to crack the triply bonded molecule diatomic of $N_2$ (N≡N) and make it bioavailable.

***Ammonification (Remineralization)***

Ammonification describes the formation of $NH_4^+$ during the destruction of organic nitrogen, e.g. remineralization of phytoplankton detritus. Decomposers release $NH_4^+$ from organic matter which can further be used by other organisms in the ecosystem.

***Anammox***

Anammox (anaerobic ammonium oxidation), is the oxidation of ammonium ($NH_4^+$) to dinitrogen ($N_2$), using nitrite ($NO_2^-$) as an electron acceptor. In contrast to denitrification, anammox is performed by chemolithoautotrophic bacteria which use carbon dioxide ($CO_2$) as a C-source and are independent of the availability of organic matter.

***DNRA***

Dissimilatory nitrate reduction to ammonium (DNRA) is a direct reduction of nitrate ($NO_3^-$) to ammonium ($NH_4^+$). DNRA conserves N within the ecosystem as $NH_4^+$ and thus competes with denitrification for $NO_3^-$ reduction. It can be performed by heterotrophic or chemolithoautotrophic organisms, using organic carbon as an electron acceptor or nitrate (or other reduced inorganic substrates) for sulfide oxidation, respectively.

## 1.2. Anthropogenic effects on the nitrogen cycle

Over the last decades the significant increase in nutrient loads and especially reactive nitrogen loads due to human-driven sources has led to widespread eutrophication in terrestrial and aquatic ecosystems.

Anthropogenic impacts, i.e. human-driven impacts, doubled the rate at which fixed N is supplied to the biosphere (Vitousek et al., 1997) and have led to N saturations in many terrestrial ecosystems, also in Europe (Aber et al., 1998; Aber et al., 1989; Tietema et al., 1998). As a consequence, this nitrogen saturation also increased delivery of N to rivers, to coastal areas, and eventually into the ocean (David and Gentry, 2000; Deutsch et al., 2006; Rabalais, 2002; Seitzinger et al., 2002), which further leads to a decrease in $O_2$ availability and an increase in $N_2O$ emissions (Naqvi et al., 2000; Nevison et al., 2004).

In general, sources of dissolved inorganic nitrogen (DIN) inputs into coastal zones are mostly linked to agriculture (Seitzinger et al., 2005) and dominate natural inputs (Figure 1.3).

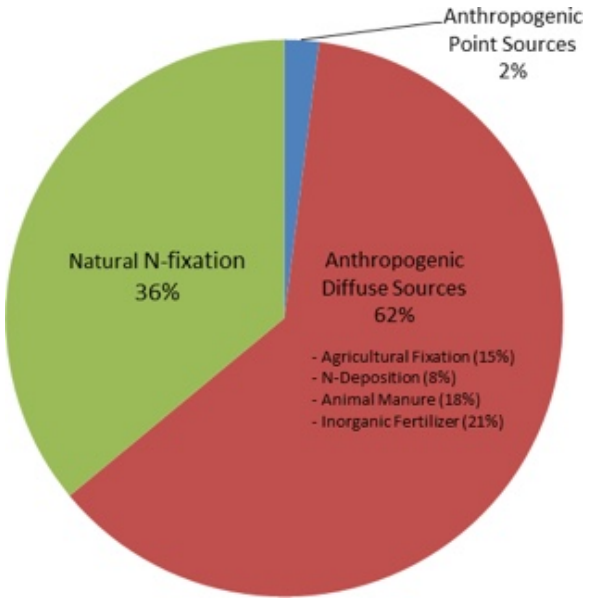


Figure 1.3: Estimated global sources of DIN to the coastal zone in percentage (after Seitzinger et al., 2005)

Within the nitrogen cycle, nitrification and denitrification are two important processes regulating the balance between nitrogen input and removal. This interplay is altered by

human activity either directly due to DIN discharge introduced upstream (e.g. Barnes and Upstill-Goddard, 2011; Ferrón et al., 2007; Garnier et al., 2006; Law et al., 1992) or indirectly because non-limiting N load favors phytoplankton growth. Enhanced phytoplankton growth also increases deposition of phyto-detritus into the sediments which can then be remineralized to $NH_4^+$, fueling nitrification (Kerner and Spitzy, 2001). In addition, denitrification rate and thus nitrogen removal is enhanced by supply of organic material, e.g. by partial excretion of photosynthetic products (Middelburg and Nieuwenhuize, 2000), and/or additional $NO_3^-$ discharge (Mulholland et al., 2008; Seitzinger, 1988).

As described in section 1.1.1., sources and sinks of $N_2O$ are closely related to the nitrogen cycle and its different turnover processes, where the main pathways for $N_2O$ production are nitrification and denitrification. As a consequence, the enhancement of both processes also leads to a very high $N_2O$ concentrations and thus emissions to the atmosphere.

Highest emissions of 10 to 12 Tg $N_2O$-N per year are released naturally in soils and water bodies by microbial nitrification and/or denitrification in the world's oceans, but with a net emission of 5.3 Tg $N_2O$-N per year anthropogenic sources are in the same order of magnitude (Davidson and Kanter, 2014).

In general, the annual source of $N_2O$ from the Earth's surface has increased from pre-industrial levels by about 40% to 50% as a result of human activity (Hirsch et al., 2006) and showed that there is an urgent need to reduce the $N_2O$ amount in our environment and to gain a closer understanding of both, GHG sources and sinks.

## 1.3. $N_2O$ in estuaries and coastal regions

Whereas $N_2O$ is known to be consumed under anoxic conditions, low oxygen conditions lead to high $N_2O$ production by nitrification and denitrification (Bakker et al., 2014). Therefore most aquatic systems are highly variable in $N_2O$ production and reduction. In addition, eutrophication also promotes hypoxia or anoxia (Howarth et al., 2011) and can further contribute to high $N_2O$ concentrations (see e.g. Naqvi et al., 2010). Hence, the function of an environment as a net source or sink depends on an overall ratio of $N_2O$ production and uptake.

Estuarine and coastal areas, which are characterized by high load of organic and mineral particles, as well as inorganic nitrogen compounds, provide ideal conditions for production of $N_2O$ by nitrification and denitrification in particular, and thus lead to high $N_2O$ emissions (e.g. Bange, 2006; Barnes and Upstill-Goddard, 2011; Murray et al., 2015).

$N_2O$ saturations up to a maximum of 6500% (Humber estuary) were found in a study of six UK estuaries by Barnes and Upstill-Goddard (2011). In all of these estuaries $N_2O$ saturations were highest during summer. Based on their DIN and $O_2$ concentration measurements, Barnes and Upstill-Goddard estimated nitrification as the main contributor to those high $N_2O$ concentrations and contribution by denitrification appeared to be negligible. In particular $NH_4^+$ derived from resuspension, ammonification and external inputs (e.g. sewage and industrial inputs as measured in the Tees estuary) leads to large $N_2O$ emissions in these UK estuaries. As in this study, also other investigations of estuaries determined water column nitrification as the main source of $N_2O$ in low salinity regions (mainly in the Maximum Turbidity Zone = MTZ), e.g. in the Schelde estuary located in the Netherlands (de Bie et al., 2002; de Wilde and de Bie, 2000) or Tagus estuary in Portugal (Gonçalves et al., 2010).

In contrast, few studies in the Colne Estuary reported sedimentary denitrification as the main $N_2O$ source (Dong et al., 2002; Robinson et al., 1998) and as asserted by other authors, denitrification is likely to contribute to $N_2O$ concentrations and should be taken in account even though considered as a minor source (e.g. Abril et al., 2000; Barnes and Owens, 1998; de Wilde and de Bie, 2000; Seitzinger and Nixon, 1985).

Net uptake of $N_2O$ will occur only when in-situ $N_2O$ concentrations in groundwater, soil and surface waters are lower than aqueous concentrations in equilibrium with the atmosphere. To date, few aquatic ecosystems have been reported to be net $N_2O$ sinks under specific, regional environmental conditions (e.g. Elkins et al., 1978; Kroeze et al., 2007) and mostly temporary (Kieskamp et al., 1991; Middelburg et al., 1995; Rees et al., 1997).

Aside from these exceptions, most estuaries and coastal waters are largely in equilibrium with the atmosphere or $N_2O$ supersaturated (Bange, 2006; Bange et al., 1996; Weiss, 1981), and those studies showed that coastal regions and estuaries are net sources of $N_2O$.

The major pathway of $N_2O$ formation in these areas always depends on oxygen concentration, nutrient distribution, as well as the microbial community (de Bie et al., 2002; Dong et al., 2002) which can be strongly influenced by anthropogenic inputs (e.g. Brion and Billen, 2000; Garnier et al., 2006; Howarth et al., 2011).

Latest studies estimated bulk $N_2O$ emissions from European estuaries of ~6.8 ± 13.2 Gg $N_2O$ per year (Barnes and Upstill-Goddard, 2011) and global fluxes of $N_2O$ from all estuarine environments (including coastal regions) in a range of 0.17 to 0.95 Tg $N_2O$ per year (Murray et al., 2015). With 1.9 Tg $N_2O$ per year, $N_2O$ emissions from freshwater and coastal systems account for about 35% of the total emissions of 5.4 Tg $N_2O$ per year in aquatic environments (Seitzinger et al., 2000).

## 1.4. The use of stable nitrogen and oxygen isotopes in aquatic environments

Two stable isotopes of nitrogen (N) exist: $^{14}N$ and $^{15}N$. With a natural abundance of 0.36% $^{15}N$ is lower than $^{14}N$ (99.64%) in the global nitrogen pool. Similar abundances are given for the three stable oxygen-isotopes, with the two commonly studied ones: $^{16}O$ (99.76%) and $^{18}O$ (0.204%), and the third one: $^{17}O$ (0.037%).

Stable isotopes values are usually expressed in delta notations ($\delta_{sample}$ = $\delta^{15}N$ or $\delta^{18}O$) which describes the ratio of $^{15}N/^{14}N$ or $^{18}O/^{16}O$ expressed in per mill [‰].

Isotopic ratios are calculated by using the following equation:

$$\delta_{sample}[‰] = \left(\frac{R_{sample}}{R_{standard}} - 1\right) * 1000$$

R describes the ratio of the heavier to the lighter isotopes ($R_{sample}$) and an international reference standard ($R_{standard}$) in relation to atmospheric nitrogen for $\delta^{15}N$ (Coplen, 1995; Gonfiantini et al., 1995) and for $\delta^{18}O$ relative to Vienna Standard Mean Ocean Water (VSMOW) (Kornexl et al., 1999; Révész et al., 1997; Silva et al., 2000).

To assess the anthropogenic impact and the role of internal nitrogen turnover in aquatic environments, dual isotopes of $NO_3^-$ and their specific compositions are well investigated and established as a common tool to complement nutrient data (e.g. Burns and Kendall, 2002; Mayer et al., 2002; Sigman et al., 2005).

The advantages of using isotopes of nitrate are their source-specific signatures (Figure 1.4). For example, $\delta^{15}N_{NO3}$ values >8‰ up to 13.9‰ indicate a dominance of waste water

and septic waste (Aravena et al., 1993; Burns et al., 2009), whereas $\delta^{15}N$ of soil nitrate mostly ranges between 2‰ and 5‰ (Kendall, 1998). Furthermore, the additional measurement of $\delta^{18}O_{NO3}$ could lead to a more precise source determination, e.g. by distinguishing nitrate fertilizers which have distinctive $\delta^{18}O_{NO3}$ values (Amberger and Schmidt, 1987).

Hence, the dominant use of stable isotope measurements in catchment areas is tracing nutrient sources, derived naturally or anthropogenically. In addition, these measurements are often combined with isotope mixing models to quantify how much is derived from each of the constant-composition sources (Phillips and Koch, 2002).

Stable isotopes are not only used to determine N sources, they also reflect natural isotopic fractionation by biological processes (Figure 1.4). Most biological processes lead to isotopic fractionation because $^{14}N$ is preferentially transformed relative to $^{15}N$. This fractionation leads commonly to an increase of 1.5:1 to 2:1 of $\delta^{15}N$ to $\delta^{18}O$ during denitrification (Böttcher et al., 1990; Mengis et al., 1999), whereas the ratio of $\delta^{15}N$ and $\delta^{18}O$ of the residual $NO_3^-$ increases 1:1 during nitrate assimilation by phytoplankton (Deutsch et al., 2009; Granger et al., 2004).

Since biological $NO_3^-$ production and consumption act simultaneously in rivers (Jenkins and Kemp, 1984; Seitzinger, 1988) they are mostly difficult to segregate. In this case, sediment incubation assays are used, based on the addition of $^{15}N$-labelled nitrogen, to disentangle nitrification, denitrification or nitrate uptake (Blackburn, 1979; Clark et al., 2006; Laws, 1984).

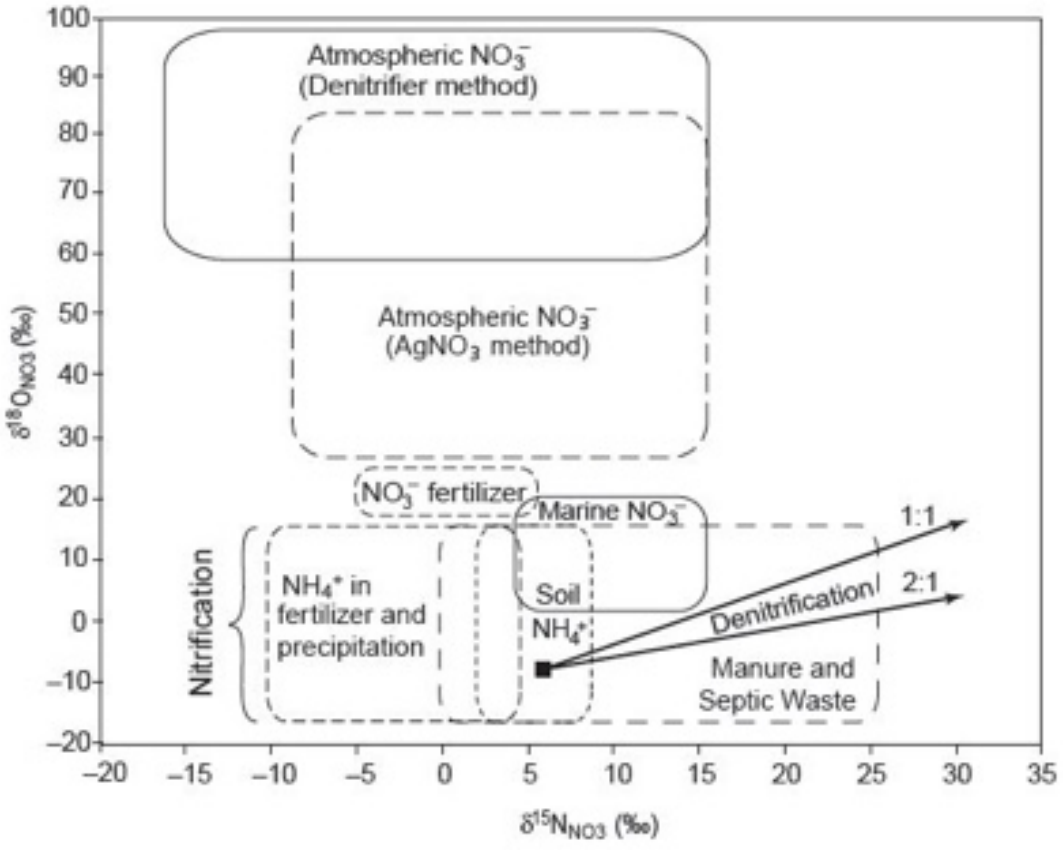


Figure 1.4: 'Typical values of $\delta^{15}N$ and $\delta^{18}O$ of nitrate derived from various N sources (Kendall et al., 2007) - boxes represent the range of $\delta^{15}N$ and $\delta^{18}O$ values of according N sources [‰]; the two slopes represent the ratio of $\delta^{15}N$ and $\delta^{18}O$ of the residual $NO_3^-$ increases during nitrate assimilation by phytoplankton (1:1) and denitrification (2:1)

## 1.5. Focus and thesis outline

The focus of this thesis was set on human alterations to the N-cycle and different aspects on nitrogen turnover. Anthropogenic discharge leads to an enhanced eutrophication, fueling nitrification and denitrification in aquatic environments (Bernhardt et al., 2002; Mulholland et al., 2008; Peterson et al., 2001; Seitzinger, 1988), and as a resulting product of these two processes, $N_2O$ emissions emerged as a highly relevant issue, especially on a larger scale (i.e. in large rivers and estuaries).

Thus, in this thesis the effect of anthropogenic input on production and consumption of nitrogen compounds was investigated in a small river, as well as in an eutrophic estuary.

This thesis consists of three chapters which have been published (Chapter 3)or submitted to scientific journals (Chapter 2) or are in preparation for submission (Chapter 4).

- **Quantifying the role of nitrification, N-retention and elimination along an anthropogenic gradient in a small river**

(Chapter 2; submitted to *Isotopes in Environmental and Health studies*)

In this chapter, the main goal was to disentangle N-turnover processes with respect to anthropogenic influences where anthropogenic nutrient enrichment leads to a change of the balance between N-retention and N-elimination in rivers and thus, contributing to strong eutrophication.

Seasonal investigations in the small river Holtemme were performed along a land-use gradient, ranging from a pristine upper region to an agricultural setting further downstream. Natural abundance of stable isotopes and a labelling experiment indicated a decreased influence on nitrogen production of soil nitrification. Its influence decreased about 70% downstream as the influence of anthropogenic discharge gains more weight with increasing human land use, even though human-driven N sources also enhanced nitrogen production rates which additionally contribute to nitrogen load in this small river.

Whereas sediment incubations in the pristine area showed a seasonally variable dependent predominance of nitrogen production or consumption, the increase of N load

due to anthropogenic discharge leads to an overall increase in $NO_3^-$ consumption rates in the agriculturally dominated area. But N was removed only inefficiently in the surface water of the anthropogenically impacted section which indicated a quick exhaustion of sediment filter capacity.

Thus, the effect of N-removal due to denitrification is exceeded by N-input and cannot lead to a further reduction of eutrophication which in turn can have adverse effects to rivers of higher orders.

- **High resolution measurements of nitrous oxide ($N_2O$) in the Elbe estuary**

(Chapter 3; published in *Frontiers in Marine Science*)

The main motivation of this study was an existing lack of recent $N_2O$ dynamics investigations in the Elbe estuary. After the German reunion in 1989 a continuous nutrient decrease could be measured in the Elbe estuary, together with an improvement of the $O_2$ regime, $N_2O$ concentrations and emissions were expected to be lower compared to measurements in the late 1980s and mid-1990s. Furthermore, the shift of DIN and oxygen concentrations raises the question if hot-spots of $N_2O$ production could be determined and which nitrogen turnover processes are the main $N_2O$ contributors along the Elbe estuary.

Results of high-resolution transect measurements of $N_2O$ concentrations in April 2015 and June 2015 showed that the Hamburg port area is a hot-spot of $N_2O$ production. Linear correlations of $N_2O_{xs}$ and apparent oxygen utilization (AOU) in the freshwater section indicated nitrification as the main contributor to $N_2O$ throughout most parts of the transect. However, at minimum oxygen concentrations measured in the port region, sedimentary denitrification obviously affected $N_2O$ concentrations.

Contrary to previous studies (BIOGEST data published in Barnes and Upstill-Goddard, 2011; Hanke and Knauth, 1990), the main $N_2O$ production pathway has changed from denitrification (1980s) to nitrification. We found that the improvement of the Elbe estuary led to a significant decrease of $N_2O$ saturations compared to the late 1980s, but no further decrease in $N_2O$ saturations could be estimated almost two decades later ($N_2O$ saturation in the mid 1990s: 202%).

Thus, with a $N_2O$ mean saturation of 201% and a sea-to-air flux density of 48 µmol $m^{-2}$ $d^{-1}$, the Elbe estuary still remains as an important $N_2O$ source to the atmosphere.

- **Tidal influences on nitrous oxide ($N_2O$) dynamics in the Port of Hamburg (Elbe estuary)**

(Chapter 4; in preparation for submission)

Stationary investigations of $N_2O$ dynamics in the Port of Hamburg was based on the idea that transect measurements reveal large amounts of $N_2O$ emissions in this region, and identified this area as a hot-spot of $N_2O$ production (Chapter 3). But especially in regions with strong tides, additional mixing with allochthonous derived $N_2O$ became likely (Leip, 2000). Hence, the motivation of this study was to investigate biotic as well as abiotic factors affecting $N_2O$ concentration and determine whether $N_2O$ in-situ production or mixing with allochthonous derived $N_2O$ can be determined as the main source in this highly productive area.

Results of high resolution measurements of $N_2O$ dynamics over four full tidal cycles indicate that allochthonous derived $N_2O$ contributes to the measured $N_2O$ concentration. As a minor source, mixing with allochthonous derived $N_2O$ was mostly seen with flood tides from a single harbor basin downstream the measurement station, but also additional mixing of $N_2O$ derived from harbor basins upstream and/or riparian zones appeared to be possible if previous water level was exceptionally high.

Nevertheless, based on tidal DIN patterns which showed $NH_4^+$, and especially $NO_2^-$, as the most significant factors influencing $N_2O$, internal N-turnover can be determined as the main contributor of measured $N_2O$ concentrations in this low oxygen region. Furthermore, biological $N_2O$ production in this area was enhanced by an average decrease of $O_2$ concentration due to an increase of remineralization and respiration, additionally fueled by higher temperatures and a lower water discharge.

Those measurements demonstrated internal N-cycling as the main source of $N_2O$ production where allochthonous derived $N_2O$ had a minor influence on $N_2O$ concentrations, leaving the Port of Hamburg as a hot-spot of biological $N_2O$ production.

# 2. Quantifying the role of nitrification, N-retention and elimination along an anthropogenic gradient in a small river

Lisa Brase, Tina Sanders, Kirstin Dähnke

Submitted to Isotopes in Environmental and Health studies (2017)

## Abstract

Anthropogenic nutrient inputs increase the N-load in many aquatic systems, leading to eutrophication and potential changes of biological N-retention capacity. In this study, nitrate inputs in a small river were investigated along a gradient of anthropogenic influence. We aimed to determine changes in nitrate load and isotope signatures in the water column and their influence on biological N-retention and N-modification in sediments. In seasonal sampling campaigns, we analysed nutrient concentrations, and stable isotopes of nitrate. To differentiate rates of nitrate production and consumption in the pristine vs. agricultural river section, intact sediment cores were incubated with $^{15}N$-labelled nitrate. $\delta^{15}N$ values of nitrate in the pristine river section were low, reflecting natural sources, but, as expected, increased with nitrate concentration in all seasons along the gradient. In general, nitrate retention and consumption were higher in the polluted than in the pristine river section, and nitrate consumption exceeded production. Our measurements show that even in a small river, the anthropogenically enhanced consumption capacity is overwhelmed by surplus N-inputs, and denitrification cannot increase in step with external loads.

## 2.1. Introduction

Excess production and application of reactive nitrogen as fertilizer has led to wide-spread eutrophication in terrestrial and aquatic ecosystems. Among other consequences, this anthropogenic nutrient enrichment leads to a change of the balance between N-retention and elimination in rivers and streams: With additional nitrate input, denitrification is promoted, which may counteract eutrophication (Seitzinger, 1988). On the other hand, additional nutrients or easily accessible carbon sources increase phytoplankton production, so that nitrogen retention in a given system is increased, at the cost of

increased biomass production (Aravena et al., 1993; Schiller et al., 2009; Starry et al., 2005).

To assess the anthropogenic impact and the role of internal turnover in rivers, not only concentration measurements of nutrients have proven usefulness. Stable isotope measurements of DIN, mainly dual isotopes in nitrate and their specific compositions, can complement nutrient data, e.g. (Aravena et al., 1993; Burns and Kendall, 2002; Mayer et al., 2002). Nitrate isotope signatures are source-specific: Atmospheric deposition has relatively low $\delta^{15}N$ values (-5‰ to 5‰,Kendall et al., 2007), whereas runoff from agricultural soils or manure is isotopically enriched (>8‰, e.g. Chang et al., 2002; Deutsch et al., 2006; Wassenaar, 1995). Furthermore, stable isotopes also reflect natural isotopic fractionation by biological processes. For example, during nitrate assimilation by phytoplankton, the ratio of $\delta^{15}N$ and $\delta^{18}O$ in the residual $NO_3^-$ increases in parallel (Granger et al., 2004), whereas during denitrification in aquifers, this increase follows a ratio of 1.5:1 to 2:1 (Böttcher et al., 1990; Mengis et al., 1999).

Many studies focused on N-turnover in large river systems (e.g. Chang et al., 2002; Mayer et al., 2002; Voss et al., 2006) where nitrification in the catchment and the stream itself regenerates significant amounts of nitrate. Nitrate concentration and isotopes in large rivers can theoretically be affected by diffuse sources, groundwater input, and by internal nitrate uptake due to assimilation or denitrification (e.g. Aravena et al., 1993; Deutsch et al., 2006; Johannsen et al., 2008). Consequently, it is notoriously difficult to address the relative importance of various sources and turnover processes separately in large rivers. One possible solution lies in incubation assays: Because biological $NO_3^-$ production and consumption act simultaneously in rivers (Jenkins and Kemp, 1984; Seitzinger, 1988), incubation assays can be used to separate these processes. The isotope dilution technique, which is based on the addition of $^{15}N$-labelled nitrate, is a useful tool to disentangle nitrification, denitrification, or nitrate uptake (Blackburn, 1979; Clark et al., 2006; Laws, 1984). This technique is often applied in sediment incubations, where N-turnover is higher than in the water column.

In this study, we combined sediment incubations with natural abundance nitrate isotope investigations to disentangle the effect of external sources vs. internal processes and their joint impact on the water column DIN and nitrate isotope inventory. We investigated a small river with a small catchment area along a land-use gradient, ranging from a pristine

upper region to an agricultural setting further downstream. To identify nitrate sources, we combined nutrient/dual nitrate isotope analyses and an isotope mixing model. Moreover, we calculated rates of $NO_3^-$ production and consumption in all seasons based on sediment incubations. We expected that nutrient concentration of the river in the uppermost section be dominated by influences of natural sources, namely atmospheric deposition and soil nitrification, whereas downstream agriculture/manure and septic waste should be dominant.

We also expected internal processing in such a small river to have a visible effect on isotope composition, and assumed that it would be possible to quantify the role of nitrate regeneration by nitrification versus assimilation or denitrification. Our main intention was to (a) quantify the role of nitrification in the river as a source of nitrate vs. nitrate derived from external sources, and (b), to assess the impact of increasing nutrient loads on N-elimination (i.e., denitrification) and retention (i.e., uptake).

## 2.2. Material and Methods

### 2.2.1. Site description

The Holtemme River in Saxony-Anhalt is ~47 km long, with a small catchment area of 278 km² and an annual mean water discharge of 1.33 $m^3 s^{-1}$ (gauge Mahndorf – station 6, Figure 2.1). Climate conditions in the catchment area of the Holtemme are typical for Central Europe, with wet summers and cold dry winters (Döring, 2004).

The Holtemme encompasses pristine regions as well as regions that are subject to anthropogenic influences. Its source is in the region of the Harz Mountains, 860 m above sea level. The headwaters lie in a forest dominated national park with steep, small waterfalls, and rapids. The national park ends at the city Wernigerode, where the regulation of the river begins. Further downstream, the river is influenced by a combination of urban runoff, a waste water treatment plant (WWTP) and agricultural fields, until it discharges into the Bode river.

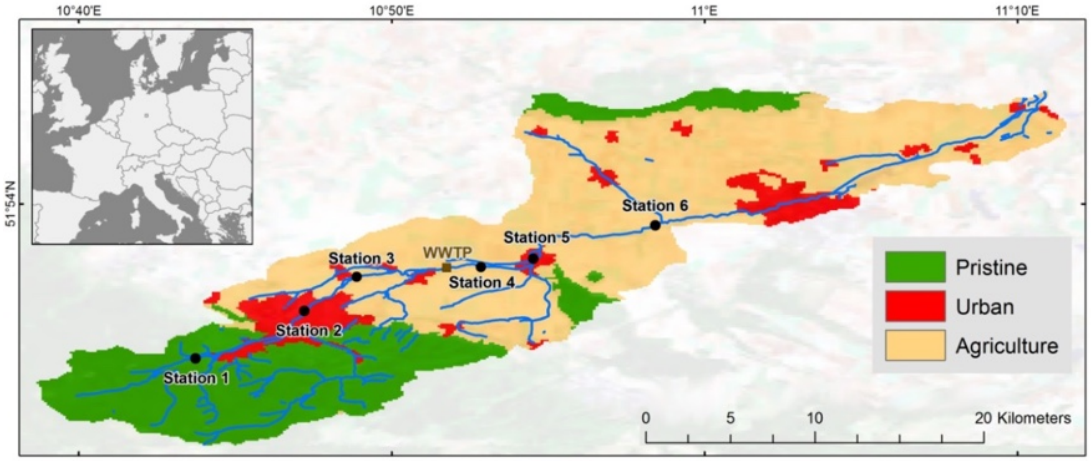


Figure 2.1: Site map of the Holtemme River created in ArcGIS; different colors indicate land use classes (pristine, urban, agriculture), the sampling stations are located as black points: station 1 - pristine area, station 2 & 3 - urban area, station 4 - WWTP (brown rectangle), station 5 & 6 - agricultural area

### 2.2.2. **Sampling**

#### *2.2.2.1. **Water samples***

Seasonal sampling campaigns took place in June 2014, September 2014, February 2015 and April 2015. Weather conditions during sampling were mainly sunny; a slight rain event in summer did not show notable effects on discharge or nutrient concentration (data not shown).

Water samples for nutrient and isotope analyses were taken along a 20 km section at six stations following a pristine-agricultural gradient (Figure 2.1,

Table 2.1). For nutrient and stable isotope analysis of nitrate, water was sampled with a bucket in the middle of the stream. Samples were filtered immediately (PVDF, 0.45µm), stored cool in PE bottles (100 ml) and were frozen within 10 hours until further analysis in the lab.

Table 2.1: Ambient conditions during transect sampling: anthropogenic influences, river kilometer and water temperatures for each station, discharge of stations 1 and 6[1], and according weather conditions

| **Season** | | | Summer | Autumn | Winter | Spring |
|---|---|---|---|---|---|---|
| **Date** | | | 6/24/2014 | 9/8/2014 | 2/6/2015 | 4/14/2015 |
| **Station** | **Anthropogenic influence** | **River km** | **Temp [°C]** | **Temp [°C]** | **Temp [°C]** | **Temp [°C]** |
| 1 | Pristine | 2.7 | 11 | 12.6 | 0.3 | 3.7 |
| 2 | Transient - Urban | 7.4 | 12.5 | 13.5 | 1.2 | 6.6 |
| 3 | Transient - Urban | 11.8 | 12.6 | 14.2 | 1.3 | 6.7 |
| 4 | WWTP | 16.2 | 16.7 | 16.4 | 3.4 | 8.4 |
| 5 | Agriculture | 18.5 | 17.1 | 16.1 | 3.1 | 9.1 |
| 6 | Agriculture | 24.4 | 16.4 | 15.8 | 2.7 | 9.4 |
| **Discharge station** | **Station name** | | **Discharge [$m^3 s^{-1}$]** | **Discharge [$m^3 s^{-1}$]** | **Discharge [$m^3 s^{-1}$]** | **Discharge [$m^3 s^{-1}$]** |
| 1 | Steinerne Renne | | 0.11 | 0.11 | 0.12 | 0.41 |
| 6 | Mahndorf | | 0.36 | 1.07 | 1.48 | 2.20 |
| **Weather conditions** | | | Mainly sunny | Mainly sunny | Snow covered | Snow melt |

[1] Data available at http://www.hochwasservorhersage.sachsen-anhalt.de/

#### *2.2.2.2.* ***Sediment samples***

Sediment cores were taken at stations 1 and 6 in spring, summer and autumn. In winter (February 2015), no cores could be taken because deeper sediment layers were frozen. At each station, twelve cores were taken (PMMA core liners, ID 3.7cm; approximately 10 cm of sediment, 13 cm of overlying water), sealed and stored in a cooling box for transportation. The middle of the river bed was covered with stones and gravel at both stations, hence, cores were taken towards the river bank where the sediment was accessible.

### 2.2.3. **Laboratory analysis**

#### *2.2.3.1.* ***Water samples for nutrient and isotopic composition***

Nitrate and ammonium concentrations in water samples were measured with a continuous flow auto analyser (AA3, SEAL Analytical) using standard colorimetric techniques (Hansen and Koroleff, 2007).

Stable isotopes of nitrate were determined using the denitrifier method (Casciotti et al., 2002; Sigman et al., 2001). The method is based on the analysis of nitrous oxide ($N_2O$) produced by denitrifying *Pseudomonas aureofaciens* (ATCC #13985). The $N_2O$ was purified, concentrated on a GasBench II and measured on an isotope ratio mass spectrometer (Delta V Advantage, Thermo Scientific). Samples were calibrated against the international standards IAEA-$NO_3$ ($\delta^{15}N$: +4.7‰, $\delta^{18}O$: +25.6‰) and USGS34 ($\delta^{15}N$: -1.8‰, $\delta^{18}O$: -27.9‰), with a standard deviation of <0.2‰ for $\delta^{15}N_{NO3}$ (n=4) and <0.5‰ for $\delta^{18}O_{NO3}$ (n=4).

#### *2.2.3.2.* ***Intact sediment core incubation – Isotope dilution experiment***

The sampled sediment cores were placed in buckets, and stored open under water which was additionally sampled from the according sampling site. To avoid anoxia in the sediment cores, river water in the buckets was oxygenated with aquarium pumps and constantly stirred (Trimmer et al., 2006). A preliminary test over 48 hours showed that this method did not lead to increased anoxia in the sediment cores. Buckets were placed in a water filled tank and pre-incubated at constant temperature (summer and autumn: 16°C, spring: 12°C, cf. Table 2.2) for 36 hours. After pre-incubation, river water in the buckets was removed until the top of the core liners was above water level, and the water

in each core was oxygenated separately using aquarium pumps. Great care was taken to avoid sediment resuspension during oxygenation of cores.

At the beginning of the experiment, the overlying water of 9 cores was labelled, aiming for a labelling percentage of 1 at% with $Na^{15}NO_3$ (98 atom % $^{15}N$, Sigma-Aldrich®). To avoid an increase in rates due to substrate addition, the label solutions had a $NO_3^-$ concentration comparable to site water. Three unlabeled cores remained and were used as control samples. All cores were then incubated for 24 hours in darkness. Samples were taken directly after label addition, after 8 and 24 hours by creating a slurry where the reactive sediment layer (1 cm) was gently mixed into the overlying water column (Crowe et al., 2012). At each time point, three labelled replicates and one control without label addition were sampled. To stop microbial activity, the slurry was filtered immediately (PVDF; 0.45 µm) and samples were stored frozen until nutrient concentration and $^{15}N_{NO3}$ enrichment were measured.

Table 2.2: Conditions during sediment core sampling and incubation experiments: river regulation, water depth and major sediment type; starting date of incubation experiment, and incubation temperature

| | **Anthropogenic influence** | **River state** | **Water depth** | **Sediment type** | **Incubation Temp [°C]** | | |
|---|---|---|---|---|---|---|---|
| Station | | | | | Summer 6/26/2014 | Autumn 9/10/2014 | Spring 4/16/2015 |
| 1 | Pristine | natural | 0.1-0.2m | gravel, sand, silt | 16 | 16 | 12 |
| 6 | Agriculture | regulated | 0.5-0.7m | clay, silt | 16 | 16 | 12 |

### 2.2.4. **Calculations**

In our assessment, we define nitrate consumption as the sum of assimilation and denitrification, nitrate production is defined as nitrification.

Nitrate production and consumption in cores were calculated based in the $^{15}N$ isotope dilution model (Koike and Hattori, 1978; Nishio et al., 2001). The following equations were used:

$$p = [\ln(I_t/I_0)]/[\ln (P_t/P_0)] (P_0-P_t/t) \quad (1)$$

where p is production in μmol $L^{-1}$ $h^{-1}$, t is incubation time, $P_0$ is the initial nitrate concentration at incubation time 0, $P_t$ is the nitrate concentration at time t, and $I_0$ and $I_t$ represent $^{15}N$ atom excess.

Nitrate consumption was calculated by using the decrease of nitrate concentration (P), the content of $^{15}N$ nitrate (p) and the natural abundance of $^{15}N$ nitrate:

$$c = \ln[(p_0-k_0P_o)/(p_t-k_tP_t)] (P_0-P_t)/\ln(P_0/P_t)/t \quad (2)$$

where c is the rate of consumption in μmol $L^{-1}$ $h^{-1}$.

Both turnover rates were then converted into mg N $m^{-2}$ $d^{-1}$, using the ratio of measured volume-to-surface area (of the boundary layer between water column and sediment) of each core (Cowan et al., 1996).

## 2.3. **Results**

### 2.3.1. **Nutrient concentrations**

Nitrate concentration increased downstream the river during all seasons (Figure 2.2a). Pristine nitrate concentrations (station 1) ranged from 15 μM to 55 μM with the highest concentration in spring and lowest in autumn. Along the transect from station 1 to 5, nitrate concentration increased up to 160 to 200 μM, with highest values in summer. There was no further increase between stations 5 and 6, and even a slight decrease in concentration between these stations in autumn and winter. In summer, nitrate concentration peaked at station 4 downstream the WWTP, with nitrate concentrations of >400 μM.

Ammonium concentration was below 1 μM at stations 1 to 3, but showed a peak at station 4 from spring to autumn (Figure 2.2b), with a maximum value of 70 μM in summer. The ammonium concentration then dropped again to 1 to 4 μM further downstream.

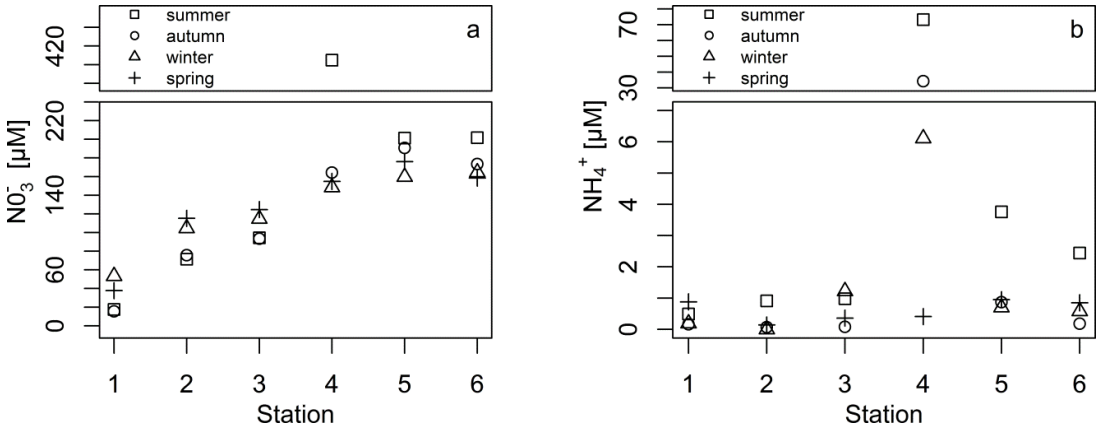


Figure 2.2: DIN concentrations for each sampling point along the river transect over all seasons. (a) Nitrate concentration in µM during summer (rectangle), autumn (circle), winter (triangle) and spring (plus) (b) Ammonium concentration in µM at the according season

### 2.3.2. **Dual stable isotopes of $NO_3^-$ ($\delta^{15}N$ and $\delta^{18}O$)**

The covariation of $^{18}O$ and $^{15}N$ along the transect reveals that samples can be divided into 3 groups: $\delta^{15}N_{NO3}$ at the pristine station 1 was approximately 0‰ in summer and autumn, and -1‰ to -2.5‰ in winter and spring. $\delta^{18}O_{NO3}$ values were relatively high and values ranged from 4‰ to 8‰. $\delta^{15}N_{NO3}$ at station 2 and 3 were always similar to each other and relatively enriched in comparison to station 1. $\delta^{15}N_{NO3}$ was higher in summer and autumn (6‰ - 7‰) than in winter and spring (1‰ - 5‰). The $\delta^{18}O_{NO3}$ was approximately 2‰ at all seasons, except in spring where it reached 4‰. At station 4, 5 and 6, dual isotope values of nitrate are similar in winter and spring. Relative to the upstream stations 2 and 3, $\delta^{15}N_{NO3}$ values were elevated (up to 10‰), and $\delta^{18}O_{NO3}$ was slightly enriched in comparison to upstream stations (3‰ - 4‰). This pattern was evident in all seasons, with a deviation in summer: While $\delta^{15}N_{NO3}$ increased to 15‰ at station 4, there was no immediate effect on $\delta^{18}O_{NO3}$, which remained stable at 1.5‰ and increased further downstream to ~6‰ (Figure 2.3).

Generally, $\delta^{15}N$ values in summer and autumn were elevated relative to winter and spring values. $\delta^{18}O$ values were highest in spring, but the seasonal variation was less pronounced than for $\delta^{15}N$ (Figure 2.3).

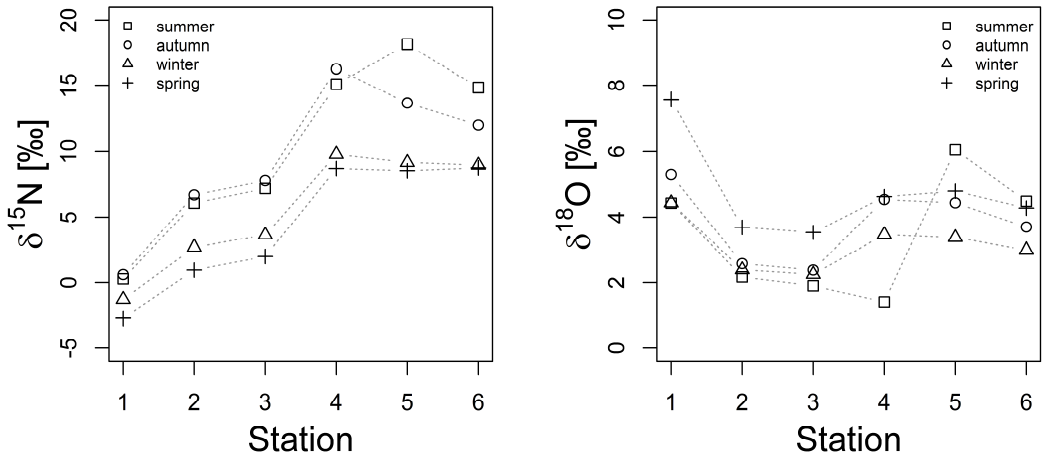


Figure 2.3: Seasonal profiles of $\delta^{15}N_{NO3}$ and $\delta^{18}O_{NO3}$ isotope vales along the Holtemme River

### 2.3.3. **Nitrate turnover in core incubations**

Sediment cores for incubations were taken at the pristine station 1 (Figure 2.4a) and at the downstream station 6 (Figure 2.4b) in spring, summer and autumn. In general, nitrate consumption and nitrate production were significantly lower at the pristine station than at the agriculturally impacted station.

We did not measure significant biological nitrate processing in spring at the pristine river site. In summer, nitrate production was active (4.3 ± 1.9 mg N $m^{-2}$ $d^{-1}$) and significantly ($p \leq 0.05$) exceeded nitrate consumption (1.5 ± 1.5 mg N $m^{-2}$ $d^{-1}$). In autumn, nitrate consumption increased (6.2 ± 2.6 mg N $m^{-2}$ $d^{-1}$) and at this time of year significantly exceeded nitrate production (2.8 ± 2.8 mg N $m^{-2}$ $d^{-1}$).

At the agriculturally impacted station 6, nitrate consumption was higher than nitrate production at all seasons, although only significantly in spring and summer (Figure 2.4b). Nitrate production ranged from 12.2 to 22.2 mg N $m^{-2}$ $d^{-1}$, whereas consumption rates in spring and summer clearly exceeded production with rates around 117 mg $m^{-2}$ $d^{-1}$ (spring: 113 ± 28.7 mg N $m^{-2}$ $d^{-1}$ , summer: 123.8 ± 38.1 mg N $m^{-2}$ $d^{-1}$).

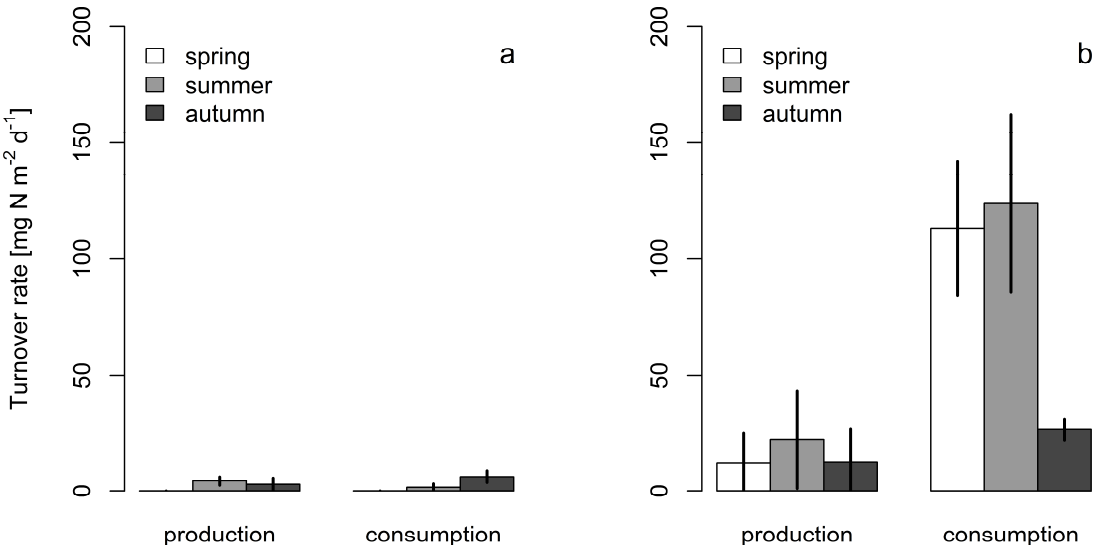


Figure 2.4: Nitrate turnover rates at the pristine station 1 (panel a) and at the agriculturally impacted station 6 (panel b) from spring to autumn

## 2.4. **Discussion**

### 2.4.1. **N-source assessment using an isotope mixing model**

Our primary goal was to disentangle the relationship between external nutrient sources vs. internal processing, using a small river as a model system, because we expected that source attribution in this case should be possible. The Holtemme follows a gradient of anthropogenic impact, and our seasonal isotope data suggested that stations can be clustered into three groups, comprised of the pristine station 1, transient stations 2+3 with an intermediate anthropogenic impact, and mainly agricultural stations 4-6.

A GIS-based analysis of the catchment of the suite of sampling stations confirms this land-use gradient (Table 2.3). There is no anthropogenic influence at the pristine station 1, the catchment of stations 2 and 3 is comprised of 20.6% anthropogenic land use, and at stations 4-6, this portion rises to 47.8%. The isotope values of $NO_3^-$ can be related to land use with an isotope mixing model to disentangle $NO_3^-$ inputs from various sources (Deutsch et al., 2006; Voss et al., 2006). If our assumptions regarding the N-sources in the catchment hold, the load weighted mean isotope values should reflect these GIS-based data. We thus applied an isotope mixing model (IMM) (Phillips and Koch, 2002) to calculate the relative proportion of potential nitrate sources at the clustered stations (Stn

1; Stns 2+3; Stns 4 – 6). We presumed three candidate sources: Nitrate from a pristine forest region ($\delta^{15}N$= -3‰, $\delta^{18}O$= 2‰), typical for the Harz mountains (Mueller et al., 2015), atmospheric deposition ($\delta^{15}N$= 0.4‰, $\delta^{18}O$= 75‰) (Beyn et al., 2014) and runoff from agricultural land including manure fertilization ($\delta^{15}N$= 13.9‰, $\delta^{18}O$= 3.4‰) (Aravena et al., 1993).

The isotope mixing model (IMM) shows that atmospheric deposition is only a relevant nitrate source at the pristine station (6.5%) and almost 90% nitrate at this station can be attributed to pristine terrestrial sources, e.g. soil nitrification (Table 2.3). $\delta^{15}N_{NO3}$ (-1.3‰ to 0.6‰) and $\delta^{18}O_{NO3}$ values (4.4‰ to 5.3‰) with according $NO_3^-$ concentrations of 17.5 µM to 38 µM in summer, autumn and winter are in the range for pristine sites (Durka et al., 1994). Depleted $\delta^{15}N_{NO3}$ and enriched $\delta^{18}O_{NO3}$ values are typical for this region (Mueller et al., 2015) and reflect a forest dominated catchment (Mayer et al., 2001) with $NO_3^-$ derived from nitrification in pristine soils (Deutsch et al., 2006; Kendall et al., 2007). The impact of atmospheric deposition is evident in spring, when depleted $\delta^{15}N_{NO3}$ and enriched $\delta^{18}O_{NO3}$ values compared to other seasons indicate a dilution with snowmelt (Hastings et al., 2004; Pardo et al., 2004; Piatek et al., 2005).

Mayer et al. (2002) estimated that nitrate concentration in forested watersheds is almost completely derived from soil nitrification processes along with a minor influence of atmospheric deposition. In contrast, Voss et al. (Voss et al., 2006) determined significant atmospheric influences in rivers receiving >50% N from agricultural runoff. These authors used deviating end-member values for atmospheric deposition ($\delta^{15}N_{NO3}$: 0.1‰ and $\delta^{18}O_{NO3}$: 51.7‰) (Deutsch et al., 2006), because different analytical methods (denitrifier vs. silver nitrate) yield substantially different $\delta^{18}O$ signatures (Kendall et al., 2007). To check the IMM sensitivity regarding the isotope signature of atmospheric deposition measured with the silver nitrate method, another IMM was applied using the source signatures applied in Voss et al. (2006). The percentage of atmospheric influence increased slightly to 9.5% at station 1, but remained negligible in the rest of the river, suggesting that atmospheric deposition is only a minor source of direct N-deposition to the Holtemme.

Table 2.3: Calculated values of the isotope mixing model (IMM) and the GIS-data based calculations of areas influencing the watershed

| | *IMM [%]* | | | *GIS [%]* | |
|---|---|---|---|---|---|
| Station | **Pristine (forest region)** | **Atmospheric Deposition** | **Agricultural Land -Manure** | **Agricultural & Urban Land** | **Pristine** |
| **1** | 89.7 | 6.5 | 3.8 | 0.0 | 100 |
| **2+3** | 63.3 | 0.8 | 35.9 | 20.6 | 79.4 |
| **4+5+6** | 17.6 | 1.2 | 81.2 | 47.8 | 52.2 |
| **total** | 21 | 1.1 | 77.9 | | |

*Source values for IMM*

| | **Pristine (forest region)** | **Atmospheric deposition** | **Agricultural Land – Manure fertilization** |
|---|---|---|---|
| **$\delta^{15}N$ [‰]** | -3 [2] | 0.4 [3] | 13.9 [4] |
| **$\delta^{18}O$ [‰]** | 2 [2] | 75 [*] | 3.4 [4] |

The GIS data indicate that stations 2 and 3 reflect a transient state with medium anthropogenic impact (Table 2.3). Isotope signatures of 1‰ to 7‰ for $\delta^{15}N_{NO3}$ and 2‰ to 3.5‰ for $\delta^{18}O_{NO3}$ are consistent with values reported for $NO_3^-$ derived from soil organic N (Kendall et al., 2007). Winter data values of $\delta^{15}N_{NO3}$ are ~6‰, and suggest that, in

[2] Mueller, C., Krieg, R., Merz, R., and Knöller, K.: Regional nitrogen dynamics in the TERENO Bode River catchment, Germany, as constrained by stable isotope patterns, Isotopes in environmental and health studies, 2015. 1-14, 2015.

[3] Beyn, F., Matthias, V., and Dähnke, K.: Changes in atmospheric nitrate deposition in Germany – An isotopic perspective, Environmental Pollution, 194, 1-10, 2014. [*] personal communication

[4] Aravena, R., Evans, M., and Cherry, J. A.: Stable isotopes of oxygen and nitrogen in source identification of nitrate from septic systems, Groundwater, 31, 180-186, 1993.

comparison to station 1, anthropogenic discharge, e.g. manure and septic waste, increase in importance. Overall, this is supported by the IMM results where agricultural nitrate increases from 3.8% to 35.9%, but the pristine influence is still dominant (63.3%).

The agricultural part of the river (station 4 to 6) showed an increase in $NO_3^-$ concentration in all seasons. $\delta^{15}N_{NO3}$ values >9‰ indicate a dominance of waste water (Burns et al., 2009), and the $\delta^{18}O_{NO3}$ values fall within a range typical of agricultural sites (2‰ to 5‰), which we attribute to an input of fertilizer and soil- or manure-derived $NO_3^-$ (Aravena et al., 1993; Chang et al., 2002) in addition to waste water inputs. The GIS data indicate an almost equal percentage of agricultural and pristine influences, whereas IMM results showed that anthropogenic sources dominate river nitrate contribution with 81.2%.

Overall, the model agrees with land-use data, but the impact of agriculture at stations 2+3 and stations 4-6 is overestimated and differs by up to 30% from GIS data (Table 2.3). Such a poor agreement of IMM and land use data sets of pristine sources was also found previously in the Baltic sea catchment (Voss et al., 2006). The authors noted that the reliability of GIS data for source attribution was rarely tested and our results confirm this: The IMM output suggest an amount of anthropogenic N that is disproportionate to land-use. An application of the IMM over the whole river (Table 2.3 'total') showed that the $NO_3^-$ concentration of the watershed is mainly influenced by agriculture/manure, with a subordinate role of $NO_3^-$ from pristine sources, while atmospheric deposition only played a minor role. This result and the accompanying isotope values are consistent with data from other rivers that are influenced by agriculture, e.g. the Warnow River (Deutsch et al., 2006), and thus appears more reliable than the GIS based source attribution.

### 2.4.2. **N-turnover in the river**

We investigated nitrate production and consumption in the river to assess the effect of sedimentary processes on DIN concentration – and potentially, isotope composition - in the water column. The balance of nutrients in a river and the proportion of nitrogen retention and elimination can be altered by external factors: It can be enhanced by additional nutrient input, temperature rise or organic matter supply (Bernhardt et al., 2002; Richardson et al., 2004; Zhu and Chen, 2002) which can also be a limiting parameter for heterotrophic denitrification (Christensen et al., 1990; Newcomer et al., 2012).

#### *2.4.2.1.* ***Pristine station***

At the pristine station, nitrate production and consumption rates were low, and do not exceed 4.3 mg N $m^{-2}$ $d^{-1}$. These lower production rates are in a good relation to other studies in forest dominated streams that found rates of 0 to 50 mg N $m^{-2}$ $d^{-1}$ (Bernhardt et al., 2002; Starry et al., 2005) while nitrate consumption seems to be highly variable in pristine areas, and can be as high as to 716 mg N $m^{-2}$ $d^{-1}$ (Bernhardt et al., 2002; Mulholland et al., 2000; Schiller et al., 2009). Our results at the pristine site clearly fall in the lower range of reported values.

In spring, there was no detectable N-turnover in sediment cores, probably due to low temperature (3.7°C) in the water column that impeded biological activity. Turnover rates then increased in summer and autumn, with a shift from dominant production in summer to nitrate consumption in autumn. This is somewhat surprising, because we expected assimilation to be highly active in summer based on higher phytoplankton activity (Basu and Pick, 1997; Wehr and Descy, 1998). However, it seems that nitrate production is more important, which has been found previously in small streams in forested catchments. We assume that nitrate production is fueled by high ammonification providing ample $NH_4^+$ for nitrification (Starry et al., 2005). Apparently, the impact of nutrients provided by soil, like $NH_4^+$ by ammonification, fosters nitrification and thus has a stronger impact on nitrate concentration in this river section during summer seasons than phytoplankton activity.

In autumn, nitrate consumption dominated over production. While we cannot disentangle denitrification and assimilation, we assume that in this case, denitrification dominates and that phytoplankton activity is lower. This is supported by chlorophyll a measurements in an other river in the same area (Bode River - Harz mountains), showing that primary production activity is decreasing at this time of the year (Rode and Kiwel, 2012). Lower primary production in autumn can lower the amount of oxygen that diffuses into the sediment (Mulholland et al., 2008). Denitrification at this time is likely stimulated by an increase of benthic organic carbon sources as an electron donor (Arango et al., 2007; Christensen et al., 1990; Newcomer et al., 2012), stemming from phytoplankton production in summer.

#### *2.4.2.2. **Agricultural station***

Contrary to the pristine river section, nitrate production and consumption rates in the agricultural area were high (up to 123.8 mg N $m^{-2}$ $d^{-1}$), indicating that the additional nutrient input fosters turnover rates (Mulholland et al., 2008). Nevertheless, nitrate consumption was the predominant turnover process in every season, suggesting that nitrate limitation is released and there is ample organic substrate fueling denitrification (Mulholland et al., 2008; Richardson et al., 2004; Schiller et al., 2009). Highest turnover rates of both, production and consumption, in the agricultural area were measured in summer, and were lowest in autumn.

In spring, we found that nitrate consumption at the agricultural site clearly exceeded production. This may be due to higher temperatures (

Table 2.1) promoting microbiological processing, and maybe additional inputs of nitrate and organic material due to the human and animal waste (Newcomer et al., 2012; Zhu and Chen, 2002). This can release the limitation of denitrification by organic matter and nutrient loads and hence, will lead to a rise of consumption rates.

In autumn, nitrate consumption decreases. Equivalent to the pristine section, we expect assimilation to decrease at this time of the year, so that the remaining uptake should mainly be due to denitrification. Mulholland et al. (Mulholland et al., 2008) found that denitrification makes up for a median of 16% of nitrate uptake in general and exceeded 43% of a total uptake in a quarter of their investigated streams. Their dataset was independent of seasons; our seasonal assessment, with a clear drop in nitrate consumption outside the growing season, reflects a shift in the relative role of assimilation vs. denitrification.

In general, both turnover rates were higher at the agricultural than at the pristine station. At the agricultural station, nitrate consumption always dominates production while at the pristine station turnover rates varied seasonally.

### 2.4.3. **The role of nitrification as an internal nitrate source**

Another focal point of our study was the role of nitrate production, i.e. nitrification, along the stream. Nitrate production dominated over consumption at the pristine station in

summer, but gross rates were low in this river section. Based on anthropogenic inputs, we see a rise not only in nitrate consumption, but also in nitrate production, in the agricultural section. The magnitude appeared to be linked to external inputs: Nitrate production was highest in summer, and at this time, we also found high DIN concentrations downstream the WWTP. We assume that high ammonium concentrations in the WWTP are a source for intense nitrification in the river (Bernhardt et al., 2002; Peterson et al., 2001). This additional $NH_4^+$ input is still detectable at the last station of the transect. Therefore, the release of nutrients by WWTP discharge controls nitrate production rates in the agricultural section.

Along with high nitrate concentration in the water column, this additional nitrate can in turn contribute to nitrate consumption, but as our rate measurements suggest that consumption exceeds production by a factor of 4 – 5, such additional nitrate consumption due to coupled nitrification-denitrification appears to be of limited importance. Along the river, our rate and isotope measurements indicate that the nitrate load is mainly affected by diffuse inputs rather than by biological activities. Hence, the supplementary input of anthropogenic derived $NO_3^-$ seemed to be the major contributor to the river N-load. Like organic matter supply, this nitrate may stimulate sedimentary nitrate consumption (e.g. Deek et al., 2012; Marti et al., 2004; Mulholland et al., 2008), but this increase in denitrification does not affect $NO_3^-$ concentration or isotopes in our study. We find that sedimentary nitrate consumption had only a minor influence on water column nitrate concentration and was inefficiently counteracting excess nitrate loads in the agricultural river section (Marti et al., 2004; Mulholland et al., 2008). Even in such a small river, and in cases where we found high sedimentary consumption, effects on water column nitrate were not detectable.

## 2.5. **Conclusions**

As expected, we find that the source of nitrate in this small river changes along the transect. Contrary to our assumptions, there was no visible effect of internal processing on isotope composition in the water column outside the pristine area, except a minor effect of WWTP discharge in summer. The importance of nitrate derived from soil nitrification in forest soils decreases, and the influence of anthropogenic derived $NO_3^-$

gains more weight. The IMM data show that in the pristine river section, nitrate derived from forest soil nitrification acts as a major contributor to riverine nitrate, but this percentage decreases by about 70% downstream with increasing human land use. Furthermore, the IMM results indicate a disproportional contribution of agriculture in comparison to GIS data.

In the pristine area, we find that nitrate production at times exceeds nitrate consumption, whereas a shift towards dominant nitrate consumption at all seasons occurred in the anthropogenically impacted section and exceeded production up to 4-times. A shift towards denitrification occurred in the sediment, independent of seasonal factors. Nevertheless, consumption only inefficiently removed N in the surface water, indicating that filter capacity of the sediment was exhausted. In conclusion, we find that even in a small river, the enhanced consumption rate cannot cope with anthropogenic derived nitrate loads and cannot reduce the potential for eutrophication. Instead, we find that additional anthropogenic DIN inputs not only rising nitrate consumption, but also production rates, which at times had a notable effect on water column nitrate concentration and isotope composition. This increased nitrate input can have additional adverse effects on rivers of higher orders.

# 3. High resolution measurements of nitrous oxide ($N_2O$) in the Elbe estuary

Lisa Brase, Hermann W. Bange, Ralf Lendt, Tina Sanders and Kirstin Dähnke

Published in Frontiers in Marine Science (2017)

## Abstract

Nitrous oxide ($N_2O$) is one of the most important greenhouse gases and a major sink for stratospheric ozone. Estuaries are sites of intense biological production and $N_2O$ emissions. We aimed to identify hot-spots of $N_2O$ production and potential pathways contributing to $N_2O$ concentrations in the surface water of the tidal Elbe estuary. During two research cruises in April and June 2015, surface water $N_2O$ concentrations were measured along the salinity gradient of the Elbe estuary by using a laser-based on-line analyzer coupled to an equilibrator. Based on these high-resolution $N_2O$ profiles, $N_2O$ saturations and fluxes across surface water/atmosphere interface were calculated. Additional measurements of DIN concentrations, oxygen concentration, and salinity were performed. Highest $N_2O$ concentrations were determined in the Hamburg port region reaching maximum values of 32.3 nM in April 2015 and 52.2 nM in June 2015. These results identify the Hamburg port region as a significant hot spot of $N_2O$ production, where linear correlations of AOU-$N_2O_{xs}$ indicate nitrification as an important contributor to $N_2O$ production in the freshwater part. However, in the region with lowest oxygen saturation, sediment denitrification obviously affected water column $N_2O$ saturation. The average N2O saturation over the entire estuary was 201% (SD: ±94%), with an average estuarine N2O flux density of 48 μmol $m^{-2}$ $d^{-1}$ and an overall emission of 0.18 Gg $N_2O$ $y^{-1}$. In comparison to previous studies, our data indicate that N2O production pathways over the whole estuarine freshwater part have changed from predominant denitrification in the 1980s toward significant production from nitrification in the present estuary. Despite a significant reduction in $N_2O$ saturation compared to the 1980s, $N_2O$ concentrations nowadays remain on a high level, comparable to the mid-90s, although a steady decrease of DIN inputs occurred over the last decades. Hence, the Elbe estuary still remains an important source of $N_2O$ to the atmosphere.

## 3.1. Introduction

Nitrous oxide ($N_2O$) is one of the most important atmospheric greenhouse gases (IPCC, 2013) and a major precursor for stratospheric ozone depletion (Crutzen, 1970; WMO, 2014). At present, the global average atmospheric dry mole fraction of $N_2O$ is ~324 ppb, with an annual growth rate of ~0.25% (IPCC, 2013). $N_2O$ is predominantly released via microbial processes, such as nitrification (oxidation of ammonium to nitrate) and denitrification (reduction of nitrate to dinitrogen, $N_2$). Both processes occur in soils, sediments, or water bodies, and release in total ~10 to 12 Tg $N_2O$-N per year (Davidson and Kanter, 2014). During the first step of nitrification (i.e. the oxidation of ammonium to nitrite via hydroxylamine), $N_2O$ can be produced as a side product of hydroxylamine oxidation (Poughon et al., 2001; Ritchie and Nicholas, 1972). During denitrification, $N_2O$ is an obligate intermediate that can be further reduced to $N_2$ (Knowles, 1982).

However, the yield of $N_2O$ production during nitrification and denitrification strongly depends on the prevailing oxygen ($O_2$) concentrations, which is especially relevant in aquatic systems: Hypoxic to anoxic conditions lead to high $N_2O$ production by both nitrification and denitrification, whereas $N_2O$ is consumed by denitrification under anoxic conditions (Bakker et al., 2014). Coastal regions receive inputs of nitrogen (N) that fuel both nitrification and denitrification. Moreover, eutrophication via N inputs also promotes hypoxia or anoxia (Howarth et al., 2011) which, in turn, may lead to additional $N_2O$ production (see e.g. Naqvi et al., 2010). In line with this, estuaries are known to release high amounts of $N_2O$ from nitrification and/or denitrification (e.g. Bange, 2006; Barnes and Upstill-Goddard, 2011; Murray et al., 2015).

The Elbe estuary has undergone a long history of eutrophication and remediation and was highly polluted until the 1990s. Since then, ecological conditions in the Elbe estuary have improved significantly due to a better management of municipal and industrial sewage and an overall reduction of pollution (Adams et al., 2001; Langhammer, 2010). As a consequence, the $O_2$ regime improved and $O_2$ concentrations rarely decrease below 2 mg $L^{-1}$ (62.5 µM), which comes along with a decrease of ammonium and nitrate concentrations in the Elbe (Amann et al., 2012).

In an early study from the late 1980s, Hanke and Knauth (1990) found $N_2O$ saturations of up to 1600% in the Elbe estuary which they attributed mostly to denitrification in the port

region and its sediments. In a follow-up study by the BIOGEST project in the 1990s, $N_2O$ saturations of less than 400% were reported (data from J. Middelburg published in Barnes and Upstill-Goddard, 2011).

Here we present the results of high-resolution measurements of dissolved $N_2O$ along the Elbe estuary in April and June 2015. This study was performed in order (i) to decipher the $N_2O$ distribution and its saturations along the transect and (ii) to identify hot spots of $N_2O$ production and potential $N_2O$ production pathways in the Elbe estuary. Moreover, we compare our results with those of previous studies (iii) to elucidate how management measures that changed the ecological conditions of the Elbe estuary over the past twenty years have affected $N_2O$ pathways and emissions.

## 3.2. Methods

### 3.2.1. Study site

The Elbe River runs from the Czech Republic through Germany and discharges into the German Bight/North Sea. Its catchment area of about 148.300 km² is inhabited by nearly 25 million people (Simon, 2005). The Elbe estuary extends over ~140 km, from a weir at stream km 586 through the Port of Hamburg to the port of Cuxhaven (stream km 730), where the estuary opens into the German Bight. The salinity gradient starts around stream km 670. The estuary is well mixed (Middelburg and Herman, 2007) and with an annual load of 2.9 kt P and 88 kt N (mostly as nitrate), it is the largest nutrient source to the German Bight (ELBE, 2010). From the Port of Hamburg (~ stream km 620) to the German Bight, the estuary has an average water depth of >10 m and ~15 m of the navigational route and it is heavily dredged on a regular basis to ensure access for large container ships to the port (Schöl et al., 2014).

### 3.2.2. Transect sampling

Samples were taken during two research cruises with the research vessel *Ludwig Prandtl* during 28/29 April 2015 and 9-11 June 2015. All sampling and on-line measurements were done during ebb tide to ensure comparable current and mixing conditions. Transects and locations of sampling stations were similar in April and June (Figure 3.1), but sampling started further downstream (stream km 626) in April compared to June (stream

km 609). Distinct samples for nutrient analyses were taken at 16 stations in April 2015 and at 20 stations in June 2015.

The ship's membrane pump continuously pumped water from two meter water depth and supplied a Ferry-Box system (Petersen et al., 2003) and the equilibrator of the $N_2O$ measurement system with a continuous flow rate of 1 L $min^{-1}$. Additionally, discrete samples for nutrient analysis were taken from a separate outlet of the ship's pump. $O_2$ concentration (µM), $O_2$ saturation (%), salinity and temperature (°C) data were recorded with the Ferry-Box system.

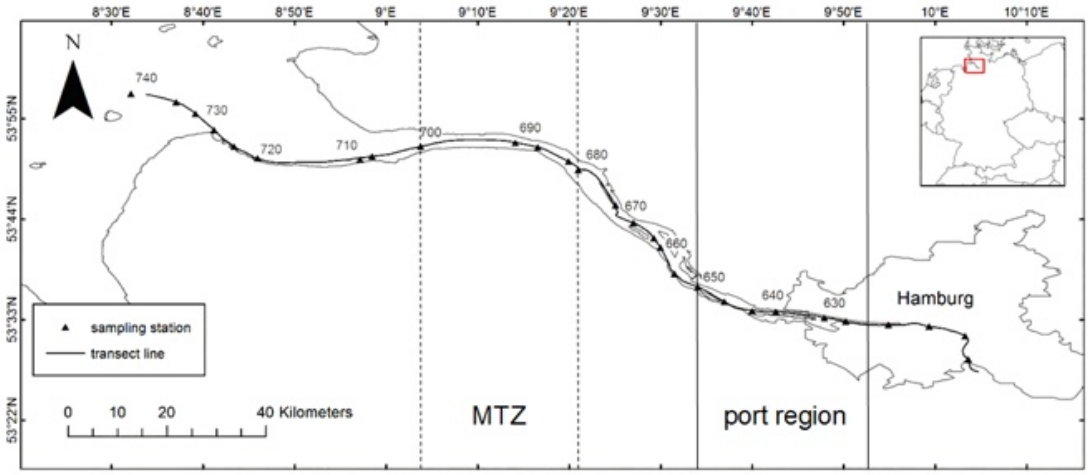


Figure 3.1: The Elbe estuary with river stream km, transect line (black line) and stations for distinct sampling (triangles); MTZ = maximum turbidity zone.

### 3.2.3. **Nutrient measurements**

Water samples for nutrient analyses were filtered immediately (GFF, 0.45 µm), and stored frozen (-18°C) for later analyses in the shore-based laboratory. Dissolved nitrate, nitrite and ammonium concentrations were measured with a continuous flow auto analyzer (AA3, SEAL Analytical) using standard colorimetric techniques (Hansen and Koroleff, 2007).

### 3.2.4. **Equilibrator based $N_2O$ measurements and calculations**

An $N_2O$ analyzer (Model 914-0022, Los Gatos Res. Inc., San Jose, CA, USA) was used to measure gas phase mole fractions of $N_2O$, as well as water vapor ($H_2O$), using off-axis integrated cavity output spectroscopy (OA-ICOS)(Baer et al., 2002).

The $N_2O$ analyzer was connected to a seawater/gas equilibrator which is described in detail by Körtzinger et al. (1996).

Comparable setups show a very good agreement with discrete measurements of dissolved $CH_4$ and $N_2O$ using traditional gas chromatographic system (Arévalo-Martínez et al., 2013; Gülzow et al., 2011) and have been successfully deployed during various campaigns to the Atlantic and Pacific Oceans and the Baltic Sea (Arévalo-Martínez et al., 2015; Arévalo-Martínez et al., 2017; Grefe and Kaiser, 2014; Gülzow et al., 2013).

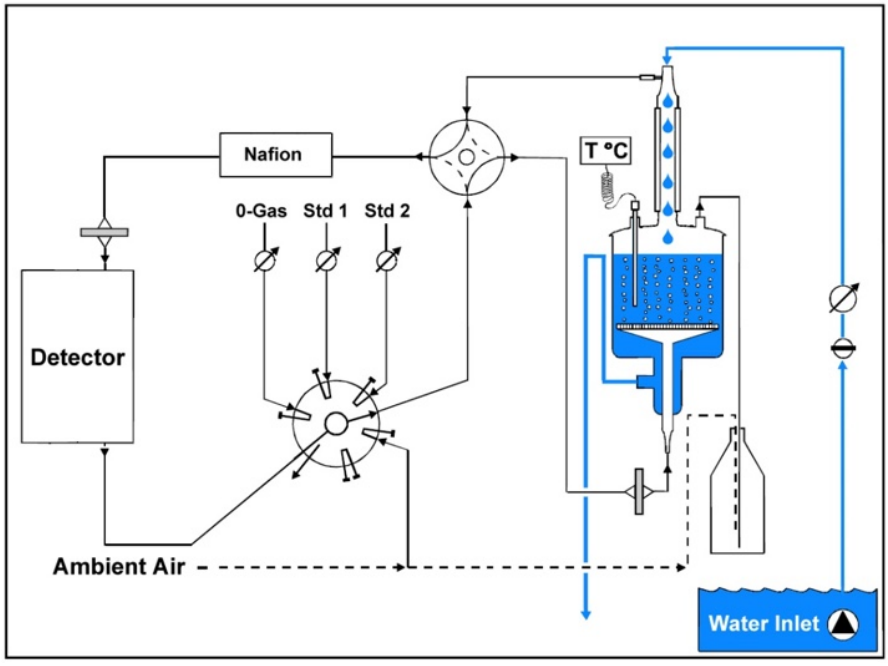


Figure 3.2: Scheme of the $N_2O$ measurement system.

The general principle of dynamic equilibration systems is based on a continuous flow of water passing through an equilibration chamber which is open to the atmosphere. This allows equilibration at ambient pressure at any time of the measurements. The continuous re-circulation of a fixed volume of headspace air ensures a permanent equilibrium with the constantly renewed water phase. For a quick equilibration, water is dripped down along the glass tube of the headspace in combination with a 'shower head and laminary flow' to enlarge the surface sample gas to water ratio (Körtzinger et al., 1996). The gas stream from the headspace was dried in a Nafion® tube embedded in silica gel beads before it reached the inlet of the analyzer (Figure 3.2). The equilibration time of $N_2O$ for

equilibrator applied in our study was determined to 7 minutes (according to Gülzow et al., 2011) and was taken into account for data processing.

The $N_2O$ analyzer covers a $N_2O$ mole fraction range from 300 ppb to 100 ppm. Its internal precision is ± 0.2 ppb for $N_2O$ (1σ, 100 seconds integration time, $N_2O$ >300 ppb). Furthermore, the instrument's software uses the parallel measured water vapor to calculate $N_2O$ dry mole fractions. Laboratory dilution experiments covering a $N_2O$ mole fraction range from 300 ppb to 5 ppm showed an analytical precision of gas phase measurement of $N_2O$ from ± 0.2 ppb (at 300 ppb $N_2O$) to ± 3 ppb (at 5 ppm $N_2O$) which corresponds to an overall precision of ± 0.06-0.07%.

For validation of the $N_2O$ measurements, standard gas mixtures of $N_2O$ in synthetic air (Standard 1: 312.9 ppb $N_2O$ and Standard 9: 573.8 ppb $N_2O$, prepared by Deuste Steininger GmbH, Mühlhausen, Germany) were measured regularly during the campaigns. In addition, a bottle of pressurized air (337 ppb $N_2O$) in the lab was used for on-site calibration of the system. Standard measurements had a precision of 0.5 ppb and an accuracy of 0.9 ppb. During our transect measurements, no drift was detected, and thus, no drift correction was performed.

For further data analyses, we calculated one minute averages of $N_2O$ dry mole fractions (ppb). The dry mole fractions were measured from the recirculating the headspace air of the equilibrator, and $N_2O$ water concentrations ($N_2O_{cw}$) (SD: ± 0.15 nM) were calculated from these, using the Bunsen solubility function of Weiss and Price (1980) and taking into account temperature differences between sample inlet and equilibrator (Rhee et al., 2009). $N_2O$ saturations (s) were calculated as shown in equation (1), based on $N_2O_{cw}$ and atmospheric $N_2O$ ($N_2O_{air}$).

$$s = 100 * \left(\frac{N_2O_{cw}}{N_2O_{air}}\right) \quad (1)$$

Atmospheric $N_2O$ was determined in regular measurements along the two transects. The average atmospheric $N_2O$ dry mole fractions were 331 ppb (SD: ± 0.5 ppb) in April 2015 and 325 ppb (SD: ± 0.8 ppb) in June 2015. The comparably high mean $N_2O$ mole fraction in April was most probably resulting from agricultural activities such as to manure- and N-fertilization (Hellebrand et al., 2008; Lampe et al., 2003): Computations of 48h air mass backward trajectories (data not shown) imply that the measured air masses

originated from the agricultural regions of western Germany, the Netherlands and Belgium.

The gas transfer coefficient (k) (Eq. 2), expressed in m $d^{-1}$, was calculated based on Borges et al. (2004) using the average wind speed at ten meter height above water surface ($u_{10}$ = 7.41 ± 2.26 m $s^{-1}$ in April, $u_{10}$ = 5.05 ± 1.31 m $s^{-1}$ in June) and the Schmidt number (Sc), which is the ratio of the kinematic viscosity of water (Siedler and Peters, 1986) to the diffusivity of $N_2O$ in water (Rhee, 2000). Air-sea flux densities (f in µmol $m^{-2}$ $d^{-1}$) (Eq. 3) were calculated according to Eq. (3):

$$k = 0.24 * (4.045 + 2.58u_{10}) * \left(\frac{Sc}{600}\right)^{-0.5} \quad (2)$$

$$f = k * (N_2O_{cw} - N_2O_{air}) \quad (3)$$

## 3.3. **Results**

### 3.3.1. **Transect measurements**

Based on the $N_2O$ concentration peaks, as well as on the lowest $O_2$ concentrations found between km 620 to 650, we in the following refer to this region of the Elbe estuary as the Hamburg port region. Its upper boundary coincides with the intensely dredged deep water section (>10 m, navigational route: ~15 m) of the Port of Hamburg (Schöl et al., 2014).

#### *3.3.1.1.* ***$N_2O$ and $O_2$ concentrations***

In general, $N_2O$ and $O_2$ concentrations were inversely correlated (Figure 3.3A). $N_2O$ was low in the upstream part of the transect (only sampled in June 2015), rose further downstream and peaked in the Hamburg port region, with maximum values of 32.3 nM and 52.2 nM in April and June, respectively. $N_2O$ concentrations then decreased and remained relatively constant between stream km 650 and 700 with average values of 18.6 ± 0.5 nM in April and 18.2 ± 1.9 nM in June. In the Elbe mouth, the $N_2O$ concentrations decreased with increasing salinity to a final concentration of ~10 nM $N_2O$ in April and June, which is near the equilibrium concentration calculated for dissolved $N_2O$ in water based on the measured $N_2O$ atmospheric mole fractions.

Upstream of the port region, the $O_2$ concentration was high (up to 424 µM) and supersaturated (>140%). The concentrations then decreased to 324 µM and approached saturation when entering the port region. In April 2015, sampling started slightly further downstream, and the $O_2$ saturation at the beginning of the transect was only 72% (230 µM). In the port region, the $O_2$ concentrations decreased to minimum values of 185 µM (April) and 153 µM (June), corresponding to saturations of 58% and 53%, respectively. Downstream of the port region, the $O_2$ concentrations rose again, reaching ~330 – 350 µM in both months in the Elbe mouth, which was equivalent to 100% saturation in April and a slight oversaturation of 5% in June.

#### *3.3.1.2.* ***DIN distribution***

DIN (dissolved inorganic nitrogen, i.e. $NO_3^-$, $NO_2^-$ and $NH_4^+$) concentrations were generally higher in April than in June (Figure 3.3B). $NO_3^-$ concentrations increased from the beginning of each transect up to the MTZ (Maximum Turbidity Zone, located between stream km 680-700), and then decreased with increasing salinity. Maximum concentrations of $NH_4^+$ (19 µM) and $NO_2^-$ (4 µM) were measured in April around stream km 640 in the port region. In June, the peaks were located slightly further upstream at stream km ~630 to ~635 in the port region, and maximum values were 7 µM for $NH_4^+$ and 2 µM for $NO_2^-$. Further downstream, ammonium and nitrite concentration fell below the detection limit (<0.5 µM). In April, a slight increase in ammonium and nitrite concentration (4 and 0.6 µM, respectively) was visible in the mouth of the estuary (stream km 710 – 740).

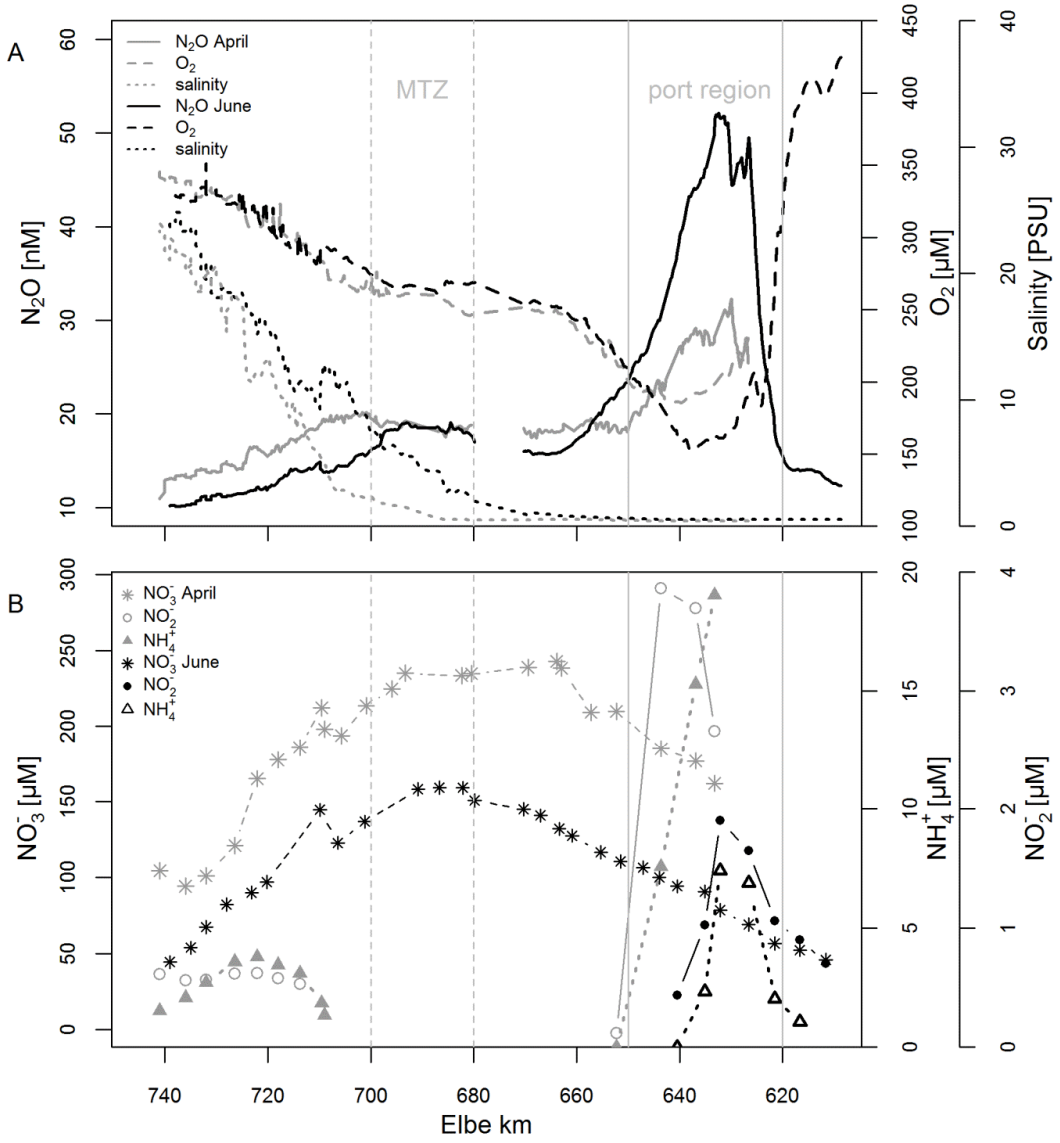


Figure 3.3: Transect measurements in April 2015 and June 2015 from Elbe stream km 609 to 745: (A) continuous measurements of $N_2O$, $O_2$ and salinity, (B) Concentrations of DIN: $NO_3^-$, $NH_4^+$ and $NO_2^-$; vertical lines indicate the Hamburg port region according to Fig. 3.1, the dashed line localized the area of the MTZ.

### 3.3.2. $N_2O$ saturations and emissions to the atmosphere

The $N_2O$ saturations were always highest in the Hamburg port region (Figure 3.4) with median $N_2O$ saturations of 237 ± 32% and 386 ± 105% in April and June, respectively. Downstream, the mean saturations dropped to 155 ± 5% in April and 175 ± 11% in June. Towards the end of the transect, at the onset of the salinity gradient, saturations decreased further and approached equilibrium (i.e. 100%) in the German Bight/North Sea region.

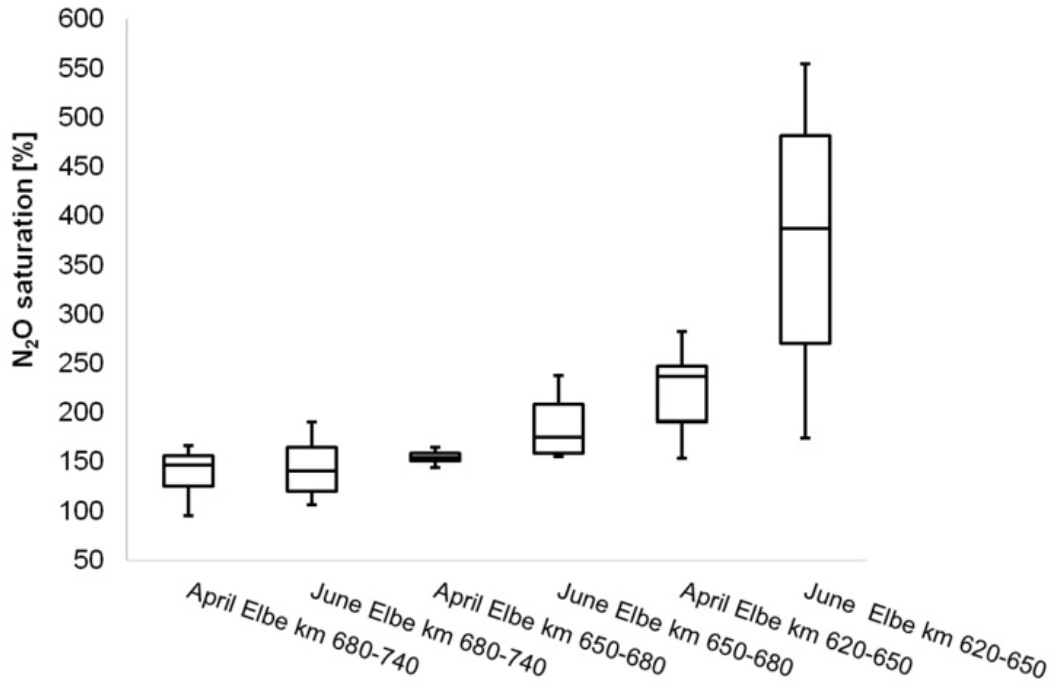


Figure 3.4: $N_2O$ water saturations (%) of different transect parts with according Elbe stream km, including the Hamburg port area (km 620-650), the Elbe river (km 650-680) and beginning of salinity gradient of the Elbe estuary up to the North Sea (km 680-740).

Similar to the $N_2O$ saturations, the $N_2O$ sea-to-air flux densities were highest between stream km 620 and 650, i.e., in the section of the estuary where the port of Hamburg is located (100 µmol $m^{-2}$ $d^{-1}$ and 199.8 µmol $m^{-2}$ $d^{-1}$ in April and June, respectively). To get an integrated picture of $N_2O$ emissions along the estuary, we divided the transect into different sections, the Port region (stream km 620-650), the residual freshwater part (stream km 650-680), beginning of salinity gradient up to the North Sea (stream km 680-740). We then calculated mean fluxes for each section, and, based on the respective

surface area (J. Kappenberg, pers. comm.), calculated the flux for the entire estuary. This calculation yielded an average sea-to-air flux density of 48 ± 41.4 µmol $m^{-2}$ $d^{-1}$, over the entire estuary, which is equivalent to an $N_2O$ emission of 0.18 ± 0.01 Gg $N_2O$ per year.

## 3.4. Discussion

### 3.4.1. $N_2O$ source regions in the estuary

$N_2O$ and DIN concentrations were low upstream of the port, where the water column was oversaturated with respect to $O_2$. In this region of the Elbe, intense phytoplankton growth led to an obvious increase of dissolved oxygen concentration (Amann et al., 2012, 2015; Schöl et al., 2014), and this clearly was also the reason for the observed $O_2$ oversaturations during our sampling campaign in early summer.

Especially in June 2015, the $O_2$ concentrations decreased sharply around stream km 620, where a sudden increase in channel depth marks the beginning of the deep Hamburg port region (Schöl et al., 2014). Due to a reduction of light availability in the port, and an increase of suspended particulate matter, primary production is inhibited in this region (Goosen et al., 1995; Wolfstein and Kies, 1999), and the fresh phytoplankton biomass brought in by the Elbe water is an optimal source for remineralization by heterotrophic bacteria (Kerner, 2000). Enhanced remineralization and decreasing phytoplankton activity leads to increased $O_2$ consumption and a decrease of $O_2$ production, respectively, leading to the observed minimal $O_2$ concentrations in the deep Hamburg port region (Schöl et al., 2014).

Furthermore, these high remineralization rates (Kerner and Spitzy, 2001; Schöl et al., 2014) can contribute to elevated ammonium concentrations (Figure 3.3B). This ammonium is the substrate for ammonia oxidation during the first step of nitrification (Kerner and Spitzy, 2001). Based on stable isotope investigations, Dähnke et al. (2008) concluded that nitrification played an important role in the estuary.

Intriguingly, recent rate measurements revealed that both nitrification and denitrification can occur at high rates in the port region: Deek et al. (2013) found highest denitrification rates in the sediments at stream km ~630, and Sanders et al. (submitted) found highest nitrification rates in the water column in the same section of the estuary. This implies that

both processes can potentially contribute to $N_2O$ production in the region of the Hamburg port where the $O_2$ minimum is most pronounced.

In addition, $N_2O$ production either due to nitrification and/or denitrification is enhanced under lower oxygen conditions (Codispoti et al., 2001; de Bie et al., 2002; e.g. Goreau et al., 1980), also seen in $N_2O$ concentration differences between June and April. Furthermore, an increase of nitrification and denitrification rates and thus $N_2O$ release, are fueled by warmer temperatures (e.g. Gödde and Conrad, 1999; Nowicki, 1994) which were also measured in June (20°C vs. 14°C in April) in the port region.

Beside this obvious hot-spot of $N_2O$ production, we also aimed to evaluate $N_2O$ production in the downstream part of the Elbe estuary. The low concentrations of $NH_4^+$ and $NO_2^-$ measured in April when entering the Elbe mouth may indicate biological N-turnover, but there was no obvious relationship with the $N_2O$ concentrations which decreased steadily. Upstream of the Elbe mouth, between stream km 680 and 700, the MTZ is located, and in many estuaries, this is regarded as a hot-spot of biogeochemical processing (e.g. Barnes and Owens, 1998; Harley et al., 2015; Kerner, 2000) due to intense decomposition of organic matter at rising salinity. This decomposition is often coupled to intense $N_2O$ production (e.g. Barnes and Owens, 1998; Barnes and Upstill-Goddard, 2011; de Wilde and de Bie, 2000). In our study, however, we only see a slight increase of 3 - 6 nM $N_2O$ at the beginning of the salinity gradient in the MTZ. This indicates that the MTZ at the time of our measurements was not a site of enhanced $N_2O$ production.

Thus, in contrast to other European estuaries, we find that the MTZ is only of minor importance with regards to estuarine $N_2O$ emissions, which leaves the Hamburg port region as the most important hot spot of $N_2O$ production in the Elbe estuary.

### 3.4.2. **Assessment of nitrification and of denitrification as $N_2O$ sources**

If we assume that significant $N_2O$ production occurs mainly in the deeper part of the Hamburg port region, this still leaves an open question as to whether this $N_2O$ production is dominated by nitrification (in the water column or in surface sediments) or by sedimentary denitrification.

The ration of nitrate to $N_2O$ can be a useful tool to investigate the origin of $N_2O$. A positive correlation to $NO_3^-$ is usually interpreted as an indication of denitrification (Dong et al., 2004). We find a solid negative correlation of nitrate and $N_2O$ concentration in the estuary freshwater part (April, stream km 633 to 680: $r^2 = 0.77$, $p \ll 0.05$, and June, stream km 626 to 679: $r^2 = 0.84$, $p \ll 0.05$). For nitrification, Harley et al. (2015) once reported a negative correlation to nitrate in an European macrotidal estuary and conclude that this must be due to nutrient distribution of $NO_3^-$. This is presumably also the case in our study area where $NO_3^-$concentration is highest in the MTZ but does not coincide with highest $N_2O$ concentration measured in the port region, and suggests that denitrification is not responsible for most of the $N_2O$ production. Instead this negative correlation points towards nitrification as candidate process.

Thus, to assess the role of nitrification versus denitrification, we investigated the correlation of excess $N_2O$ ($N_2O_{xs}$) and apparent oxygen utilization (AOU). Nitrification consumes oxygen, and a linear correlation of AOU and $N2O_{xs}$ is usually regarded as an indicator for a dominant role of nitrification in $N_2O$ production (e.g. Cohen and Gordon, 1979; Nevison et al., 2003; Walter et al., 2004). $N_2O_{xs}$ was calculated based on the difference between the $N_2O$ concentration in the water ($N_2O_{cw}$) and the theoretical equilibrium concentration ($N_2O_{air}$):

$$N_2O_{xs} = N_2O_{cw} - N_2O_{air} \quad (4)$$

This can be correlated to the apparent oxygen utilization (AOU in µM) defined as Eq. (5),

$$AOU = O_2' - O_2 \quad (5)$$

where $O_2$ is the dissolved $O_2$ measured in the water phase and $O_2'$ is the theoretical equilibrium concentration of the water body with respect to atmospheric $O_2$ concentration (Garcia and Gordon, 1992).

In our study, mixing along the salinity gradient obviously exerts a major control on both AOU and $N_2O_{xs}$, and when mixing is dominant, the correlation of both parameters cannot be used as a proxy for nitrification. Therefore, only parts of the data can be used to investigate the correlation of AOU and $N_2O_{xs}$. All stations with clearly rising salinities are disregarded due to dominant mixing effects, and so are all upstream stations that showed an oversaturation in $O_2$. Hence, only the freshwater part of the Elbe was plotted (stream

km 620, where mean water depth decreases due to dredging (Schöl et al., 2014), up to stream km 670), Figure 3.5.

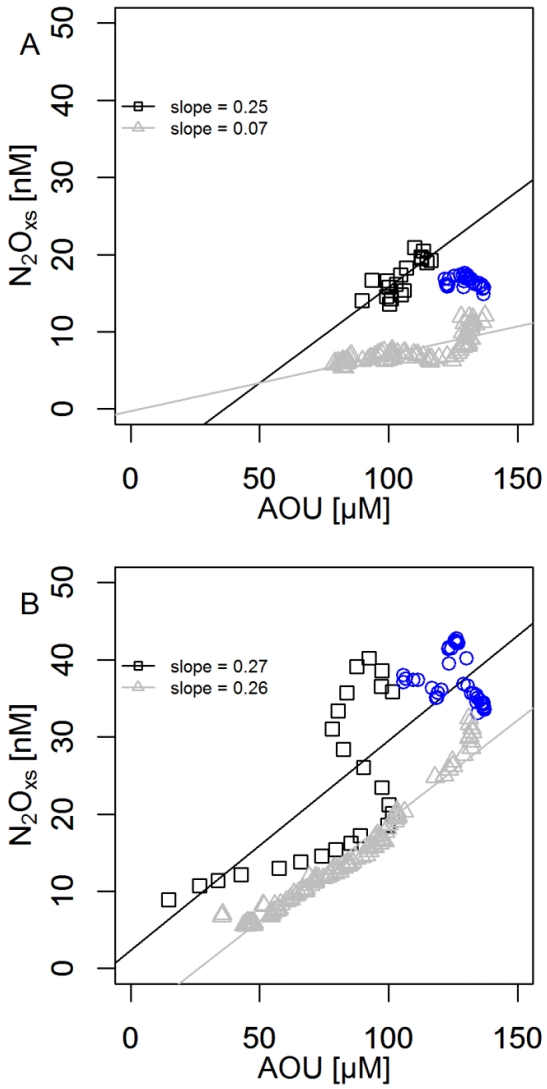


Figure 3.5: Relationship between $N_2O$ excess ($N_2O_{xs}$) and apparent oxygen utilization (AOU) in the Elbe river with according regression slopes in April (A) and June (B). Black □: Elbe river upstream of the region with lowest $O_2$ concentration, grey Δ: Elbe river downstream of the region with lowest $O_2$ concentration region, blue o: within the oxygen minimum.

AOU-$N_2O_{xs}$ cross plots showed a significant linear relationship in most parts of the transect (Figure 3.5), which only breaks down at lowest $O_2$ concentrations, where $N_2O$ production is elevated (blue symbols in Figure 3.5). Such a linear relation is regarded as

an indicator for a dominant role of nitrification in $N_2O$ production (Cohen and Gordon, 1979; Walter et al., 2004). The slope itself generally reflects the biological $N_2O$ yield per mole $O_2$ consumed (Cohen and Gordon, 1979; Najjar, 1992; Suntharalingam and Sarmiento, 2000). As we find a linear correlation throughout most of the transect, we thus conclude that nitrification dominates $N_2O$ production in the Elbe estuary.

Regression slopes were remarkably similar in the upstream part of the river in April and June. Furthermore in June, the slopes, upstream and downstream of the $O_2$ minimum are also comparable. For nitrification, regression slopes of 0.08 to 0.3 nM $N_2O$/µM $O_2$ have been calculated (Suntharalingam and Sarmiento, 2000), in our study, the slopes (0.25 to 0.27) are thus in the high end of this range, reflecting a high relative $N_2O$ yield. In the light of comparatively low $O_2$ concentrations in our study, this is in line with an expected increase of nitrous oxide production with decreasing $O_2$ (Bakker et al. 2014).

We note that the slopes can also be affected by mixing processes (Nevison et al., 2003; Suntharalingam and Sarmiento, 2000), and assume that this is the case in June 2015, where we, despite significant linearity (Figure 3.5B – black symbols, $r^2 = 0.39$, $p \ll 0.05$), see a curved pattern of AOU vs. $N_2O_{xs}$. We assume that this reflects local mixing with water masses from adjacent harbor basins and/or waste water discharge by a neighboring waste water treatment plant (stream km ~630). Nevertheless, nitrification remained as the dominant contributor to dissolved $N_2O$, indicated by significant linear correlations of $N_2O_{xs}$ and AOU throughout much of the measured transect freshwater part (Cohen and Gordon, 1979; Walter et al., 2004).

While we did not perform $N_2O$ measurements in the sediment, at minimum $O_2$ concentrations, we find that the linear correlation of $N_2O_{xs}$ and AOU breaks up (Figure 3.5). Our measured $O_2$ concentration which was measured at 2 m water depth is too high to allow denitrification in the water column. But the linearity break up is accompanied by high AOU values, which indicate high $O_2$ consumption in water masses and/or sediment of the Elbe River, either due to nitrification and/or due to respirational processes (Amann et al., 2015; Schöl et al., 2014). Therefore, we speculate that the resulting hypoxic conditions can favor denitrification as an additional contributor to $N_2O$ in the Elbe estuary and previous studies showed that denitrification in sediments is highly active in this region (Deek et al., 2013; Schroeder et al., 1990). It is thus plausible that also a portion of the $N_2O$ that is produced in the sediment during denitrification escapes to the water

column. In consequence, this would affect linearity of $N_2O_{xs}$/AOU by increasing the relative amount of $N_2O$, which is exactly what we find in our measurements. Hence, we assume that the additional $N_2O_{xs}$ in the oxygen minimum region must be explained by sedimentary denitrification contributing to an elevated concentration of $N_2O$ in the water column.

However, this break-up of linearity only occurred at lowest oxygen concentrations and in a small part of the transect (~ stream km 627/633 to 638/640). Thus, we conclude that sedimentary denitrification is an additional contributor to $N_2O$ concentration in this specific region. Nevertheless, the main portion of $N_2O$ is apparently produced by nitrification in the freshwater estuary.

### 3.4.3. **Trends in $N_2O$ saturation in the estuary and emissions**

In comparison to other European estuaries, $N_2O$ saturation in the Elbe appears to be in the midrange of values reported so far, even if seasonal variability can affect the comparison. The mean $N_2O$ saturation of 201% (SD: ± 94%) in the Elbe is high compared to Tamar, Temmesjoki, Gironde and Tagus estuaries, but relatively low compared to the Schelde and the Humber (UK) estuary (Table 3.1), where nitrification is the main source of $N_2O$ (Barnes and Owens, 1998; de Bie et al., 2002; de Wilde and de Bie, 2000). In addition, de Bie et al. (2002) also speculated that additional $N_2O$ may derive from denitrification, which occurs at high rates in the inner Humber estuary (Barnes and Owens, 1998).

Despite the moderate $N_2O$ saturations in the Elbe estuary, we found very high sea-to-air fluxes which are closer to those measured in the Schelde and the Humber estuary than to other European estuaries. While a major uncertainty derives from estimations of gas transfer velocity, which highly depends on wind, water currents, turbulences, etc. (Abril et al., 2009; Zappa et al., 2003), the average sea-to-air flux density of 48.1 µmol $m^{-2}$ $d^{-1}$ still suggests that the Elbe is a significant source for $N_2O$. The calculated total $N_2O$ emissions of 0.18 Gg $N_2O$ per year are rather comparable to the Gironde (France) (Table 3.1) than to the Humber estuary (0.41 Gg $N_2O$ $y^{-1}$), even though the DIN concentrations in the Elbe are comparable to that of the Humber estuary. Zhang et al. (2010) showed that DIN and $N_2O$ emissions are often correlated, and the Elbe data from our study nicely match the correlation they show.

Table 3.1: Comparison of $N_2O$ saturations, fluxes and emissions from European estuaries.

| **Estuary/Country** | **$N_2O$ saturation [%]** | **$N_2O$ flux [µmol $m^{-2}$ $d^{-1}$]** | **$N_2O$ emissions [Gg $N_2O$ $y^{-1}$]** | **Area [km²]** | Reference |
|---|---|---|---|---|---|
| **Elbe, Germany** | 200.9 | 48.1 | 0.18 | 371.9 | This study |
| Elbe, Germany | 199-1600 | n.a. | n.a. | n.a. | Hanke and Knauth, 1990 |
| Elbe, Germany | 202 | 33.6 | 0.12 | 224 | BIOGEST - Barnes and Upstill-Goddard, 2011 |
| Humber Estuary, UK | 395.7 | 77.5 | 0.41 | 303.6 | Barnes and Upstill-Goddard, 2011 |
| Tamar, UK | 145 | 8.03 | 0.006 | 39.6 | Barnes and Upstill-Goddard, 2011 |
| Schelde, The Netherlands | 710 | 66.2 | 0.28 | 269 | De Bie et al., 2002<br>De Wilde and de Bie, 2000 |
| Temmesjoki, Finland | 136 | 14.7 | 0.09 | 407.6 | Silvennoinen et al., 2008 |
| Gironde, France | 132 | n.a. | 0.18 | 442 | Bange et al., 1996<br>Barnes and Upstill-Goddard, 2011 |
| Tagus, Portugal | 125 | 5.8 | 0.03 | 320 | Gonçalves et al., 2010 |
| | | | | | |
| European estuaries | 327 | 45.7 | 1.35 | 1,840 | Barnes and Upstill-Goddard, 2011 |

Thus, as this correlation holds, and because nutrient loads in the Elbe Estuary have decreased during the last decades, we compared trends in nutrient loads and $N_2O$ concentrations over time. Previous investigations in the 1980s (Hanke and Knauth, 1990) found $N_2O$ saturations from 199% up to 1600%, which were much higher than the saturation range from 139% to 374% reported in the BIOGEST study from the 1990s (Barnes and Upstill-Goddard, 2011). One main reason for the difference between the results of Hanke and Knauth (1990) and later studies including ours probably is the

reduced nutrient load of the Elbe estuary and the increased oxygen concentration (Figure 3.6A). Hanke and Knauth (1990) reported ammonium concentrations of ~15 µM to 110 µM along the whole transect, while in our study ammonium concentrations were below <19 µM. In line with high nutrient loads and low oxygen saturation at that time, Hanke and Knauth (1990) concluded that denitrification was the dominant contributor to $N_2O$ production. The importance of denitrification appears to have ceased in the contemporary Elbe estuary since then (Dähnke et al., 2008), and our data support that this also affects $N_2O$ production: The clear correlation of $N_2O_{xs}$ and AOU rather points towards nitrification as dominant $N_2O$ source.

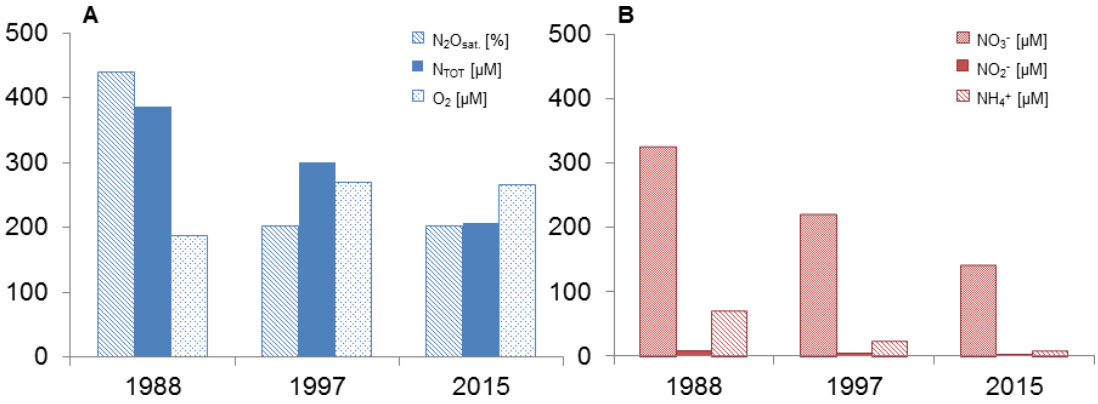


Figure 3.6: Comparison of Elbe transect measurements for the years 1988, 1997 and 2015: (A) average $N_2O$ saturation, and annual average total N and $O_2$ concentrations; (B) Annual average concentrations of dissolved $NO_3^-$, $NO_2^-$ and $NH_4^+$. [5]

Since the study by Hanke and Knauth (1990), the DIN load decreased markedly, and a significant improvement of the environmental condition in the Elbe estuary occurred as a consequence of reduced nutrient inputs (Figure 3.6B). A reduced input of DIN correlates with a reduction in $N_2O$ production (Zhang et al., 2010), and we thus expected to find lower $N_2O$ concentrations than during the BIOGEST study in the 1990s (Figure 3.6). However, in comparison to the BIOGEST data, it is remarkable that $N_2O$ saturations have

[5] Nutrient and $O_2$ data are available at

http://www.elbe-datenportal.de/FisFggElbe/content/start/BesucherUnbekannt.action

obviously not decreased any further some 20 years later, even though a steady decrease of the total nitrogen load occurred over the last decades (Pätsch and Lenhart, 2004; Radach and Pätsch, 2007; see also Fig. 3.6A). It is yet unclear why $N_2O$ saturations remained unchanged at this high level, but it appears plausible that internal N-cycling, i.e. intense nitrification, and denitrification in the port region, may compensate for the reduction in overall nutrient loads.

## 3.5. **Conclusions**

$N_2O$ saturations in the range from 118% to 554% and high sea-to-air fluxes were observed along two transects along the salinity gradient of the Elbe estuary in April and June 2015, indicating that the Elbe estuary was a moderate source of $N_2O$ to the atmosphere. We found highest $N_2O$ concentrations in the Hamburg port area, which was a hot-spot of biological $N_2O$ production with maximum sea-to-air flux densities of 100 µmol $m^{-2}$ $d^{-1}$ and 200 µmol $m^{-2}$ $d^{-1}$ April and June, respectively. Our DIN and $O_2$ measurements suggest that intense remineralization and respiration took place in this area leading to maximum ammonium concentrations, which serves as a substrate for nitrification. Moreover, nitrification was identified to be mainly responsible for $N_2O$ production as indicated by linear correlations of apparent oxygen utilization and $N_2O_{xs}$ throughout much of the transect in the freshwater part. However, we found that the linear correlation of AOU-$N_2O_{xs}$ breaks up at highest $N_2O$ concentrations associated with the lowest measured $O_2$ concentrations, which shows a signal of $N_2O$ production by sedimentary denitrification.

In comparison to previous studies, our data indicate that the main $N_2O$ production pathway with respect over the whole Elbe estuary freshwater part has changed from predominant denitrification in the 1980s to nitrification in the present estuary. Although a significant reduction in $N_2O$ saturations (and its subsequent emissions to the atmosphere) occurred since the 1980s, the Elbe estuary remains as an important source of $N_2O$, especially as nutrient reduction measures do not seem to further reduce $N_2O$ production. Thus, the future development of the Elbe estuary as a greenhouse gas source is unclear, and the seasonality of $N_2O$ production as well as determining factors should be evaluated in future studies.

# 4. Tidal influences on nitrous oxide ($N_2O$) dynamics in the Port of Hamburg (Elbe estuary)

Lisa Brase, Ralf Lendt and Kirstin Dähnke

in preparation for submission

## Abstract

The Port of Hamburg represents one of the most productive $N_2O$ emission sites in the Elbe estuary. Transect measurements reveal strong $N_2O$ emissions in this region, but nothing is reported about $N_2O$ dynamics in this area in a tide controlled context and the potential influence by the surrounding harbor basins. Thus, we aim to identify potential biotic and abiotic factors in dependence of the tides leading to alterations of $N_2O$ dynamics in the surface water, and try to disentangle whether biological $N_2O$ production or allochthonous derived $N_2O$ can be determined as the main source. During two stationary campaigns in May and July 2015, $N_2O$ concentrations were measured by using a laser-based $N_2O$ analyzer coupled to an equilibrator. In both months, on-line measurements were performed over a period of four full tidal cycles. Ancillary measurements of DIN, oxygen and chlorophyll concentrations, and water levels were performed. Based on these high-resolution $N_2O$ concentration signals, $N_2O$ saturations and sea-to-air fluxes were calculated. Highest $N_2O$ concentrations of up to 343 nM were determined with ebb tides, where peaks of ammonium and nitrite indicate high rates of biological $N_2O$ production due to nitrification and denitrification. An enhanced remineralization, a further oxygen decrease and a lower water discharge led to high internal N-turnover rates and thus an increased $N_2O$ concentration, which marks $N_2O$ in-situ production as a main source. In addition, alterations of $N_2O$ concentration due to allochthonous $N_2O$ derived from harbor basins can be demonstrated during flood tides, and under high water level conditions with ebb tides. Average saturations of 330 ± 55% and 1025 ± 753% lead to $N_2O$ flux densities of 68 ± 16 µmol $m^{-2}$ $d^{-1}$ and 573 ± 317 µmol $m^{-2}$ $d^{-1}$, in May and July respectively. Total emissions of 4.5 ± 1.1 Mg $N_2O$ in May and of 37.8 ± 20.9 Mg $N_2O$ in July over a water surface area of 48 m² were derived from this data, marking the Port of Hamburg as a constant net source of $N_2O$ emissions to the atmosphere.

## 4.1. Introduction

Nitrous oxide ($N_2O$) is known as a powerful atmospheric greenhouse gas. Its global warming potential is 298 times higher compared to carbon dioxide ($CO_2$) (Ramaswamy et al., 2001), with an atmospheric average residence time of 114 years (EPA, 2010). Additionally, it is a major contributor to stratospheric ozone destruction (Crutzen, 1970; WMO, 2014). Atmospheric $N_2O$ concentration rises about 0.25% per year, reaching a present global average atmospheric dry mole fraction of ~324 ppb (IPCC, 2013).

Nitrous oxide production is strongly linked to the microbial turnover by nitrifying and denitrifying bacteria. It is produced as a side product during the first step of nitrification, the ammonium oxidation to nitrite ($NH_4^+ \rightarrow NO_2^-$) during oxidation of hydroxylamine ($NH_2OH$) (Poughon et al., 2001; Ritchie and Nicholas, 1972). Also denitrification (stepwise reduction of nitrate to dinitrogen: $NO_3^- \rightarrow N_2$) is known as a $N_2O$ source, where $N_2O$ as an obligate intermediate (Knowles, 1982) is either released or further reduced to $N_2$. Hence, the load of dissolved inorganic nitrogen (DIN) is one of the most important factors affecting nitrogen (N) cycling and thus $N_2O$ formation (e.g. Barnes and Owens, 1998; de Wilde and de Bie, 2000; Dong et al., 2002).

In addition, the yield of $N_2O$ production is highly dependent on the prevailing oxygen ($O_2$) concentration, especially in aquatic systems, where its availability is playing an important key role in intensifying the rate of nitrification and favoring denitrification (e.g. Codispoti et al., 2001; de Bie et al., 2002; Goreau et al., 1980). While $N_2O$ is known to be consumed by denitrification under anoxic conditions, hypoxic to anoxic conditions fuel nitrification and denitrification and lead to high $N_2O$ production (Bakker et al., 2014). Furthermore, additional $N_2O$ production can be caused by eutrophication via N inputs (see e.g. Naqvi et al., 2010) which promotes hypoxia or anoxia (Howarth et al., 2011).

In line with this, estuaries that receive enhanced inputs of N are known as highly active regions for nitrogen turnover processes and thus to release large amounts of $N_2O$ (e.g. Barnes and Upstill-Goddard, 2011; Murray et al., 2015). Former studies in the Elbe estuary reveal the Port of Hamburg as one of the most active regions for nitrogen turnover (e.g. Deek et al., 2013; Deutsch et al., 2009) where large amounts of $N_2O$ release, attributed to $N_2O$ in-situ production, were measured during transect measurements (BIOGEST data published in Barnes and Upstill-Goddard, 2011; Brase et al., 2017;

Hanke and Knauth, 1990). However, additional mixing with allochthonous derived $N_2O$ is likely, especially in regions with strong tides (Leip, 2000) and an often higher input of DIN derived from anthropogenic N-loads upstream (e.g. Ferrón et al., 2007; Murray et al., 2015).

In this context, we investigate $N_2O$ dynamics in the Port of Hamburg in May 2015 and July 2015 by using stationary high resolution measurements. The aim of this study was to investigate potential biotic and abiotic factors affecting $N_2O$ concentration, saturation and subsequently emissions. Furthermore, we wanted to segregate in-situ produced $N_2O$ from allochthonous derived $N_2O$, and determine whether in-situ production or external mixing is the main source of this $N_2O$ productive region.

## 4.2. Material and Methods

### 4.2.1. Study site

The Elbe river is one the major rivers in Central Europe with a total length of 1,094 km. It rises at the Czech Republic near Labská bouda with its flow downstream through Bohemia (Czech Republic), Germany and discharges into the North Sea. Its catchment area is about 148,300 km², inhabited by nearly 25 million people, with a mean annual discharge of 704 $m^3 s^{-1}$ at the last non-tidal gauge Neu Darchau (river-km 536) (Amann et al., 2012).

The Elbe Estuary is well mixed (Middelburg and Herman, 2007) and the largest nutrient source for the German Bight (ELBE, 2010). The inner estuary extends over 140 km, with a tide influenced freshwater part starting from a weir at stream km 586 to a part where strong salt and freshwater mixing occurs (MTZ = maximum turbidity zone). It ends at the port of Cuxhaven (stream km 730) where the estuary opens to the German Bight.

At the entrance into the tidal estuary, 120 km upstream from the Elbe mouth, the Port of Hamburg is located, which is the second busiest port in Europe. Its size is about 73.99 km² with 43.31 km² land area. Although the Port of Hamburg is not located next to the North Sea, still the description as a sea port is correct: This is given by the deepening of the navigational route providing a capacity for vessels with a draught up to 15 m to enter the Port of Hamburg up to stream km 620.

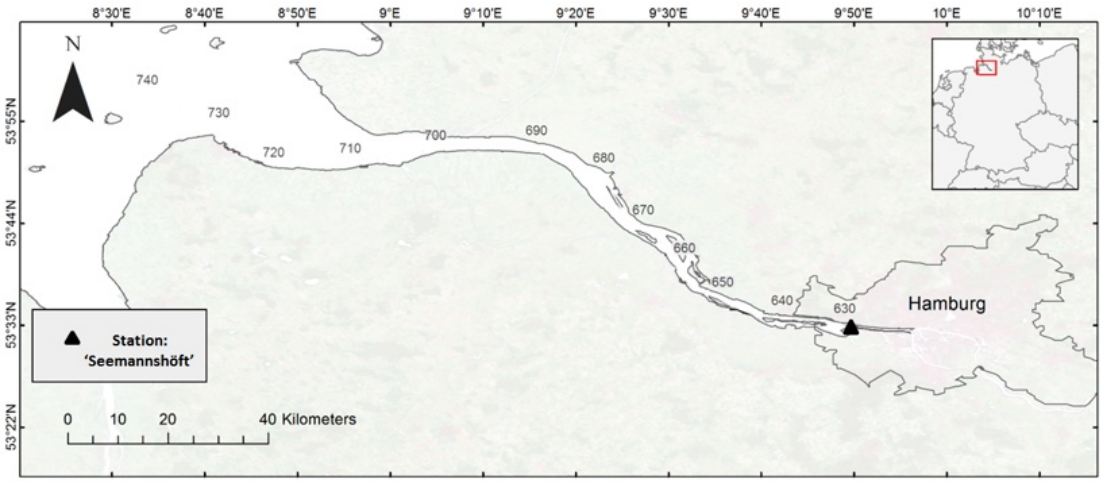


Figure 4.1: Location of the measurement station 'Seemannshöft' in the Elbe estuary

### 4.2.2. **Tidal measurements and sampling**

Samples were taken during two sampling campaigns in May 2015 (5/19 – 5/22) and July 2015 (7/7 - 7/10) with support of the Institute for Hygiene and Environment Hamburg (HU) providing their local research station for long term measurements located in Seemannshöft, at Elbe km 628.9 in the Hamburg Port region. (Figure 4.1)

The research station is supplied with a continuous flow of Elbe water provided by a submerged pump (SCUBA 5, Xylem Water solutions Deutschland GmbH) placed 1 m under the water surface.

Discrete samples for nutrient and isotope measurements were taken with an automatic water sampler (Basic solid SE, ORI Wassertechnik GmbH) every two hours. Water temperature (°C), chlorophyll (µg $l^{-1}$) (FluoroProbe, bbe Moldaenke) and oxygen amount (mg $l^{-1}$) (IQ sensor FDO 700 IQ, WTW) were measured by the HU. The corrected data set is available as download from http://www.hamburg.de/daten/113066/daten.html. The tidal range (water level in cm) and discharge (Neu Darchau, Elbe km 568.97 in $m^3$ $s^{-1}$) were downloaded from

https://www.portaltideelbe.de/Funktionen/Liste_der_vorhandenen_Daten/index.php.html.

A branch connection from the measurement station's pipe line was installed, providing a continuous flow of Elbe water for $N_2O$ measurements.

#### *4.2.2.1.* ***Nutrient measurements***

Water samples for DIN measurements were filtrated immediately (PVDF, 45µm) - or the next morning for overnight samples -, and stored frozen (-18°C) in PE bottles (100ml) for later analysis in the laboratory. Dissolved DIN concentrations (nitrate ($NO_3^-$), nitrite ($NO_2^-$) and ammonium ($NH_4^+$)) were measured with a continuous flow auto analyzer (AA3, SEAL Analytical) using standard colorimetric techniques (Hansen and Koroleff, 2007).

#### *4.2.2.2.* ***Equilibrator based $N_2O$-Measurements and calculations***

An $N_2O$ analyzer (Model 914-0022, Los Gatos Res. Inc., San Jose, CA, USA) was used to measure gas-phase mole fractions of $N_2O$ (ppb) as well as water vapor ($H_2O$, ppm) using off-axis integrated cavity output spectroscopy (OA-ICOS) (Baer et al., 2002).

To obtain an equilibrated gas phase, the analyzer was connected to a glass equilibrator as described by Körtzinger et al. (1996). For a faster equilibration, water is dripped down along the glass tube of the headspace in combination with a 'shower head and laminary flow' to enlarge the surface sample gas to water ratio (Körtzinger, 1995). The gas stream from the headspace was dried in a Nafion® tube embedded in silica gel beads before it reached the inlet of the analyzer. (Figure 4.2)

For drift corrections and validation of the $N_2O$ measurements, standard gas mixtures of $N_2O$ in synthetic air (Standard 1: 312.9 ppb $N_2O$ and Standard 9: 573.8 ppb $N_2O$, prepared by Deuste Steininger GmbH, Mühlhausen, Germany) were measured regularly during the campaigns and a bottle of pressurized air (337 ppb $N_2O$) in the lab was used to check for on-site calibration of the system.

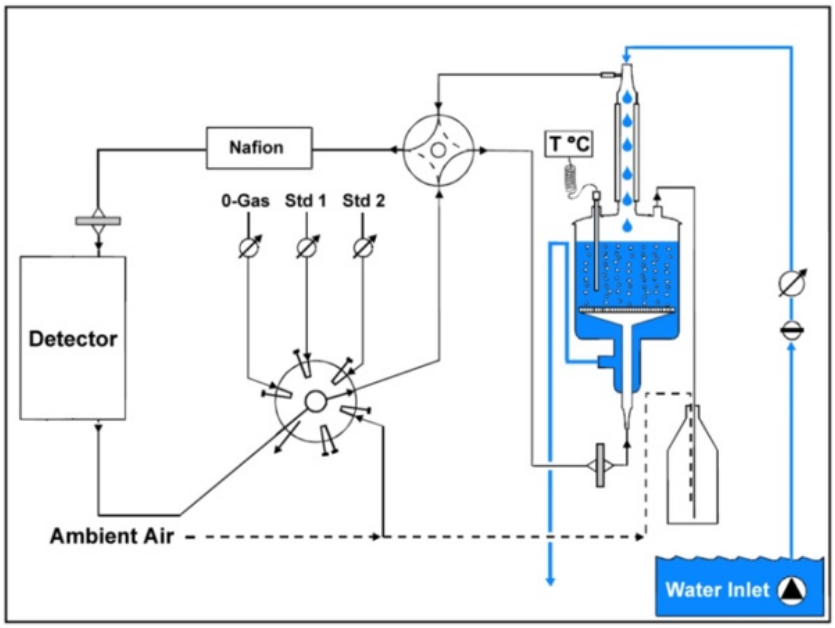


Figure 4.2: Scheme of the $N_2O$ measurement system.

15 minute averages of measured $N_2O$ dry-mole fractions (ppb) were calculated and used for further data analyzes. $N_2O$ water concentrations ($N_2O_{cw}$) (SD May: ± 0.17 nM, SD July: ± 1.85 nM) were calculated from the dry mole fractions measured in the headspace of the equilibrator using the Bunsen solubility function of Weiss and Price (1980), taking into account temperature differences between sample inlet and equilibrator (Rhee et al., 2009). $N_2O$ saturations (s) were calculated as shown in equation (1), based on $N_2O_{cw}$ and atmospheric $N_2O$ ($N_2O_{air}$).

$$s = 100 * \left(\frac{N_2O_{cw}}{N_2O_{air}}\right) \quad (1)$$

Atmospheric $N_2O$ was determined in regular measurements with average atmospheric $N_2O$ dry mole fractions of 333 ppb (SD: ± 0.8 ppb) in May and 343 ppb (SD: ± 5 ppb) in July. The comparably high mean $N_2O$ mole fraction in May was most probably resulting from agricultural activities such as manure- and N-fertilization where the application of fertilizers in April can lead to increased $N_2O$ emissions until mid of June (Hellebrand et al., 2008). Computations of 120h air mass backward trajectories (data not shown) on a smaller scale (new trajectory every 24h) implied that the measured air masses in July originated from turbulences around the city of Hamburg and thus included also the Port of

Hamburg where lots of industrial and vessel emissions can contribute to such high $N_2O$ mole fractions in the atmosphere.

The gas transfer coefficient (k) (Eq. 2), expressed in m $d^{-1}$, was calculated based on Borges et al. (2004) by using the average wind speed at ten meter height above water surface ($u_{10}$ = 3.2 m $s^{-1}$ in May, $u_{10}$ = 6.4 m $s^{-1}$ in July) and the Schmidt number (Sc) which is the ratio of the kinematic viscosity of water (Siedler and Peters, 1986) over the diffusivity of $N_2O$ (Rhee, 2000). Air-sea flux densities (f in µmol $m^{-2}$ $d^{-1}$) (Eq. 3) were calculated according to Eq. (3):

$$k = 0.24 * (4.045 + 2.58u_{10}) * \left(\frac{Sc}{600}\right)^{-0.5} \quad (2)$$

$$f = k * (N_2O_{cw} - N_2O_{air}) \quad (3)$$

## 4.3. **Results**

### 4.3.1. **Tidal dependent $N_2O$ measurements**

#### *4.3.1.1.* ***Oxygen, Chlorophyll and $N_2O$***

We observed a clear increase in $N_2O$ concentration in the surface water with ebb tides in May and July 2015.

In May, $N_2O$ concentrations were highest with low tides in a range of 37 nM to 50 nM, while a minimum $N_2O$ concentration of 28 nM was measured at high tides (Figure 4.3.1a). The average $N_2O$ concentration in May was 37.1 ± 6 nM. Chlorophyll (average 11.7 µg $L^{-1}$) and oxygen concentrations (average 6.7 ± 0.3 mg $L^{-1}$) showed a highly positive significant correlation with $N_2O$ and to each other, following the tides and not a day-night rhythm.

In July (Figure 4.3.2a), the $N_2O$ concentration was significantly higher than in May, but showed a similar pattern with highest $N_2O$ values measured at low tides and vice versa (maximum $N_2O$ concentration: 343.4 nM, minimum: 61.5 nM). The average $N_2O$ amount over all measured cycles was 120.5 ± 61 nM and thus more than three times higher compared to May. The pattern of oxygen and chlorophyll differed clearly in comparison

to May by showing a significant negative correlation of oxygen and $N_2O$ ($r^2 = 0.3$, $p \ll 0.05$). No correlation between $O_2$ and chlorophyll was detectable.

In general, the strong tidal influence on chlorophyll concentration as observed during May disappeared almost completely in July. Mean concentration was lower than two months before (Chlorophyll May: 11.7 µg $L^{-1}$, Chlorophyll July: 8.3 µg $L^{-1}$). Oxygen concentration also decreased from May to July by about ~2.5 mg $L^{-1}$ to a mean value of 4.3 ± 0.7 mg $L^{-1}$.

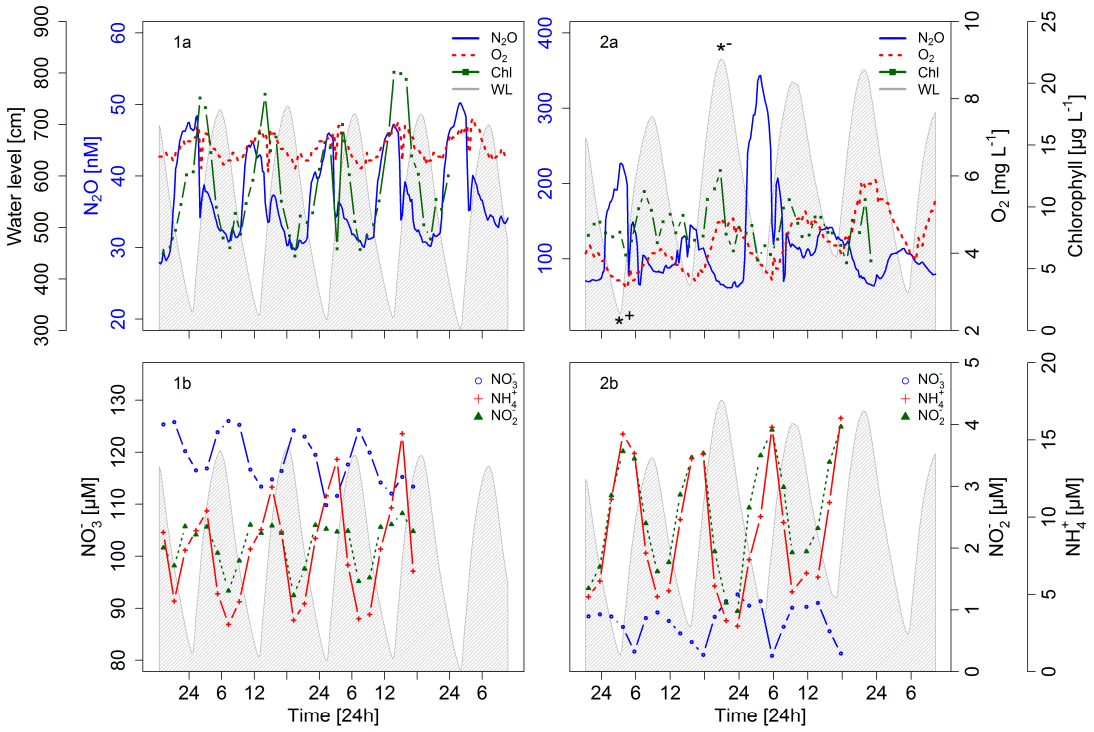


Figure 4.3: Tidal dependent measurements in May (1) and July (2) (water level is indicated by the grey line, the tanned bars mark the ebb tides): (a) $N_2O$, $O_2$ and chlorophyll concentration, (b) dissolved inorganic nutrients: $NO_3^-$ (o), $NH_4^+$ (+), $NO_2^-$ (▲); - in July (2a): lowest water level ($*^+$) and highest water level ($*^-$)

### *4.3.1.2.* ***DIN distribution***

DIN (dissolved inorganic nitrogen, i.e. $NO_3^-$, $NO_2^-$ and $NH_4^+$) concentrations generally showed the same pattern with ebb and flood tides in both months (Figure 4.3.1b, Figure 4.3.2b): Concentrations of ammonium ($NH_4^+$) and nitrite ($NO_2^-$) were highest when the water level reached its minimum while in May the peak of $NO_2^-$ was not as clear as in

July. Nitrate concentration ($NO_3^-$) was lowest during low tides and increased with increasing water level. Mean concentration of $NH_4^+$ and $NO_2^-$ showed only a slight increase of 0.5 µM ($NO_2^-$) and 1 µM ($NH_4^+$) from May to July, accompanied by a significant decrease of nitrate concentration (~30 µM).

### 4.3.2. **Calculated $N_2O$ saturations and sea-to-air fluxes**

In July, water saturations were significantly higher than in May. Water saturations show similar median $N_2O$ saturation values in the respective month with 337% (ebb tides) and 317% (flood tides) in May, and 1160% (ebb tides) and 1131% (flood tides) in July (Figure 4.4).

$N_2O$ saturations did not show differences in maximum saturation values between the tides in May, but saturation value maxima differed extremely between ebb tides and flood tides in July, with a maximum saturation of 3795% during ebb tides.

According to $N_2O$ saturations, mean calculated sea-to-air flux densities differed by ~500 µmol $m^{-2}$ $d^{-1}$ between May (68 ± 16 µmol $m^{-2}$ $d^{-1}$) and July (573 ± 317 µmol $m^{-2}$ $d^{-1}$). Maximum $N_2O$ fluxes were 103 µmol $m^{-2}$ $d^{-1}$ in May and 1726 µmol $m^{-2}$ $d^{-1}$ in July.

Total $N_2O$ emissions from the Hamburg port region, derived from the flux data, were 4.5 ± 1.1 Mg $N_2O$ and 37.8 ± 20.9 Mg $N_2O$ in May and July respectively, calculated over the water surface area at mean water level (~48.35 km²; J. Kappenberg, pers. comm.).

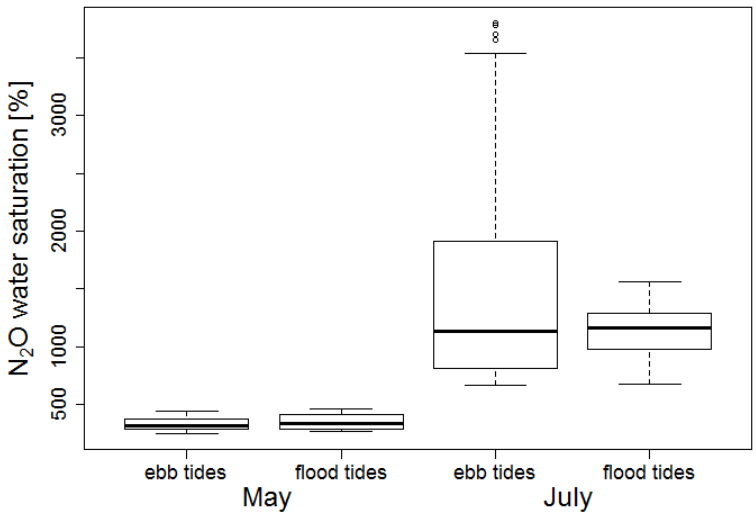


Figure 4.4: Box plot of $N_2O$ water saturation during ebb tides and flood tides between May and July at Elbe km 628.9 (station Seemannshöft)

## 4.4. Discussion

### 4.4.1. The relationship between $N_2O$ and oxygen

#### *4.4.1.1. $N_2O$ vs. $O_2$ during seasons of enhanced phytoplankton growth*

$N_2O$ is known to be closely linked to oxygen concentrations and related processes. A lower $O_2$ content leads to increased nitrification and/or denitrification rates and thus to an increased production of $N_2O$ (e.g. Codispoti et al., 2001; de Bie et al., 2002; Goreau et al., 1980). Under oxic conditions nitrification is the predominant process consuming oxygen and releasing $N_2O$. With decreasing $O_2$ concentrations denitrification as a $N_2O$ source becomes more important. Hence, both processes lead to a negative correlation between $O_2$ and $N_2O$ concentration.

Figure 4.5 shows different relationships between $O_2$ and $N_2O$ concentration during our two campaigns. In May a positive correlation between $N_2O$ and oxygen concentration exists (Figure 4.5.1a). Due to a close positive relationship between $O_2$ and chlorophyll concentration (Figure 4.5.2a), we assume that $O_2$ production from phytoplankton masks the expected $O_2$ consuming processes. As seen in Figure 4.3.1a, the typical day-night-signal of chlorophyll concentration is overlain by the tidal signal in this area. Since there is no evidence for $N_2O$ production during phytoplankton growth (Goreau et al., 1980), the oxygen signal in May obviously reflects $O_2$ produced by phytoplankton upstream from the port. The slightly oxygen enriched water is then transported into the port with ebb tides, which explains the strong correlation between oxygen and chlorophyll in our investigation.

The commonly known anti-correlated relationship between $O_2$ and $N_2O$, as seen during transect measurements in April and June (Brase et al., 2017) is masked during tidal measurements, especially during seasons of enhanced phytoplankton growth. A similar effect of a masked $O_2$ signal by higher photosynthetic rates was reported once before during the warm season, in a mangrove area (Barnes et al., 2006).

In July, the end of the phytoplankton bloom is indicated by lower chlorophyll concentrations and a significant negative correlation between $O_2$ and $N_2O$ concentration (Figure 4.5.1b) occurred.

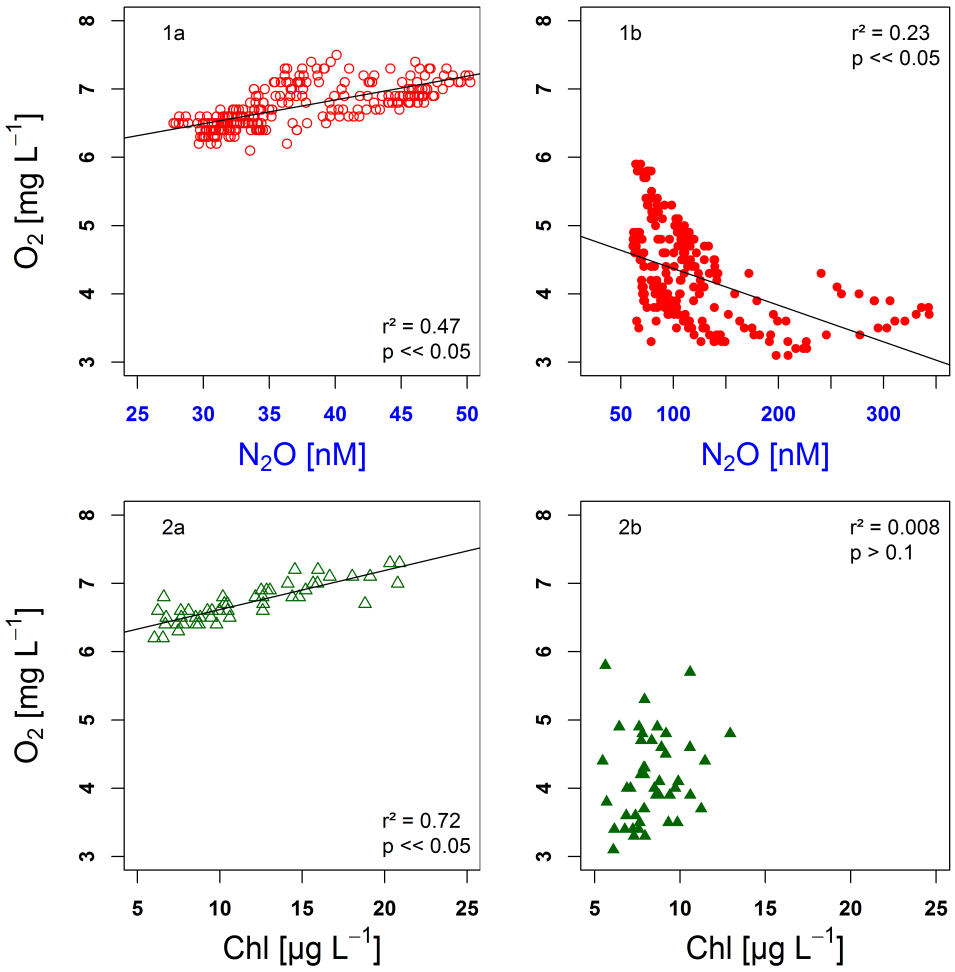


Figure 4.5: $O_2$ concentration vs. (1) $N_2O$ concentration (circle) or (2) chlorophyll concentration (triangle) in (a) May (open symbols) and (b) July (closed symbols) with according regression lines)

#### *4.4.1.2. $N_2O$ vs. $O_2$ and enhanced rates of remineralization*

In contrast to the upstream region, where intense phytoplankton growth elevates dissolved oxygen (Amann et al., 2012, 2015; Schöl et al., 2014), $O_2$ concentration begins to sharply decrease when the river water enters the Hamburg port region at stream km 620 (Schöl et al., 2014). In the deep port region, primary production is then inhibited due to an increase of suspended particulate matter leading to a reduction of light availability (Goosen et al., 1995; Wolfstein and Kies, 1999). Thus, $O_2$ consumption by remineralization of organic matter starts to exceed production (Kerner and Spitzy, 2001; Schöl et al., 2014).

During both months, i.e. May and July, remineralization can be expected in the port region (Amann et al., 2012). In May a significant positive correlation between oxygen and chlorophyll indicates predominant primary production. For July no clear relation between oxygen and chlorophyll (Figure 4.5.2b) was noticed, which might be a hint that remineralization exceeds primary production. This suggestion is in good agreement with the results of Schöl (2012) and Schöl et al. (2014). In July, remineralization is additionally forced by higher water temperatures (15°C in May, 22°C in July) and these enhanced remineralization rates further contribute to minimal oxygen concentrations in the Hamburg port (Schöl et al., 2014).

### 4.4.2. **Internal N-turnover – effects of nitrification and denitrification on $N_2O$**

Aside from the oxygen concentration, $N_2O$ production is highly dependent on ambient DIN concentrations, providing substrate for nitrification and denitrification (e.g. de Wilde and de Bie, 2000; Murray et al., 2015).

High remineralization rates in the port area (Kerner and Spitzy, 2001; Schöl et al., 2014) can contribute to an elevated ammonium concentration (Figure 4.3.1b, Figure 4.3.2b), which is also a substrate for nitrification (Kerner and Spitzy, 2001). Nitrification contributes to $N_2O$ production during oxidation of hydroxylamine ($NH_2OH$) as an intermediate during the conversion of $NH_4^+$ to $NO_2^-$ (Poughon et al., 2001; Ritchie and Nicholas, 1972).

The simultaneous increase in $N_2O$ and $NH_4^+$ concentrations with ebb tides provides evidence for nitrification, resulting in a subsequent production of $N_2O$ in both months (de Wilde and de Bie, 2000), see Figure 4.3. Furthermore, a negative correlation of $NH_4^+$ and $O_2$ concentration is reported as a result of in situ $N_2O$ production during nitrification (Gonçalves et al., 2010). Due to phytoplankton masked $O_2$ pattern this relation is not possible to be determined in May but in July, where a significant negative correlation to $NH_4^+$ was given ($r^2 = 0.53$, $p << 0.05$). Since no $N_2O$ production is expected during nitrite oxidation, a negative correlation (May, Figure 4.6a) to no significant correlation of $N_2O$ and $NO_3^-$ concentration (July, Figure 4.6b) additionally identifies nitrification as an essential $N_2O$ source (Barnes and Upstill-Goddard, 2011; Harley et al., 2015). The negative correlation in this case is presumably an artefact caused by the nutrient distribution in the Elbe estuary, where highest $NO_3^-$ concentration is determined in the

maximum turbidity zone downstream (Dähnke et al., 2008; Schlarbaum et al., 2010). Thus, a $NO_3^-$ concentration increase can be expected with flood tides, bringing downstream water masses enriched in $NO_3^-$ into the Hamburg port.

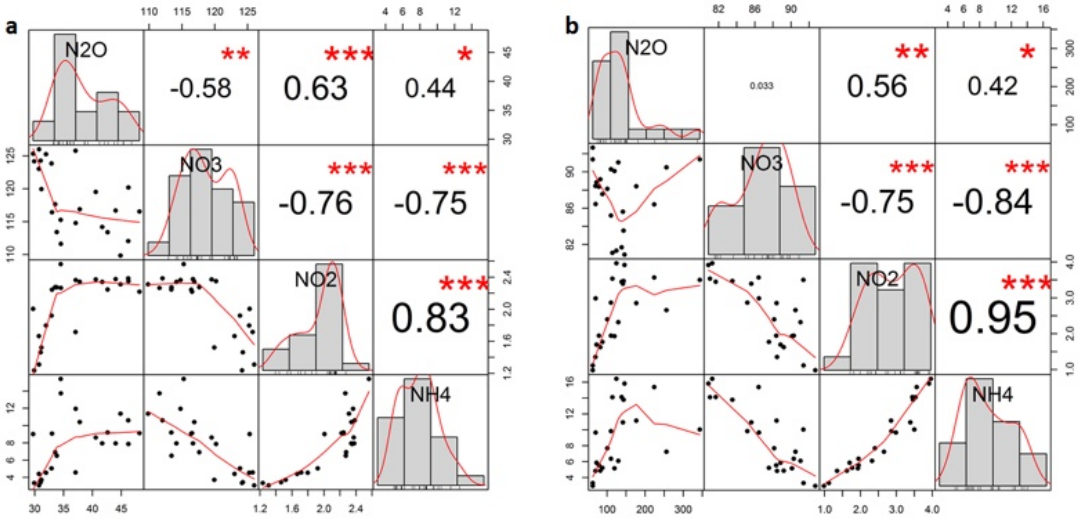


Figure 4.6: Correlation matrixes of (a) May and (b) July; Scales on the sides are given in µM for DIN and for $N_2O$ in nM; The distribution of each variable is shown on the diagonal; On the bottom of the diagonal: the bivariate scatter plots with a fitted line are displayed, and on the top of the diagonal: the value of the correlation plus the significance level as stars where each significance level (p-value) is associated to a symbol (0, '***' 0.001, '**' 0.01, '*' 0.05, '.' 0.1, ' ' 1 )

The interaction of an increased remineralization rate, ammonium increase and the related oxygen decrease may enhance the rate of nitrification and, as a subsequent result, $N_2O$ production, which was reported to be highest during the summer months in other European estuaries (e.g. de Wilde and de Bie, 2000; McElroy et al., 1978).

Besides remineralization, the observed ammonium peaks can also derive from mineralization that is coupled to heterotrophic denitrification where $N_2O$ is an intermediate and can be released during reduction of nitrate ($NO_3^- \rightarrow NO_2^- \rightarrow N_2O$). The $O_2$ amount in this study was measured 1 m beneath the water surface. A higher $O_2$ consumption either due to nitrification and/or due to respirational processes ( Amann et al., 2015; Schöl et al., 2014) can be assumed with increasing water depth, leading to hypoxic and anoxic sites in the sediment, which then provides good conditions for denitrifying bacteria. Due to an increased supply of organic matter, i.e. easily degradable carbon derived from algal detritus, the Elbe estuary becomes heterotrophic in this region

and depleted in oxygen during warmer months (Schöl et al., 2014). Furthermore, the produced $NO_3^-$ from nitrification is likely to diffuse from the water column into the sediment and leads to an additional increase of denitrification (Middelburg et al., 1995).

Recent studies showed highest rates of denitrification in the region of the Port of Hamburg (Deek et al., 2013; Schroeder et al., 1990), and Brase et al. (submitted) conclude that $N_2O$ is significantly increased by denitrification in this area. This suggests denitrification processes within our study which additionally contributes to $N_2O$ release from the sediment into the water column besides nitrification.

A combined influence of nitrification and denitrification is further indicated by a strong correlation of $NO_2^-$ and $N_2O$ concentration in May as well as in July (Figure 4.6), which shows that $N_2O$ production is also significantly driven by $NO_2^-$ concentration (comp. Dong et al., 2004). During both processes, nitrification and denitrification, $NO_2^-$ is an intermediate product. While Gonçalves et al. (2010) determined a positive relation of $N_2O$ to $NO_2^-$ concentration during nitrification, Dong et al. (2002) showed that rates of denitrification were also, and even more stimulated by increasing $NO_2^-$ beside $NO_3^-$ concentration. Thus, the increased $NO_2^-$ concentration can fuel sedimentary denitrification but can also be caused by an increased rate of $NH_4^+$ oxidation.

Especially at the sediment-water interface a relative contribution of coupled nitrification and denitrification of 36% was measured in this area (Deek et al., 2013). This can further contribute to high amounts of $N_2O$ in July, fueled by an increased remineralization rate and a lower oxygen amount compared to May. Direct measurements of $N_2O$ concentrations in the sediments would be a helpful tool to get more information on these processes.

### 4.4.3. **Additional sources influencing $N_2O$ concentration**

#### *4.4.3.1.* ***Water level & discharge***

Water discharge was less in July than in May, which led to a longer water residence time ($238 \pm 21$ m³ s$^{-1}$ vs. $472 \pm 97$ m³ s$^{-1}$ – measurement station: Neu Darchau). Tidal estuaries are known to have high content of suspended organic matter which serves as a substrate for nitrification and can be modified by nitrifying bacteria under long residence time conditions (Gonçalves et al., 2010; Middelburg and Herman, 2007). A longer water

residence time allows an extensive level of remineralization, contributing to a domination of consumption over production and hence to a further $O_2$ decrease (Frankignoulle and Middelburg, 2002). This oxygen decrease in turn will lead to enhanced rates of nitrification and favors denitrification as well (e.g. Codispoti et al., 2001; de Bie et al., 2002; Goreau et al., 1980), which both contribute to higher $N_2O$ concentrations, especially seen in July.

In addition, a very low water level in combination with low water discharge can enhance conditions of remineralization and biological turnover processes in July (see $*^+$ in Figure 4.3.2a). Taking tidal pumping into account, the higher $N_2O$ release during low water level conditions was presumed due to mixing of water column nitrification derived $N_2O$ and $N_2O$ released from the sediment (McElroy et al., 1978). But water level can also be an influencing factor when it exceeds its normal height which was also seen in July: Here, the highest $N_2O$ concentration was measured after a high water level peak (~827 cm, see $*^-$ in Figure 4.3.2a). Due to this preceding exceptionally high water level, the incoming water can have passed a larger area of riparian zones also known as high $N_2O$ productive sites (Groffman et al., 2000). Additionally, an intensified mixing with water from upstream harbor basins can be acquired under this circumstance and both options happen to affect $N_2O$ amount in the main stream.

#### *4.4.3.2.* ***Harbor basins***

As in many other ports, the Port of Hamburg also includes a lot of harbor basins where nutrient concentrations, water currents, depth etc., can differ extremely from those of the Elbe main stream. Due to tidal influences, water exchanges of harbor basin water with the main stream channel is possible, resulting in an alteration of $N_2O$ concentration based on mixing with allochthonous derived $N_2O$.

A clear influence of harbor basin mixing can be seen in May measurements and is attributed to the closely located *Köhlfleethafen* downstream from the research station. As seen in Figure 4.3a, with rising flood tides $N_2O$ and $O_2$ concentrations suddenly drop down and increased quickly again, followed by a continuous decrease up to high tides. These short term concentration changes are most likely to reflect a mixing with water masses derived from the *Köhlfleethafen* when ebb tides and flood tides counteract (Werner Blohm, pers. comm.). Clear $O_2$ peaks like these were not detectable in other

stationary measurements in the Port of Hamburg aside from harbor basins, e.g. in Blankenese[6] (the opposite bank of Seemannshöft). This, in turn, can provide additional evidence of $N_2O$ alteration due to harbor basin water mixing at station Seemannshöft, since peaks of $N_2O$ and $O_2$ concentration appeared simultaneously.

As seen in July, those specific $N_2O$ and $O_2$ concentration peaks did not always appear as clear as in May during our tidal measurements which indicates additional dependency of other influences, e.g. water level and discharge, as discussed before.

### 4.4.4. $N_2O$ water saturations, sea-to-air fluxes and emissions

Saturations significantly differed between May and July (Figure 4.4), but no significant differences can be calculated in $N_2O$ water saturations with flood and ebb tides within the single months. The saturation discrepancy between the months was presumably due to higher bacterial nitrogen turnover activities, enhancing $N_2O$ concentration in the water column during summer, which was also seen in other European estuaries, e.g. the Colne, Schelde or Humber estuary (Barnes and Owens, 1998; de Bie et al., 2002; Dong et al., 2004). Furthermore, the trend to higher $N_2O$ saturations in July with ebb tides coincides with the general assumption of an $N_2O$ increase when the tides dropped due to harbor basins mixing from anthropogenic N-loads upstream (e.g. Ferrón et al., 2007; Murray et al., 2015).

In general, average $N_2O$ saturations of 330 ± 55% spring and 1025 ± 753% in summer, and resulting sea-to-air flux densities of 68 ± 16 µmol $m^{-2}$ $d^{-1}$ and 573 ± 317 µmol $m^{-2}$ $d^{-1}$ (May and July) were extremely high compared to other tidal dependent measurements in estuaries (Barnes et al., 2006; Ferrón et al., 2007; Gonçalves et al., 2010). But those measurements were performed in pristine or low nutrient areas, which is an important factor due to an often demonstrated correlation of DIN to $N_2O$ concentration (Zhang et al., 2010). Unlike those low nutrient estuaries, tidal measurements in the Colne estuary showed comparable saturation values to our measurements (up to a maximum value of 5190% $N_2O$), and also no significant differences of $N_2O$ saturations with ebb and flood tides (Robinson et al., 1998). The Colne estuary is attributed to high $N_2O$ production due

[6] Data available at http://www.hamburg.de/daten/113066/daten.html

to sedimentary denitrification and this contention is supported by the absences of any significant production of $N_2O$ in the water column (Ogilvie et al., 1997; Robinson et al., 1998). In contrast, in the Port of Hamburg, a strong correlation of $N_2O$ concentration with $NH_4^+$ and $NO_2^-$ concentration was demonstrated in our surface water measurements (Figure 4.6), suggesting an influence of both sedimentary denitrification and water column nitrification, contributing to $N_2O$ saturations than either of them dominates.

Furthermore, seasonal variability plays an important key role in $N_2O$ dynamics in estuaries. To set our stationary measurements into a better context for seasonal comparison, data from transect measurements of April and June 2015 (Brase et al., submitted) were taken into account by only considering the Hamburg port region.

As expected, $N_2O$ emissions in the Port of Hamburg showed an increase from the coldest to the warmest month where emission values of April and May were almost similar but differed strongly between June and July (Table 4.1). $N_2O$ fluxes and emissions almost doubled between May and June and were about 5-8 times higher in July. Despite temperature differences which increase $N_2O$ production (e.g. Gödde and Conrad, 1999; Pfenning and McMahon, 1997), also a further decrease in oxygen concentration was seen.

Table 4.1: $N_2O$ sea-to-air fluxes and emissions as well as ancillary measurements ($O_2$, temperature) during spring and summer in the Port of Hamburg)

| Month | $N_2O$ flux [µmol $m^{-2}$ $d^{-1}$] | $N_2O$ emission [Mg per month] (area: 48.35 m²) | Oxygen [mg $L^{-1}$] | Temperature [°C] |
|---|---|---|---|---|
| April* | 66.9 | 4.3 | 6.9 | 14.1 |
| May | 68.1 | 4.5 | 6.7 | 15.3 |
| June* | 123.3 | 7.9 | 5.9 | 18.9 |
| July | 572.8 | 37.8 | 4.3 | 21.9 |
| | *data from transect measurements in the Hamburg port region (Brase et al., submitted) | | | |

While $O_2$ values for April and May were almost similar, a continuous $O_2$ decrease from May to July was determined, which contributes to enhanced biological $N_2O$ production

(Codispoti et al., 2001; de Bie et al., 2002). The measured temperature increase, as well as oxygen decrease, can provide a good explanation for $N_2O$ differences between spring and summer months. Moreover, it is likely that the interplay of oxygen and temperature values reached some borders in July, i.e. conditions for nitrogen turnover were closer to their specific optimum (e.g. de Bie et al., 2002; Gödde and Conrad, 1999; Goreau et al., 1980), and hence resulted in an extreme increase in $N_2O$ concentrations and emissions.

## 4.5. **Conclusions**

Stationary $N_2O$ measurements showed large mean sea-to-air flux densities from $68 \pm 16$ µmol $m^{-2}$ $d^{-1}$ to $573 \pm 317$ µmol $m^{-2}$ $d^{-1}$, calculated over ebb and flood tides in May and July 2015, and identified the Port of Hamburg as a constant net source of $N_2O$ to the atmosphere. Mean $N_2O$ saturations of 330% to 1035% in May and July respectively, indicate independency of the tides, but also showing a trend towards higher saturations in July with ebb tides.

DIN pattern of $NH_4^+$ and $NO_2^-$ concentration indicate internal N-turnover as the dominant source contributing to high values of $N_2O$ measured. $NH_4^+$ can be a substrate for ammonium oxidation to $NO_2^-$, but can also derive from mineralization that is coupled to denitrification, where $NO_2^-$ is an intermediate during nitrate reduction. Due to the strongest correlation found between of $N_2O$ and $NO_2^-$, $NO_2^-$ was identified as the most significant factor which regulates $N_2O$ concentrations. This provides evidence for the influence of nitrification and denitrification on the $N_2O$ concentration in this low oxygen area rather than one of them dominating. The internal $N_2O$ production can be further enhanced by an increase of remineralization and $O_2$ consumption in this area during warmer temperatures, indicated in July by lower chlorophyll concentrations accompanied by an ongoing decrease in $O_2$ concentrations. In addition, a lower water discharge seems to intensify this interplay of remineralization, $O_2$ decrease, N-turnover and thus enhancement of $N_2O$ production.

Despite $N_2O$ in-situ production as the main source, a mixing of allochthonous $N_2O$ from harbor basins upstream and/or riparian zones is likely with ebb tides, especially if the previous water level was unusually high. Furthermore, obvious alterations of $N_2O$ dynamics were observed with flood tides, presumably caused by mixing with allochthonous $N_2O$ derived from a single harbor basin downstream from the research

station. However, it is difficult to disentangle in-situ $N_2O$ production from allochthonous derived $N_2O$ completely. Further investigations are needed for future estimations by taking seasonality and ancillary measurements within the harbor basins into account, which lead to leave the Port of Hamburg as an important $N_2O$ source to the atmosphere.

# 5. Conclusions and Outlook

## 5.1. Conclusions

In this thesis I examined differences in aquatic nitrogen transformations in a small river and the Elbe estuary. Internal nitrogen cycling processes are major contributors to $N_2O$ concentrations in the eutrophic Elbe estuary, especially in the Port of Hamburg, whereas the impact of N-turnover in a small river is mostly exceeded by external nitrogen inputs.

In the small Holtemme River, external derived nitrogen loads lead to a general increase of sediment turnover rates, where nitrate consumption largely exceeds nitrate production, independent of the seasons. Although this general increase in nitrate turnover was detected, internal processing had no visible effect on isotopic composition in the water column with increasing anthropogenic gradient. This was also confirmed by IMM data which demonstrated that nitrate derived from soil nitrification decreases drastically with increasing human land use and is dominated by anthropogenic derived $NO_3^-$. Furthermore, even though enlargement of nitrate consumption rates was determined, N removal in the water column appeared to be inefficient and indicated exhaustion of sediment filter capacity. This means in turn, that enhanced rates of consumption in the sediment cannot reduce potential for eutrophication. Hence, smaller rivers are only inefficient filters for surplus reactive nitrogen and rather contribute to eutrophication in streams of higher orders.

Unlike this small river, it was pointed out that internal nitrogen turnover appears to be the major source for $N_2O$ oversaturations in the water column in the Elbe estuary. Although a continuous nutrient decrease after the German reunion 1989 can be measured, and thus also improvement of $N_2O$ supersaturations, the Elbe estuary still remains an important source of $N_2O$. In particular, this is seen by comparing $N_2O$ mean saturation of ~200% measured in the mid-90s to the present measured saturation values (chapter 3), where no further $N_2O$ decrease could be quantified. Highest saturation values and sea-to-air fluxes during transect measurements were found in the area of the Hamburg port and thus the Hamburg port region was identified as a hot-spot of $N_2O$ production. In this area, intense remineralization and respiration must take place, indicated by a peak of $NH_4^+$ and a massive $O_2$ concentration decrease. A linear correlation of $N_2O_{xs}$ vs. AOU cross-plots identified nitrification as the main $N_2O$ producing pathway throughout much of the

freshwater transect. This predominance of nitrification also indicated a change in the present estuary from predominant denitrification in the late 80s. However, at lowest oxygen values, associated with highest $N_2O$ concentrations in a small part of the Hamburg port region, the linear correlation breaks up and thus still showed a contribution of $N_2O$ production by sedimentary denitrification.

Stationary measurements confirm $N_2O$ production due to internal nitrogen turnover, i.e. biological $N_2O$ production, in this low oxygen region of the Port of Hamburg. Although influences of allochthonous $N_2O$ derived from mixing with surrounding harbor basins and/or riparian zones can be observed, those influences were relevant only as a minor $N_2O$ source or need special abiotic conditions, e.g. unusual high water level, to lead to visible alterations of $N_2O$ dynamics in the main stream of the Elbe estuary. A strong correlation of $N_2O$ to $NH_4^+$ concentration and an even stronger one to $NO_2^-$ concentration, indicate that $N_2O$ production is mostly driven by nutrients providing substrate for nitrification (i.e. $NH_4^+$) and/or stimulating denitrification (i.e. $NO_2^-$). A change from a significant positive correlation of chlorophyll and $O_2$ in May to no significant relationship in July indicated intensification of remineralization, leading to a further oxygen decrease and thus, enhancement of biological $N_2O$ production. This interplay seemed to be fueled by a lower water discharge and additionally raises internal $N_2O$ production by enhancing abiotic conditions for nitrification and denitrification.

## 5.2. **Outlook**

Although this thesis and the conclusion above could provide new insights into aquatic nitrogen cycling associated to DIN inputs - with regards to external nutrient loads, as well as $N_2O$ production, - it also led to a couple of new interesting tasks.

Investigations in a small river showed a significant increase of nitrogen turnover rates in the sediment due to external N-inputs fulling nitrification and denitrification which are also known as main sources of $N_2O$. Former measurements demonstrated there is a large potential of denitrification in the Elbe river and its estuary (e.g. Deek et al., 2013; Deutsch et al., 2009; Fischer et al., 2005) where the relative contribution of coupled nitrification-denitrification was 36% in the Hamburg port region (Deek et al., 2013). This in turn can contribute to large $N_2O$ saturation values and the linearity break up of AOU-

$N_2O_{xs}$ cross plots and nutrient distribution in the Port of Hamburg during surface water measurements, which indicated denitrification as an additional contributor to $N_2O$ concentration. However, no sedimentary measurements were performed and thus closer investigations of $N_2O$ production in the sediment can complete the concluded assumptions of additional $N_2O$ release due to denitrification.

In general, all $N_2O$ investigations in the Elbe estuary and the Port of Hamburg were done in the spring and summer months with an increase in in-situ production with warmer temperatures. As seen in other studies, and hinted by $N_2O$ measurements in July, annual measurements determined seasonal variabilities in $N_2O$ water saturation with very broad ranges where the different investigation areas showed highest values in various seasons (e.g. de Bie et al., 2002; Gonçalves et al., 2010; Silvennoinen et al., 2008). Several studies in the Elbe estuary also demonstrated differences between the seasons regarding nutrient distribution and oxygen regime (e.g. ELBE, 2010; Schöl et al., 2014) which are the main factors influencing nitrogen transformation and thus causing alterations in $N_2O$ production. Therefore, to obtain a complete understanding of $N_2O$ dynamics in the Elbe estuary, it will be necessary to undertake further investigations throughout every season.

## Figure captions

## Table captions

## List of abbreviations and symbols

| | |
|---|---|
| anammox | anaerobic ammonium oxidation |
| AOU | apparent oxygen utilization |
| DIN | dissolved inorganic nitrogen |
| DNRA | dissimilatory nitrate reduction to ammonium |
| GHG | greenhouse gas |
| h | Planck constant ($6.626 \times 10^{-34}$ Js) |
| HNO | nitroxyl |
| IAEA | International Atomic Energy Agency |
| IPCC | Intergovernmental Panel on Climate Change |
| n | number of analyses |
| $N_2$ | dinitrogen |
| $N_2O$ | nitrous oxide |
| $N_2O_2H_2$ | hyponitrous acid |
| $NH_2OH$ | hydroxylamine |
| $NH_3$ | ammonia |
| $NH_4^+$ | ammonium |
| NO | nitric oxide |
| $NO_2^-$ | nitrite |
| $NO_3^-$ | nitrate |
| $NO_x$ | atmospheric NO and NO2 |
| O* | electronically excited oxygen atoms |
| p | level of significance |
| ppb | parts per billion |

| | |
|---|---|
| ppm | parts per million |
| USGS | United States Geological Survey |
| VSMOW | Vienna Standard Mean Ocean Water |
| δ | isotope ratio relative to standard isotope ratio |
| ν | frequency |

## References

Aber, J., McDowell, W., Nadelhoffer, K., Magill, A., Berntson, G., Kamakea, M., McNulty, S., Currie, W., Rustad, L., and Fernandez, I.: Nitrogen saturation in temperate forest ecosystems, BioScience, 48, 921-934, 1998.

Aber, J. D., Nadelhoffer, K. J., Steudler, P., and Melillo, J. M.: Nitrogen saturation in northern forest ecosystems, BioScience, 39, 378-286, 1989.

Abril, G., Commarieu, M.-V., Sottolichio, A., Bretel, P., and Guérin, F.: Turbidity limits gas exchange in a large macrotidal estuary, Estuarine, Coastal and Shelf Science, 83, 342-348, 2009.

Abril, G., Riou, S. A., Etcheber, H., Frankignoulle, M., de Wit, R., and Middelburg, J. J.: Transient, Tidal Time-scale, Nitrogen Transformations in an Estuarine Turbidity Maximum—Fluid Mud System (The Gironde, South-west France), Estuarine, Coastal and Shelf Science, 50, 703-715, 2000.

Adams, M. S., Ballin, U., Gaumert, T., Hale, B. W., Kausch, H., and Kruse, R.: Monitoring selected indicators of ecological change in the Elbe River since the fall of the Iron Curtain, Environmental Conservation, 28, 333-344, 2001.

Amann, T., Weiss, A., and Hartmann, J.: Carbon dynamics in the freshwater part of the Elbe estuary, Germany: Implications of improving water quality, Estuarine, Coastal and Shelf Science, 107, 112-121, 2012.

Amann, T., Weiss, A., and Hartmann, J.: Inorganic Carbon Fluxes in the Inner Elbe Estuary, Germany, Estuaries and Coasts, 38, 192-210, 2015.

Amberger, A. and Schmidt, H.-L.: Natürliche Isotopengehalte von Nitrat als Indikatoren für dessen Herkunft, Geochimica et Cosmochimica Acta, 51, 2699-2705, 1987.

Arango, C. P., Tank, J. L., Schaller, J. L., Royer, T. V., Bernot, M. J., and David, M. B.: Benthic organic carbon influences denitrification in streams with high nitrate concentration, Freshwater Biology, 52, 1210-1222, 2007.

Aravena, R., Evans, M., and Cherry, J. A.: Stable isotopes of oxygen and nitrogen in source identification of nitrate from septic systems, Groundwater, 31, 180-186, 1993.

Arévalo-Martínez, D. L., Beyer, M., Krumbholz, M., Piller, I., Kock, A., Steinhoff, T., Körtzinger, A., and Bange, H. W.: A new method for continuous measurements of oceanic and atmospheric $N_2O$, CO and $CO_2$: performance of off-axis integrated cavity output spectroscopy (OA-ICOS) coupled to non-dispersive infrared detection (NDIR), Ocean Science, 9, 1071-1087, 2013.

Arévalo-Martínez, D. L., Kock, A., Löscher, C., Schmitz, R. A., and Bange, H. W.: Massive nitrous oxide emissions from the tropical South Pacific Ocean, Nature Geoscience, 8, 530-533, 2015.

Arévalo-Martínez, D. L., Kock, A., Steinhoff, T., Brandt, P., Dengler, M., Fischer, T., Körtzinger, A., and Bange, H. W.: Nitrous oxide during the onset of the Atlantic Cold Tongue, Journal of Geophysical Research: Oceans, 122, 171-184, 2017.

Baer, D. S., Paul, J. B., Gupta, M., and O'Keefe, A.: Sensitive absorption measurements in the near-infrared region using off-axis integrated cavity output spectroscopy, 2002, 167-176.

Bakker, D. C., Bange, H. W., Gruber, N., Johannessen, T., Upstill-Goddard, R. C., Borges, A. V., Delille, B., Löscher, C. R., Naqvi, S. W. A., and Omar, A. M.: Air-sea interactions of natural long-lived greenhouse gases ($CO_2$, $N_2O$, $CH_4$) in a changing climate. In: Ocean-Atmosphere Interactions of Gases and Particles, Springer, 2014.

Bange, H. W.: Nitrous oxide and methane in European coastal waters, Estuarine, Coastal and Shelf Science, 70, 361-374, 2006.

Bange, H. W., Rapsomanikis, S., and Andreae, M. O.: Nitrous oxide in coastal waters, Global Biogeochemical Cycles, 10, 197-207, 1996.

Barnes, J. and Owens, N. J. P.: Denitrification and Nitrous Oxide Concentrations in the Humber Estuary, UK, and Adjacent Coastal Zones, Marine Pollution Bulletin, 37, 247-260, 1998.

Barnes, J., Ramesh, R., Purvaja, R., Nirmal Rajkumar, A., Senthil Kumar, B., Krithika, K., Ravichandran, K., Uher, G., and Upstill-Goddard, R.: Tidal dynamics and rainfall control $N_2O$ and $CH_4$ emissions from a pristine mangrove creek, Geophysical Research Letters, 33, 2006.

Barnes, J. and Upstill-Goddard, R.: $N_2O$ seasonal distributions and air-sea exchange in UK estuaries: Implications for the tropospheric $N_2O$ source from European coastal waters, Journal of Geophysical Research: Biogeosciences, 116, 2011.

Basu, B. and Pick, F.: Phytoplankton and zooplankton development in a lowland, temperate river, Journal of Plankton Research, 19, 237-253, 1997.

Bernhardt, E. S., Hall Jr, R. O., and Likens, G. E.: Whole-system estimates of nitrification and nitrate uptake in streams of the Hubbard Brook Experimental Forest, Ecosystems, 5, 419-430, 2002.

Beyn, F., Matthias, V., and Dähnke, K.: Changes in atmospheric nitrate deposition in Germany – An isotopic perspective, Environmental Pollution, 194, 1-10, 2014.

Blackburn, T. H.: Method for measuring rates of $NH_4^+$ turnover in anoxic marine sediments, using a $^{15}N$-$NH_4^+$ dilution technique, Applied and Environmental Microbiology, 37, 760-765, 1979.

Borges, A. V., Vanderborght, J.-P., Schiettecatte, L.-S., Gazeau, F., Ferrón-Smith, S., Delille, B., and Frankignoulle, M.: Variability of the gas transfer velocity of $CO_2$ in a macrotidal estuary (the Scheldt), Estuaries, 27, 593-603, 2004.

Böttcher, J., Strebel, O., Voerkelius, S., and Schmidt, H.-L.: Using isotope fractionation of nitrate-nitrogen and nitrate-oxygen for evaluation of microbial denitrification in a sandy aquifer, Journal of Hydrology, 114, 413-424, 1990.

Brase, L., Bange, H. W., Lendt, R., Sanders, T., and Dähnke, K.: High Resolution Measurements of Nitrous Oxide ($N_2O$) in the Elbe Estuary, Frontiers in Marine Science, 4, 162, 2017.

Brion, N. and Billen, G.: Wastewater as a source of nitrifying bacteria in river systems: the case of the River Seine downstream from Paris, Water Research, 34, 3213-3221, 2000.

Burns, D. A., Boyer, E. W., Elliott, E. M., and Kendall, C.: Sources and transformations of nitrate from streams draining varying land uses: evidence from dual isotope analysis, Journal of Environmental quality, 38, 1149-1159, 2009.

Burns, D. A. and Kendall, C.: Analysis of $\delta^{15}N$ and $\delta^{18}O$ to differentiate $NO_3^-$ sources in runoff at two watersheds in the Catskill Mountains of New York, Water Resources Research, 38, 9-1-9-11, 2002.

Casciotti, K., Sigman, D., Hastings, M. G., Böhlke, J., and Hilkert, A.: Measurement of the oxygen isotopic composition of nitrate in seawater and freshwater using the denitrifier method, Analytical Chemistry, 74, 4905-4912, 2002.

Chang, C. C., Kendall, C., Silva, S. R., Battaglin, W. A., and Campbell, D. H.: Nitrate stable isotopes: tools for determining nitrate sources among different land uses in the Mississippi River Basin, Canadian Journal of Fisheries and Aquatic Sciences, 59, 1874-1885, 2002.

Christensen, P. B., Nielsen, L. P., Sørensen, J., and Revsbech, N. P.: Denitrification in nitrate-rich streams: Diurnal and seasonal variation related to benthic oxygen metabolism, Limnol Oceanogr, 35, 640-651, 1990.

Clark, D. R., Fileman, T. W., and Joint, I.: Determination of ammonium regeneration rates in the oligotrophic ocean by gas chromatography/mass spectrometry, Marine Chemistry, 98, 121-130, 2006.

Codispoti, L., Brandes, J. A., Christensen, J., Devol, A., Naqvi, S., Paerl, H. W., and Yoshinari, T.: The oceanic fixed nitrogen and nitrous oxide budgets: Moving targets as we enter the anthropocene?, Scientia Marina, 65, 85-105, 2001.

Codispoti, L. and Christensen, J.: Nitrification, denitrification and nitrous oxide cycling in the eastern tropical South Pacific Ocean, Marine Chemistry, 16, 277-300, 1985.

Cohen, Y. and Gordon, L. I.: Nitrous oxide production in the ocean, Journal of Geophysical Research: Oceans, 84, 347-353, 1979.

Coplen, T.: Reference and Intercomparison Materials for Stable Isotopes of Light Elements, IAEA-TECDOC-825, International Atomic Energy Agency: Vienna, 1995.

Cowan, J., Pennock, J., and Boynton, W. R.: Seasonal and interannual patterns of sediment-water nutrient and oxygen fluxes in Mobile Bay, Alabama (USA): regulating factors and ecological significance, Marine Ecology Progress Series, 141, 229-245, 1996.

Crowe, S. A., Canfield, D. E., Mucci, A., Sundby, B., and Maranger, R.: Anammox, denitrification and fixed-nitrogen removal in sediments from the Lower St. Lawrence Estuary, Biogeosciences, 9, 4309, 2012.

Crutzen, P. J.: The influence of nitrogen oxides on the atmospheric ozone content, Quarterly Journal of the Royal Meteorological Society, 96, 320-325, 1970.

Dähnke, K., Bahlmann, E., and Emeis, K.: A nitrate sink in estuaries? An assessment by means of stable nitrate isotopes in the Elbe estuary, Limnol Oceanogr, 53, 1504-1511, 2008.

David, M. B. and Gentry, L. E.: Anthropogenic inputs of nitrogen and phosphorus and riverine export for Illinois, USA, Journal of Environmental Quality, 29, 494-508, 2000.

Davidson, E. A. and Kanter, D.: Inventories and scenarios of nitrous oxide emissions, Environmental Research Letters, 9, 105012, 2014.

de Bie, M. J., Middelburg, J. J., Starink, M., and Laanbroek, H. J.: Factors controlling nitrous oxide at the microbial community and estuarine scale, Marine Ecology Progress Series, 240, 1-9, 2002.

de Wilde, H. P. J. and de Bie, M. J. M.: Nitrous oxide in the Schelde estuary: production by nitrification and emission to the atmosphere, Marine Chemistry, 69, 203-216, 2000.

Deek, A., Dähnke, K., van Beusekom, J., Meyer, S., Voss, M., and Emeis, K.: $N_2$ fluxes in sediments of the Elbe Estuary and adjacent coastal zones, Marine Ecology Progress Series, 493, 9-21, 2013.

Deek, A., Emeis, K., and van Beusekom, J.: Nitrogen removal in coastal sediments of the German Wadden Sea, Biogeochemistry, 108, 467-483, 2012.

Deutsch, B., Mewes, M., Liskow, I., and Voss, M.: Quantification of diffuse nitrate inputs into a small river system using stable isotopes of oxygen and nitrogen in nitrate, Organic Geochemistry, 37, 1333-1342, 2006.

Deutsch, B., Voss, M., and Fischer, H.: Nitrogen transformation processes in the Elbe River: distinguishing between assimilation and denitrification by means of stable isotope ratios in nitrate, Aquatic sciences, 71, 228-237, 2009.

Dong, L. F., Nedwell, D., Colbeck, I., and Finch, J.: Nitrous oxide emission from some English and Welsh rivers and estuaries, Water, Air, & Soil Pollution: Focus, 4, 127-134, 2004.

Dong, L. F., Nedwell, D. B., Underwood, G. J., Thornton, D. C., and Rusmana, I.: Nitrous oxide formation in the Colne estuary, England: the central role of nitrite, Applied and Environmental Microbiology, 68, 1240-1249, 2002.

Döring, J.: Zu den Klimaverhältnissen im östlichen Harzvorland, Hercynia-Ökologie und Umwelt in Mitteleuropa, 37, 137-154, 2004.

Durka, W., Schulze, E.-D., Gebauer, G., and Voerkeliust, S.: Effects of forest decline on uptake and leaching of deposited nitrate determined from $^{15}N$ and $^{18}O$ measurements, Nature, 372, 765-767, 1994.

ELBE, F.: Elbebericht 2008–Ergebnisse des nationalen Überwachungsprogramms Elbe der Bundeländer über den ökologischen und chemischen Zustand der Elbe nach EG-WRRL sowie der Trendentwicklung von Stoffen und Stoffgruppen, Gemeinsamer Bericht der Bundesländer und der Bundesrepublik Deutschland. Hamburg, 2010. 2010.

Elkins, J. W., Wofsy, S. C., McElroy, M. B., Kolb, C. E., and Kaplan, W. A.: Aquatic sources and sinks for nitrous oxide, Nature, 275, 602-606, 1978.

EPA, A.: Methane and Nitrous Oxide Emissions from Natural Sources. US Environmental Protection Agency Washington, DC, USA, 2010.

Ferrón, S., Ortega, T., Gómez-Parra, A., and Forja, J. M.: Seasonal study of dissolved $CH_4$, $CO_2$ and $N_2O$ in a shallow tidal system of the bay of Cádiz (SW Spain), Journal of Marine Systems, 66, 244-257, 2007.

Fischer, H., Kloep, F., Wilzcek, S., and Pusch, M.: A River's Liver – Microbial Processes within the Hyporheic Zone of a Large Lowland River, Biogeochemistry, 76, 349-371, 2005.

Francis, C. A., Beman, J. M., and Kuypers, M. M.: New processes and players in the nitrogen cycle: the microbial ecology of anaerobic and archaeal ammonia oxidation, The ISME journal, 1, 19-27, 2007.

Frankignoulle, M. and Middelburg, J. J.: Biogases in tidal European estuaries: the BIOGEST project, Biogeochemistry, 59, 1-4, 2002.

Garcia, H. E. and Gordon, L. I.: Oxygen solubility in seawater: Better fitting equations, Limnol Oceanogr, 37, 1307-1312, 1992.

Garnier, J., Cébron, A., Tallec, G., Billen, G., Sebilo, M., and Martinez, A.: Nitrogen Behaviour and Nitrous Oxide Emission in the Tidal Seine River Estuary (France) as Influenced by Human Activities in the Upstream Watershed, Biogeochemistry, 77, 305-326, 2006.

Gödde, M. and Conrad, R.: Immediate and adaptational temperature effects on nitric oxide production and nitrous oxide release from nitrification and denitrification in two soils, Biology and Fertility of Soils, 30, 33-40, 1999.

Gonçalves, C., Brogueira, M. J., and Camões, M. F.: Seasonal and tidal influence on the variability of nitrous oxide in the Tagus estuary, Portugal, Scientia Marina, 74, 57-66, 2010.

Gonfiantini, R., Stichler, W., and Rozanski, K.: Standards and intercomparison materials distributed by the International Atomic Energy Agency for stable isotope measurements, 1995. 1995.

Goosen, N. K., van Rijswijk, P., and Brockmann, U.: Comparison of heterotrophic bacterial production rates in early spring in the turbid estuaries of the Scheldt and the Elbe, Hydrobiologia, 311, 31-42, 1995.

Goreau, T. J., Kaplan, W. A., Wofsy, S. C., McElroy, M. B., Valois, F. W., and Watson, S. W.: Production of $NO_2^-$ and $N_2O$ by nitrifying bacteria at reduced concentrations of oxygen, Applied and Environmental Microbiology, 40, 526-532, 1980.

Granger, J., Sigman, D. M., Needoba, J. A., and Harrison, P. J.: Coupled nitrogen and oxygen isotope fractionation of nitrate during assimilation by cultures of marine phytoplankton, Limnol Oceanogr, 49, 1763-1773, 2004.

Grefe, I. and Kaiser, J.: Equilibrator-based measurements of dissolved nitrous oxide in the surface ocean using an integrated cavity output laser absorption spectrometer, Ocean Sci., 10, 501-512, 2014.

Groffman, P. M., Gold, A. J., and Addy, K.: Nitrous oxide production in riparian zones and its importance to national emission inventories, Chemosphere-Global change science, 2, 291-299, 2000.

Gülzow, W., Rehder, G., Deimling, J. S. v., Seifert, T., and Tóth, Z.: One year of continuous measurements constraining methane emissions from the Baltic Sea to the atmosphere using a ship of opportunity, Biogeosciences, 10, 81, 2013.

Gülzow, W., Rehder, G., Schneider, B., Deimling, J. S. v., and Sadkowiak, B.: A new method for continuous measurement of methane and carbon dioxide in surface waters using off-axis integrated cavity output spectroscopy (ICOS): An example from the Baltic Sea, Limnology and Oceanography: Methods, 9, 176-184, 2011.

Hanke, V.-R. and Knauth, H.-D.: $N_2O$-Gehalte in Wasser- und Luftproben aus den Bereichen der Tideelbe und der Deutschen Bucht, Vom Wasser, 75, 357-374, 1990.

Hansen, H. P. and Koroleff, F.: Determination of nutrients, Methods of Seawater Analysis, Third Edition, 2007. 159-228, 2007.

Harley, J. F., Carvalho, L., Dudley, B., Heal, K. V., Rees, R. M., and Skiba, U.: Spatial and seasonal fluxes of the greenhouse gases $N_2O$, $CO_2$ and $CH_4$ in a UK macrotidal estuary, Estuarine, Coastal and Shelf Science, 153, 62-73, 2015.

Hastings, M. G., Steig, E., and Sigman, D.: Seasonal variations in N and O isotopes of nitrate in snow at Summit, Greenland: Implications for the study of nitrate in snow and ice cores, Journal of Geophysical Research: Atmospheres (1984–2012), 109, 2004.

Hellebrand, H. J., Scholz, V., and Kern, J.: Fertiliser induced nitrous oxide emissions during energy crop cultivation on loamy sand soils, Atmospheric Environment, 42, 8403-8411, 2008.

Hirsch, A., Michalak, A., Bruhwiler, L., Peters, W., Dlugokencky, E., and Tans, P.: Inverse modeling estimates of the global nitrous oxide surface flux from 1998–2001, Global Biogeochemical Cycles, 20, 2006.

Howarth, R., Chan, F., Conley, D. J., Garnier, J., Doney, S. C., Marino, R., and Billen, G.: Coupled biogeochemical cycles: eutrophication and hypoxia in temperate estuaries

and coastal marine ecosystems, Frontiers in Ecology and the Environment, 9, 18-26, 2011.

IPCC: Climate Change 2013: The Physical Science Basis. Contribution of Working Group I to the Fifth Assessment Report of the Intergovernmental Panel on Climate Change, Cambridge University Press, Cambridge, United Kingdom and New York, NY, USA, 2013.

Itokawa, H., Hanaki, K., and Matsuo, T.: Nitrous oxide production in high-loading biological nitrogen removal process under low COD/N ratio condition, Water Research, 35, 657-664, 2001.

Jenkins, M. C. and Kemp, W. M.: The coupling of nitrification and denitrification in two estuarine sediments, Limnol Oceanogr, 29, 609-619, 1984.

Johannsen, A., Dähnke, K., and Emeis, K.: Isotopic composition of nitrate in five German rivers discharging into the North Sea, Organic Geochemistry, 39, 1678-1689, 2008.

Kendall, C.: Tracing nitrogen sources and cycling in catchments. W: Isotope tracers in catchment hydrology (red. C. Kendall, JJ McDonnell). Elsevier, Amsterdam, 1998.

Kendall, C., Elliott, E. M., and Wankel, S. D.: Tracing anthropogenic inputs of nitrogen to ecosystems, Stable isotopes in ecology and environmental science, 2, 375-449, 2007.

Kerner, M.: Interactions between local oxygen deficiencies and heterotrophic microbial processes in the Elbe estuary, Limnologica-Ecology and Management of Inland Waters, 30, 137-143, 2000.

Kerner, M. and Spitzy, A.: Nitrate regeneration coupled to degradation of different size fractions of DON by the picoplankton in the Elbe Estuary, Microbial ecology, 41, 69-81, 2001.

Kieskamp, W. M., Lohse, L., Epping, E., and Helder, W.: Seasonal variation in denitrification rates and nitrous oxide fluxes in intertidal sediments of the western Wadden Sea, Marine ecology progress series. Oldendorf, 72, 145-151, 1991.

Kirchman, D.: The uptake of inorganic nutrients by heterotrophic bacteria, Microbial Ecology, 28, 255-271, 1994.

Knowles, R.: Denitrification, Microbiological reviews, 46, 43, 1982.

Koike, I. and Hattori, A.: Simultaneous determinations of nitrification and nitrate reduction in coastal sediments by a $^{15}N$ dilution technique, Applied and Environmental Microbiology, 35, 853-857, 1978.

Kornexl, B. E., Gehre, M., Hofling, R., and Werner, R. A.: On-line $\delta^{18}O$ measurement of organic and inorganic substances, Rapid Communications in Mass Spectrometry, 13, 1685-1693, 1999.

Körtzinger, A.: Anthropogenes $CO_2$ im Nordatlantik-Methodische Entwicklungen und Messungen zur Quantifizierung des anthropogenen $CO_2$-Signals, 1995. 1995.

Körtzinger, A., Thomas, H., Schneider, B., Gronau, N., Mintrop, L., and Duinker, J. C.: At-sea intercomparison of two newly designed underway $pCO_2$ systems — encouraging results, Marine Chemistry, 52, 133-145, 1996.

Kroeze, C., Bouwman, L., and Slomp, C. P.: Sinks for Nitrous Oxide at the Earth's Surface, Greenhouse gas sinks, 2007. 227, 2007.

Lampe, C., Dittert, K., Sattelmacher, B., Wachendorf, M., Butterbach-Bahl, K., Papen, H., Gasche, R., and Taube, F.: Einfluss der N-Düngung auf die $N_2O$-Emissionen auf Grünland, Die 10.000 kg-Herde auf dem Grünland, 2003. 36-42, 2003.

Langhammer, J.: Water quality changes in the Elbe River basin, Czech Republic, in the context of the post-socialist economic transition, GeoJournal, 75, 185-198, 2010.

Law, C., Rees, A., and Owens, N.: Nitrous oxide: estuarine sources and atmospheric flux, Estuarine, Coastal and Shelf Science, 35, 301-314, 1992.

Laws, E.: Isotope-Dilution Models and the Mystery of the Vanishing $^{15}N$, Limnol Oceanogr, 29, 379-386, 1984.

Leip, A.: Nitrous Oxide ($N_2O$) Emissions from a Coastal Catchment in the Delta of the Po River: Measurement and Modelling of Fluxes from a Mediterranean Lagoon and Agricultural Soils, Office for Official Publ. of the Europ. Communities, 2000.

Lu, H. and Chandran, K.: Factors promoting emissions of nitrous oxide and nitric oxide from denitrifying sequencing batch reactors operated with methanol and ethanol as electron donors, Biotechnology and bioengineering, 106, 390-398, 2010.

Marti, E., Aumatell, J., Godé, L., Poch, M., and Sabater, F.: Nutrient retention efficiency in streams receiving inputs from wastewater treatment plants, Journal of Environmental Quality, 33, 285-293, 2004.

Mayer, B., Bollwerk, S. M., Mansfeldt, T., Hütter, B., and Veizer, J.: The oxygen isotope composition of nitrate generated by nitrification in acid forest floors, Geochimica et Cosmochimica Acta, 65, 2743-2756, 2001.

Mayer, B., Boyer, E. W., Goodale, C., Jaworski, N. A., Van Breemen, N., Howarth, R. W., Seitzinger, S., Billen, G., Lajtha, K., and Nadelhoffer, K.: Sources of nitrate in rivers draining sixteen watersheds in the northeastern US: Isotopic constraints, Biogeochemistry, 57, 171-197, 2002.

McElroy, M., Elkins, J., Wofsy, S., Kolb, C., Duran, A., and Kaplan, W.: Production and release of $N_2O$ from the Potomac Estuary, Limnol. Oceanogr, 23, 1168-1182, 1978.

Meinshausen, M., Smith, S. J., Calvin, K., Daniel, J. S., Kainuma, M. L. T., Lamarque, J.-F., Matsumoto, K., Montzka, S. A., Raper, S. C. B., Riahi, K., Thomson, A., Velders, G. J. M., and van Vuuren, D. P. P.: The RCP greenhouse gas concentrations and their extensions from 1765 to 2300, Climatic Change, 109, 213-241, 2011.

Mengis, M., Schif, S., Harris, M., English, M., Aravena, R., Elgood, R., and MacLean, A.: Multiple geochemical and isotopic approaches for assessing ground water $NO_3^-$ elimination in a riparian zone, Groundwater, 37, 448-457, 1999.

Middelburg, J. J. and Herman, P. M.: Organic matter processing in tidal estuaries, Marine Chemistry, 106, 127-147, 2007.

Middelburg, J. J., Klaver, G., Nieuwenhuize, J., Markusse, R. M., Vlug, T., and van der Nat, F. J. W.: Nitrous oxide emissions from estuarine intertidal sediments, Hydrobiologia, 311, 43-55, 1995.

Middelburg, J. J. and Nieuwenhuize, J.: Nitrogen uptake by heterotrophic bacteria and phytoplankton in the nitrate-rich Thames estuary, Marine Ecology Progress Series, 203, 13-21, 2000.

Mueller, C., Krieg, R., Merz, R., and Knöller, K.: Regional nitrogen dynamics in the TERENO Bode River catchment, Germany, as constrained by stable isotope patterns, Isotopes in environmental and health studies, 2015. 1-14, 2015.

Mulholland, P. J., Helton, A. M., Poole, G. C., Hall, R. O., Hamilton, S. K., Peterson, B. J., Tank, J. L., Ashkenas, L. R., Cooper, L. W., and Dahm, C. N.: Stream denitrification across biomes and its response to anthropogenic nitrate loading, Nature, 452, 202-205, 2008.

Mulholland, P. J., Tank, J. L., Sanzone, D. M., Wollheim, W. M., Peterson, B. J., Webster, J. R., and Meyer, J. L.: Nitrogen cycling in a forest stream determined by a $^{15}N$ tracer addition, Ecological Monographs, 70, 471-493, 2000.

Murray, R. H., Erler, D. V., and Eyre, B. D.: Nitrous oxide fluxes in estuarine environments: Response to global change, Global change biology, 2015. 2015.

Najjar, R. G.: Marine biogeochemistry, Climate system modeling, 1992. 241-280, 1992.

Naqvi, S., Bange, H. W., Farias, L., Monteiro, P., Scranton, M., and Zhang, J.: Marine hypoxia/anoxia as a source of $CH_4$ and $N_2O$, Biogeosciences, 7, 2010.

Naqvi, S. W. A., Jayakumar, D. A., Narvekar, P. V., Naik, H., Sarma, V. V. S. S., D'Souza, W., Joseph, S., and George, M. D.: Increased marine production of $N_2O$ due to intensifying anoxia on the Indian continental shelf, Nature, 408, 346-349, 2000.

Nevison, C., Butler, J. H., and Elkins, J.: Global distribution of $N_2O$ and the $\Delta N_2O$-AOU yield in the subsurface ocean, Global Biogeochemical Cycles, 17, 2003.

Nevison, C. D., Lueker, T. J., and Weiss, R. F.: Quantifying the nitrous oxide source from coastal upwelling, Global Biogeochemical Cycles, 18, 2004.

Newcomer, T. A., Kaushal, S. S., Mayer, P. M., Shields, A. R., Canuel, E. A., Groffman, P. M., and Gold, A. J.: Influence of natural and novel organic carbon sources on denitrification in forest, degraded urban, and restored streams, Ecological Monographs, 82, 449-466, 2012.

Nishio, T., Komada, M., Arao, T., and Kanamori, T.: Simultaneous determination of transformation rates of nitrate in soil, Japan Agricultural Research Quarterly: JARQ, 35, 11-17, 2001.

Nowicki, B. L.: The Effect of Temperature, Oxygen, Salinity, and Nutrient Enrichment on Estuarine Denitrification Rates Measured with a Modified Nitrogen Gas Flux Technique, Estuarine, Coastal and Shelf Science, 38, 137-156, 1994.

Ogilvie, B., Nedwell, D., Harrison, R., Robinson, A., and Sage, A.: High nitrate, muddy estuaries as nitrogen sinks: the nitrogen budget of the River Colne estuary (United Kingdom), Marine Ecology Progress Series, 150, 217-228, 1997.

Pardo, L. H., Kendall, C., Pett-Ridge, J., and Chang, C. C.: Evaluating the source of streamwater nitrate using $\delta^{15}N$ and $\delta^{18}O$ in nitrate in two watersheds in New Hampshire, USA, Hydrological Processes, 18, 2699-2712, 2004.

Pätsch, J. and Lenhart, H.-J.: Daily loads of nutrients, total alkalinity, dissolved inorganic carbon and dissolved organic carbon of the European continental rivers for the years 1977-2002, Inst. für Meereskunde, 2004.

Payne, W.: Reduction of nitrogenous oxides by microorganisms, Bacteriological Reviews, 37, 409, 1973.

Petersen, W., Petschatnikov, M., Schroeder, F., and Colijn, F.: FerryBox systems for monitoring coastal waters, Elsevier Oceanography Series, 69, 325-333, 2003.

Peterson, B. J., Wollheim, W. M., Mulholland, P. J., Webster, J. R., Meyer, J. L., Tank, J. L., Martí, E., Bowden, W. B., Valett, H. M., and Hershey, A. E.: Control of nitrogen export from watersheds by headwater streams, Science, 292, 86-90, 2001.

Pfenning, K. S. and McMahon, P. B.: Effect of nitrate, organic carbon, and temperature on potential denitrification rates in nitrate-rich riverbed sediments, Journal of Hydrology, 187, 283-295, 1997.

Phillips, D. L. and Koch, P. L.: Incorporating concentration dependence in stable isotope mixing models, Oecologia, 130, 114-125, 2002.

Piatek, K. B., Mitchell, M. J., Silva, S. R., and Kendall, C.: Sources of nitrate in snowmelt discharge: evidence from water chemistry and stable isotopes of nitrate, Water, Air, and Soil Pollution, 165, 13-35, 2005.

Poughon, L., Dussap, C. G., and Gros, J. B.: Energy model and metabolic flux analysis for autotrophic nitrifiers, Biotechnology and bioengineering, 72, 416-433, 2001.

Rabalais, N. N.: Nitrogen in aquatic ecosystems, AMBIO: A Journal of the Human Environment, 31, 102-112, 2002.

Radach, G. and Pätsch, J.: Variability of continental riverine freshwater and nutrient inputs into the North Sea for the years 1977–2000 and its consequences for the assessment of eutrophication, Estuaries and Coasts, 30, 66-81, 2007.

Ramaswamy, V., Boucher, O., Haigh, J., Hauglustaine, D., Haywood, J., Myhre, G., Nakajima, T., Shi, G., Solomon, S., and Betts, R. E.: Radiative forcing of climate change, Pacific Northwest National Laboratory (PNNL), Richland, WA (US), 2001.

Rees, A., Owens, N., and Upstill-Goddard, R.: Nitrous oxide in the Bellingshausen sea and drake passage, Journal of Geophysical Research: Oceans, 102, 3383-3391, 1997.

Révész, K., Böhlke, J., and Yoshinari, T.: Determination of $\delta^{18}O$ and $\delta^{15}N$ in nitrate, Analytical Chemistry, 69, 4375-4380, 1997.

Rhee, T., Kettle, A., and Andreae, M.: Methane and nitrous oxide emissions from the ocean: A reassessment using basin-wide observations in the Atlantic, Journal of Geophysical Research: Atmospheres, 114, 2009.

Rhee, T. S.: The process of air-water gas exchange and its application, 2000. Texas A&M University College Station, Texas, USA, 2000.

Richards, F.: Anoxic basins and fiords. In: Chemical Oceanography, Riley, J. P. and Skjrrolu, G. (Eds.), Academic Press, London, 1965.

Richardson, W. B., Strauss, E. A., Bartsch, L. A., Monroe, E. M., Cavanaugh, J. C., Vingum, L., and Soballe, D. M.: Denitrification in the Upper Mississippi River: rates, controls, and contribution to nitrate flux, Canadian Journal of Fisheries and Aquatic Sciences, 61, 1102-1112, 2004.

Ritchie, G. and Nicholas, D.: Identification of the sources of nitrous oxide produced by oxidative and reductive processes in *Nitrosomonas europaea*, Biochemical Journal, 126, 1181-1191, 1972.

Robinson, A., Nedwell, D., Harrison, R., and Ogilvie, B.: Hypernutrified estuaries as sources of $N_2O$ emission to the atmosphere: the estuary of the River Colne, Essex, UK, Marine Ecology Progress Series, 164, 59-71, 1998.

Rode, M. and Kiwel, U.: How to use new online monitoring techniques to improve river water quality modeling at the river reach scale, 2012. 2012.

Schiller, D. v., Martí, E., and Riera, J. L.: Nitrate retention and removal in Mediterranean streams bordered by contrasting land uses: a $^{15}N$ tracer study, Biogeosciences, 6, 181-196, 2009.

Schlarbaum, T., Daehnke, K., and Emeis, K.: Turnover of combined dissolved organic nitrogen and ammonium in the Elbe estuary/NW Europe: Results of nitrogen isotope investigations, Marine Chemistry, 119, 91-107, 2010.

Schlegel, H. G.: Allgemeine Mikrobiologie, 7. überarbeitete Auflage/unter Mitarbeit von Christiane Zaborosch. Georg Thieme Verlag, Stuttgart New York, 1992.

Schöl, A.: Modelling the oxygen budget of the Elbe-Estuary–Scenarios concerning the impact of shallow water zones and reduced algal and detritus load, TIDE HPA/BfG contribution, WP3_Task, 6, 2012.

Schöl, A., Hein, B., Wyrwa, J., and Kirchesch, V.: Modelling water quality in the Elbe and its estuary - Large scale and long term applications with focus on the oxygen budget of the estuary, Die Küste, 80, 2014.

Schroeder, F., Klages, D., and Knauth, H.-D.: Bell-jar experiments and suspension measurements for the quantification of oxygen consumption and nitrogen conversion in sediments of the Elbe estuary. In: Estuarine Water Quality Management, Springer, 1990.

Seitzinger, S. P.: Denitrification in freshwater and coastal marine ecosystems: ecological and geochemical significance, Limnol Oceanogr, 33, 702-724, 1988.

Seitzinger, S. P., Harrison, J., Dumont, E., Beusen, A. H., and Bouwman, A.: Sources and delivery of carbon, nitrogen, and phosphorus to the coastal zone: An overview of Global Nutrient Export from Watersheds (NEWS) models and their application, Global Biogeochemical Cycles, 19, 2005.

Seitzinger, S. P., Kroeze, C., and Styles, R. V.: Global distribution of $N_2O$ emissions from aquatic systems: natural emissions and anthropogenic effects, Chemosphere - Global Change Science, 2, 267-279, 2000.

Seitzinger, S. P. and Nixon, S. W.: Eutrophication and the rate of denitrification and $N_2O$ production in coastal marine sediments, Limnol Oceanogr, 30, 1332-1339, 1985.

Seitzinger, S. P., Styles, R. V., Boyer, E. W., Alexander, R. B., Billen, G., Howarth, R. W., Mayer, B., and Van Breemen, N.: Nitrogen retention in rivers: model development

and application to watersheds in the northeastern USA, Biogeochemistry, 57, 199-237, 2002.

Siedler, G. and Peters, H.: Properties of sea water: Physical properties. In: Oceanography, Sündermann, J. (Ed.), Springer Berlin Heidelberg, Berlin, Heidelberg, 1986.

Sigman, D., Casciotti, K., Andreani, M., Barford, C., Galanter, M., and Böhlke, J.: A bacterial method for the nitrogen isotopic analysis of nitrate in seawater and freshwater, Analytical chemistry, 73, 4145-4153, 2001.

Sigman, D. M., Granger, J., DiFiore, P. J., Lehmann, M. M., Ho, R., Cane, G., and van Geen, A.: Coupled nitrogen and oxygen isotope measurements of nitrate along the eastern North Pacific margin, Global Biogeochemical Cycles, 19, 2005.

Silva, S., Kendall, C., Wilkison, D., Ziegler, A., Chang, C., and Avanzino, R.: A new method for collection of nitrate from fresh water and the analysis of nitrogen and oxygen isotope ratios, Journal of Hydrology, 228, 22-36, 2000.

Silvennoinen, H., Liikanen, A., Rintala, J., and Martikainen, P. J.: Greenhouse gas fluxes from the eutrophic Temmesjoki River and its Estuary in the Liminganlahti Bay (the Baltic Sea), Biogeochemistry, 90, 193-208, 2008.

Simon, M.: Die Elbe und ihr Einzugsgebiet: Ein geographisch-hydrologischer und wasserwirtschaftlicher Überblick, Internat. Komm. zum Schutz der Elbe, 2005.

Starry, O. S., Valett, H. M., and Schreiber, M. E.: Nitrification rates in a headwater stream: influences of seasonal variation in C and N supply, Journal of the North American Benthological Society, 24, 753-768, 2005.

Stüven, R., Vollmer, M., and Bock, E.: The impact of organic matter on nitric oxide formation by *Nitrosomonas europaea*, Archives of Microbiology, 158, 439-443, 1992.

Suntharalingam, P. and Sarmiento, J.: Factors governing the oceanic nitrous oxide distribution: Simulations with an ocean general circulation model, Global Biogeochemical Cycles, 14, 429-454, 2000.

Tietema, A., Boxman, A., Bredemeier, M., Emmett, B., Moldan, F., Gundersen, P., Schleppi, P., and Wright, R.: Nitrogen saturation experiments (NITREX) in coniferous

forest ecosystems in Europe: a summary of results, Environmental Pollution, 102, 433-437, 1998.

Trimmer, M., Risgaard-Petersen, N., Nicholls, J. C., and Engstrom, P.: Direct measurement of anaerobic ammonium oxidation (anammox) and denitrification in intact sediment cores, Marine Ecology Progress Series, 326, 37-47, 2006.

Vitousek, P. M., Aber, J. D., Howarth, R. W., Likens, G. E., Matson, P. A., Schindler, D. W., Schlesinger, W. H., and Tilman, D. G.: Human alteration of the global nitrogen cycle: sources and consequences, Ecological applications, 7, 737-750, 1997.

Von Schulthess, R., Wild, D., and Gujer, W.: Nitric and nitrous oxides from denitrifying activated sludge at low oxygen concentration, Water Science and Technology, 30, 123-132, 1994.

Voss, M., Deutsch, B., Elmgren, R., Humborg, C., Kuuppo, P., Pastuszak, M., Rolff, C., and Schulte, U.: Source identification of nitrate by means of isotopic tracers in the Baltic Sea catchments, Biogeosciences, 3, 663-676, 2006.

Walter, S., Bange, H. W., and Wallace, D. W.: Nitrous oxide in the surface layer of the tropical North Atlantic Ocean along a west to east transect, Geophysical research letters, 31, 2004.

Wassenaar, L. I.: Evaluation of the origin and fate of nitrate in the Abbotsford Aquifer using the isotopes of $^{15}N$ and $^{18}O$ in $NO_3^-$, Applied Geochemistry, 10, 391-405, 1995.

Wehr, J. D. and Descy, J. P.: Use of phytoplankton in large river management, Journal of Phycology, 34, 741-749, 1998.

Weiss, R.: The temporal and spatial distribution of tropospheric nitrous oxide, Journal of Geophysical Research: Oceans, 86, 7185-7195, 1981.

Weiss, R. F. and Price, B. A.: Nitrous oxide solubility in water and seawater, Marine Chemistry, 8, 347-359, 1980.

WMO: Scientific Assessment of Ozone Depletion: 2014, Global Ozone Research and Monitoring Project–Report No. 55, World Meteorological Organization, Geneva, Switzerland, 2014.

Wolfstein, K. and Kies, L.: Composition of suspended participate matter in the Elbe estuary: Implications for biological and transportation processes, Deutsche Hydrografische Zeitschrift, 51, 453-463, 1999.

Wrage, N., Velthof, G., Van Beusichem, M., and Oenema, O.: Role of nitrifier denitrification in the production of nitrous oxide, Soil Biology and Biochemistry, 33, 1723-1732, 2001.

Zappa, C. J., Raymond, P. A., Terray, E. A., and McGillis, W. R.: Variation in surface turbulence and the gas transfer velocity over a tidal cycle in a macro-tidal estuary, Estuaries, 26, 1401-1415, 2003.

Zhang, G.-L., Zhang, J., Liu, S.-M., Ren, J.-L., and Zhao, Y.-C.: Nitrous oxide in the Changjiang (Yangtze River) Estuary and its adjacent marine area: Riverine input, sediment release and atmospheric fluxes, Biogeosciences, 7, 3505-3516, 2010.

Zhu, S. and Chen, S.: The impact of temperature on nitrification rate in fixed film biofilters, Aquacultural Engineering, 26, 221-237, 2002.

# Appendix

## A. Experiments with the $N_2O$-isotope-analyzer (LGR)

### A.1. Instrumental specification: $N_2O$-Isotope-analyzer

An $N_2O$ analyzer (Los Gatos Research, Model 914-0022, LGR) was used to measure gas-phase mole fractions of $N_2O$, as well as water vapor ($H_2O$), using off-axis integrated cavity output spectroscopy (ICOS) (Baer et al., 2002).

The analyzer is specified for isotope measurements of $N_2O$ ($\delta^{15}N^{\alpha}$, $\delta^{15}N^{\beta}$, $\delta^{15}N_{bulk}$ and $\delta^{18}O$) and has an additional port for discrete injection which can be used for small volume samples via syringe (minimum 80ml). Its precision is noted with 0.2 ppb for $N_2O$ and better than 1‰ for isotopes (1σ, 100 seconds, $N_2O$ >300 ppb). The measurement range is covered between 300 ppb to 100 ppm for all specs with a maximum drift of 1 ppb for $N_2O$ and less than 1‰ for all isotopes (15 min. average).

The measurement rate can be set up to a frequency of 1 Hz in 'flow through' mode which describes continuous measurements of the sample gas. Measurement rates > 0.5 Hz required an additional external pump and are performed with a flow rate of ~690 ml $min^{-1}$ ('high flow') which implies that a lot of sample gas is needed. Thus, all experiments were done with a measurements rate of 0.5 Hz (= 2 seconds), described as 'low flow', with a flow rate between 70-90 ml $min^{-1}$.

For measurements of the batch injection an average of 143 measured points are calculated by the analyzer itself.

Water vapor is detected additionally and used by the analyzer to automatically calculate the dry mole fraction of $N_2O$ up to a water content of 20,000 ppm:

$$N_2O_{dry} = \frac{x\,(N_2O)}{1 - x\,(H_2O)}$$

Where $N_2O_{dry}$ is the dry mole fraction and x are the mole fractions of the according gas.

All LGR analyzers measure under stable pressure and temperature for comparable gas values. Our instrument has a working temperature of 45.5°C (± 0.5°C) and a constant pressure of 45.23 Torr (= 6.03 bar). Under ambient $N_2O$ concentration and water vapor (~15,000 ppm) the mirror ring down time is 13.28 µs.

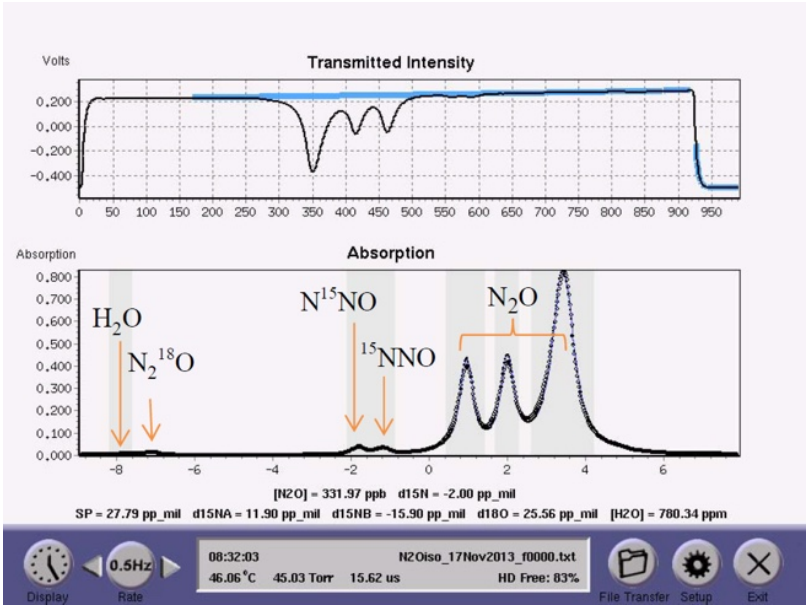


Figure A.1: Transmitted intensity and absorption spectrum as seen during measurements with the LGR-$N_2O$-isotpe-analyzer. (Picture: N2O_ISOTOPE_manual, LGR®)

The used $N_2O$ sample gas for the experiments was *Distickstoffmonoxid UHP* (100% $N_2O$, > 99,999Vol%, Air Liquide Deutschland GmbH, Stelle, Germany), calibrated by Prof. Jan Kaiser (University of East Anglia) against his laboratory's internal standard 'MPI-1' with the following isotopic ratios:

| | | |
|---|---|---|
| $\delta^{15}N$, average | = -0.50 ± 0.01‰ | (vs. Air-$N_2$) |
| $\delta^{15}N$, terminal/β | = 0.24 ± 0.05‰ | (vs. Air-$N_2$) |
| $\delta^{15}N$, central/α | = -1.23 ± 0.04‰ | (vs. Air-$N_2$) |
| $\delta^{18}O$ | = 40.37 ± 0.02‰ | (vs. VSMOW) |
| SP (**s**ite-**p**reference) | = -1.47 ± 0.04‰ | (calculated: SP = $\delta^{15}N^{\alpha}$ - $\delta^{15}N^{\beta}$) |

## A.2. $N_2O$ alteration with water vapor increase

To check for alterations caused by water vapor concentration increase, $N_2O$ sample gas was mixed with zero air ($N_2O$-free, ZA) in a 5 liter 'mixing bottle' (culture bottle with 4 ports). The gas mixture was established by injecting $N_2O$ sample gas into a permanent stream of ZA via a fused silica capillary (100 µm diameter, SGE Analytical Science). $N_2O$ dry mole fraction was regulated by the ZA flow rate. Additionally an open tube was

used to outbalance arising overpressures in the mixing bottle. The third port was used to connect the bottle via a Viton® tube with the analyzer's inlet.

After $N_2O$ dry mole fraction stabilization of 1230 ppb, 10 ml water was injected in the bottle to investigate the effect on $N_2O$ mole fraction measurements, and according isotope values due to a water vapor increase.

Results show that an increased vapor also altered $N_2O$ mole fraction below the declared water content of 20,000 ppm (Fig. A.2).

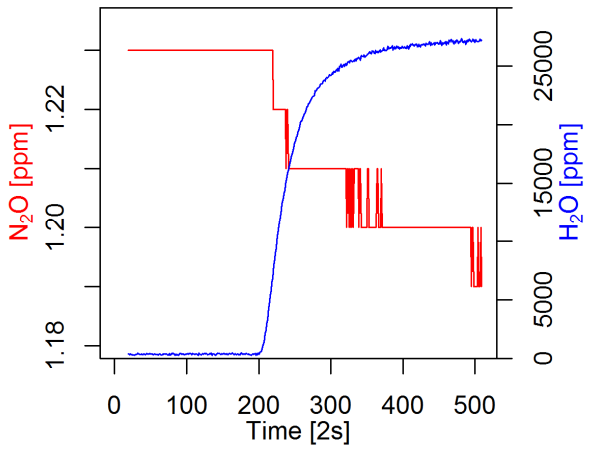


Figure A.2: Alteration of $N_2O$ mole fraction with increasing water vapor vs. time.

Additionally, the water vapor increased affected isotope measurements which led to a dilution in $\delta^{15}N_{bulk}$ (Fig. A.3a), while $\delta^{18}O$ seemed to follow the $H_2O$ line (Fig. A.3b).

The increase of water vapor not just lowered $N_2O$ mole fraction, it also led to an almost stair like decrease, interrupted by uncoordinated jumps of ~10 ppb between the lowering steps. This phenomenon was probably caused by a higher density (and presumably light refractions) of the $H_2O$ vapor which forced the analyzer to new internal adjustments of the absorption spectrum.

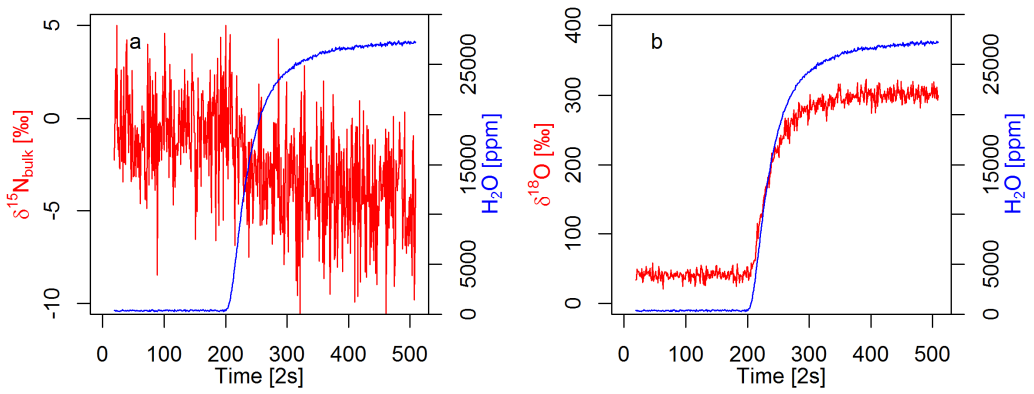


Figure A.3: Isotopic ratio alteration of $N_2O$ with increasing water vapor vs. time; a) $\delta^{15}N_{bulk}$ depletion with increasing water vapor, b) $\delta^{18}O$ enrichment with increasing water vapor

Based on those results, the necessity of a water trap for further $N_2O$ measurements was demonstrated. Due to an alteration of $N_2O$ mole fraction, $\delta^{15}N_{bulk}$ and $\delta^{18}O_{N2O}$, it is important to keep $H_2O$ vapor under 5000 ppm.

## A.3. **Continuous measurements with and without a Nafion® tube water trap**

In this experiment pressurized air was used as the sampling gas with a $N_2O$ mole fraction of 345 ppb. Influence on $N_2O$ isotopic composition was tested with a water trap during the 'low flow-through mode' of the instrument. The measurement rate was set to 0.5 Hz (= 2 s, time).

The water trap was built of a Nafion® tube (PermaPure, Modell PPME-110-18COMP-4) embedded in silica gel beads (orange, PanReac AppliChem) in a plastic box and mounted at the inlet of the analyzer.

In general, the usage of the Nafion® trap led to larger variations in the analyzer's single point measurements, i.e. every two seconds (Fig. A.4).

Nevertheless, there was no significant difference of $\delta^{15}N_{bulk}$ between measurements with and without the Nafion® water trap (mean values of $\delta^{15}N_{bulk}$: 79 ± 7‰ with trap and 77 ± 2‰ without trap (Fig. A.4a)). The single site specific N-isotope mean values were 76 ± 8‰ (trap) and 77 ± 2‰ (no trap) for $\delta^{15}N^{\alpha}$, and 82 ± 10‰ (trap) & 77 ± 3‰ (no trap) for $\delta^{15}N^{\beta}$.

However, $\delta^{18}O_{N2O}$ values were strongly affected by the water trap with mean values of 159 ± 21‰ and 214 ± 5‰ with and without the water trap, respectively (Fig. A.4b). This indicated a dependency of $\delta^{18}O_{N2O}$ values and the ambient water content in the measured sample which was also determined before (section A.2.). Hence, care should be taken with absolute values of $\delta^{18}O_{N2O}$ if a water trap is used to keep $H_2O$ vapor on a constant level.

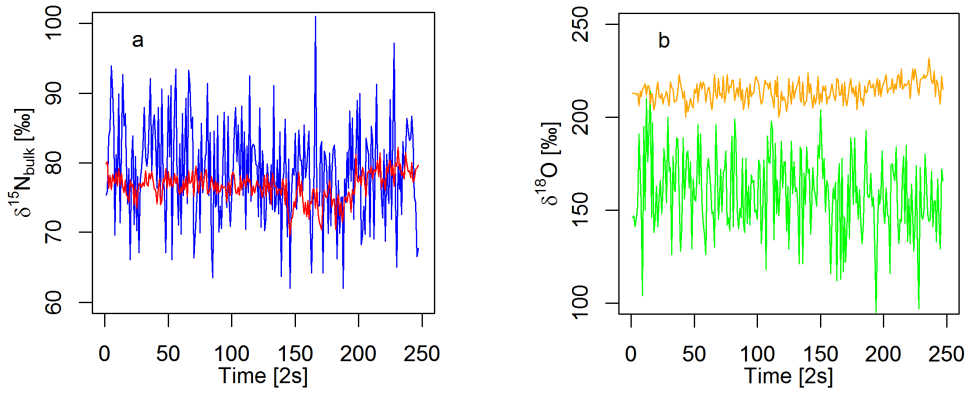


Figure A.4: Differences between isotopes measurements of $N_2O$ vs. time, with and without the Nafion® water trap; a) $\delta^{15}N_{bulk}$: red = without water trap, blue = Nafion® trap, b) $\delta^{18}O_{N2O}$: orange = without water trap, green = Nafion® trap

## A.4. Dilution-Experiments

### A.4.1. 'Simple' mixing of $N_2O$ dry mole fraction

An $N_2O$ dry mole fraction dilution test was done to check for isotopic composition stability and reproducibility over a time period of four days. To check for alterations due to a mole fraction increase, sample gas was mixed in the culture bottle as described in section A.2., using the UHP sample gas.

The head description 'simple' is used because no calibration of correct isotope values was done before, and in addition dilution was done continuously which means no stepwise increase of $N_2O$ mole fraction was performed (e.g. measurements of ten minutes before the next stepwise increase was induced). $N_2O$ mole fraction ranges from ~300 ppb up to ~1.5 ppm. For each day, the measurements over the full concentration range were repeated.

Values of $\delta^{15}N_{bulk}$ stabilized at a $N_2O$ level above 1 ppm (Fig. A.5a).

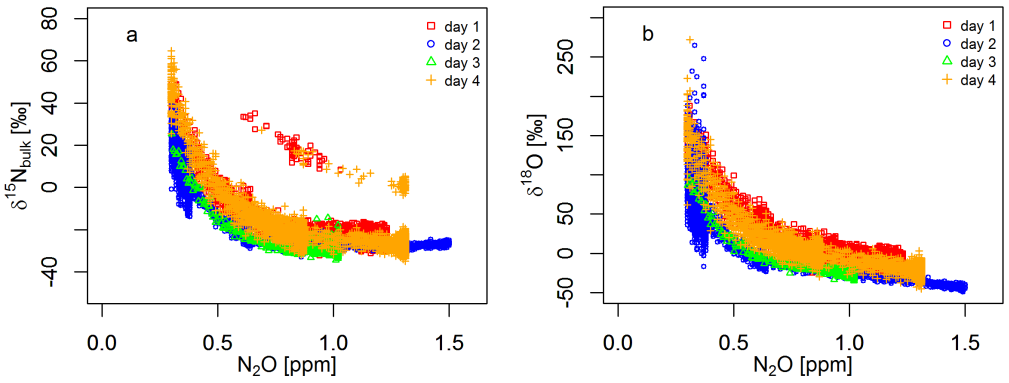


Figure A.5: Comparison of isotopic ratios of $N_2O$ vs. $N_2O$ mole fraction between four days; a) $\delta^{15}N_{bulk}$ vs. $N_2O$, b) $\delta^{18}O_{N2O}$ vs. $N_2O$

Despite large standard deviations of isotope values during the measurements, single outliers were seen at day 1 and day 4. Those outliers indicated instability of the analyzer in a random pattern for unknown reasons, because performance of dilution and experimental setup were not altered during this time period. On the other hand, the data for $\delta^{18}O_{N2O}$ showed no inconsistency which might be an indicator of an internal measurement/calculation problem of the analyzer for $\delta^{15}N_{N2O}$ rather than handling errors during the experiment (Fig. A.5b).

Although an improvement was estimated above 1 ppm, no stabilization of $\delta^{18}O_{N2O}$ values was reached (Fig. A.5b). There is no doubt of a more stable isotope measurement at increased $N_2O$ mole fractions, but a slight isotopic depletion was still visible.

Differences of stabilization measurements of $\delta^{15}N_{bulk}$ and $\delta^{18}O_{N2O}$ are also reflected in their standard deviations from the four days. Deviation of $\delta^{18}O_{N2O}$ values above 1 ppm was ± 12.1‰ within the four days and hence too large for an adequate isotopes determination. Despite the outliers, standard deviation of $\delta^{15}N_{bulk}$ was ± 2.7‰ which sets those values in a more comparable range by providing more reliable measurement results.

### A.4.2. **Stepwise mixing of $N_2O$ dry mole fraction**

$N_2O$ dry mole fraction dilution tests were done to check step by step the stability of isotopic composition.

Between the dilution tests, the support of LGR did internal calibrations to improve stabilization of isotopomer measurements by altering the internal software code according to our results.

*A.4.2.1. Pre-mixed sample gas in Tedlar® gas sampling bags*

To investigate alterations of $N_2O$ isotope compositions with increasing $N_2O$ mole fraction, 14 Tedlar® bags (3L, Restek Pure Chromatography, Bad Homburg, Germany) with different $N_2O$ mole fractions were pre-mixed. A determined amount of UHP sample gas was added to a Tedlar® bag filled with ZA to get roughly the required $N_2O$ mole fraction.

For this experiment the analyzer was calibrated to the according $\delta$-$N_2O$-values of our UHP sample gas at a $N_2O$ mole fraction of 1.296 ppm but the calibration was done 10 days before the beginning of the experiment. Thus an occurring shift of delta values between the days cannot be excluded and care must be taken to use the measured $\delta$-values. Thereof, the focus was mainly set to differences between $N_2O$ isotope values and $N_2O$ dry mole fraction rather than to calibrated $N_2O$ isotope values.

Five minute averages were taken of the measured sample gas values. Samples were measured by connecting the Tedlar® bags directly to the inlet port by using a tube (~20 cm, Viton®) equipped with a Swagelok® connector.

Since the 'simple' mole fraction dilution experiment (section A.4.1.) indicated a stabilization of $\delta^{15}N_{bulk}$ values when exceeding $N_2O$ concentrations of 1 ppm, measurement range was extended to a $N_2O$ dry mole fraction of ~5 ppm.

As expected, results of $\delta^{15}N^{\alpha\beta}$ showed stable values if $N_2O$ mole fraction exceeded 1 ppm (Fig. A.6a). In addition, the deviation of the single $\delta^{15}N^{\alpha\beta}$ isotopes improved at higher mole fractions of $N_2O$. A closer look at the site-specific N-isotopes of $N_2O$ at larger $N_2O$ mole fractions pointed out: Stabilization of $\delta$-values was even better above 2 ppm (Fig. A.6b), because no significant difference in isotope values could be calculated between the single concentration levels.

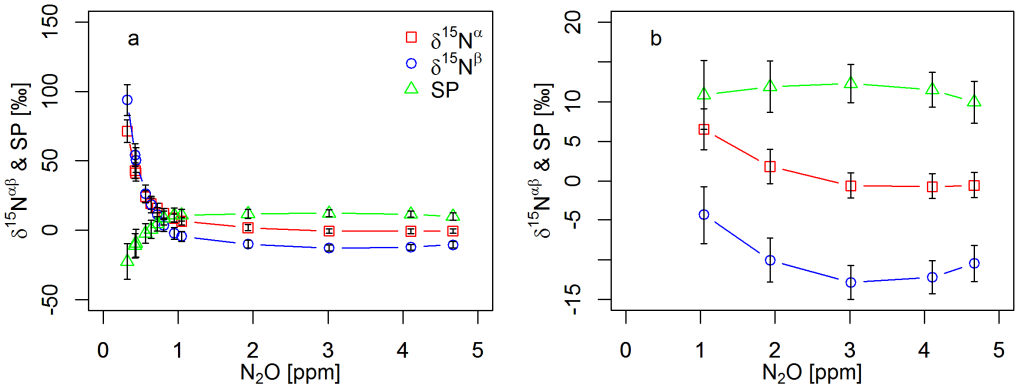


Figure A.6: $\delta^{15}N^{\alpha\beta}$ and SP values vs. $N_2O$ mole fraction; a) $\delta^{15}N^{\alpha\beta}$ and SP over the whole $N_2O$ mole fraction range, b) Zoom: $\delta^{15}N^{\alpha\beta}$ and SP exceeding $N_2O$ mole fraction of 1 ppm (note the different scale on the y-axis)

In comparison to $\delta^{15}N^{\alpha\beta}$, $\delta^{18}O_{N2O}$ values did not show a stabilization when $N_2O$ mole fractions exceed 2 ppm, as seen in figure A.7a. Although, standard deviations got smaller with increasing $N_2O$ mole fraction range, still significant differences were calculated for $\delta^{18}O_{N2O}$.

Furthermore, an increase in $H_2O$ vapor was detected with increasing $N_2O$ mole fraction. In contrast to the former $H_2O$ vapor increase experiment (section A.2.), $\delta^{18}O_{N2O}$ became more depleted (Fig. A.7b) instead of enriched. This was unexpected and led to further studies to determine possible reasons for this conspicuous pattern (see section A.5.).

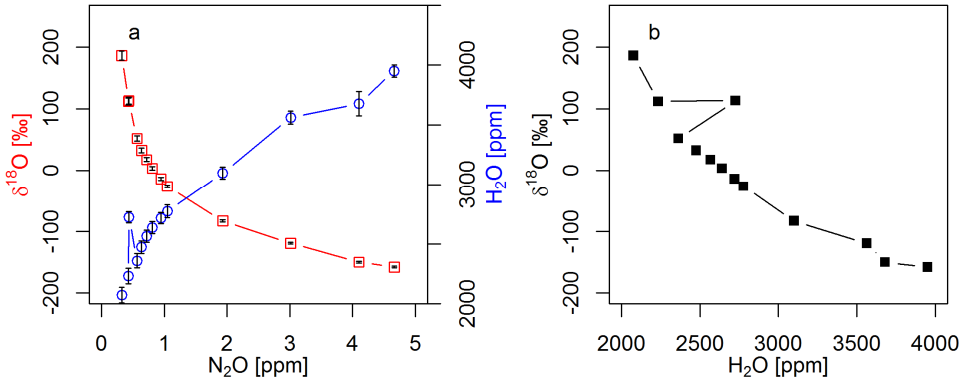


Figure A.7: Plots of $\delta^{18}O_{N2O}$ and $H_2O$ vapor with increasing $N_2O$ mole fraction; a) $\delta^{18}O_{N2O}$ & $H_2O$ vs. $N_2O$ mole fraction, b) $\delta^{18}O_{N2O}$ vs. $H_2O$

### *A.4.2.2. $N_2O$ dilution in a bottle*

A $N_2O$ dry mole fraction dilution test was done to check for stability of isotopic composition with increasing $N_2O$ concentration. To determine possible alterations due to a $N_2O$ mole fraction increase, sample gas was mixed in a 5 liter culture bottle with ZA (compare section A.2.). The concentration level was adjusted stepwise and measured for ~ 10 minutes to get a better overview of stabilization. For standard deviation calculations, a 5 min average (n = 250) was taken for each $N_2O$ mole fraction level.

Since lots of those dilution tests were done, two tests were chosen as examples, comparing the first dilution test (further referred as 'test-1') and the latest one so far ('test-2'), despite the Tedlar® bag test.

As seen in figure A.8, all measurements of different $N_2O$ mole fractions were highly constant (SD: ± 0.1 ppb to ± 1 ppb) and did not show large variation within a single concentration level.

Results of test-1 showed large standard deviations between single measurements of $\delta^{15}N^{\alpha\beta}$ isotopes (SD: ± 8‰) up to a $N_2O$ level of 1.5 ppm, and improved by exceeding this mole fraction (SD: ± 4‰) (Fig. A.8a).

A similar improvement of variations of δ-values in dependency of the $N_2O$ mole fractions was also found in $\delta^{18}O_{N2O}$, where the standard deviation was larger up to 1.5 ppm (SD: ± 15‰) and improved at a $N_2O$ mole fraction of 2.5 ppm (SD: ± 6‰). Improvement of $\delta^{18}O_{N2O}$ values finally ended with a standard deviation of ± 3.6‰ exceeding a $N_2O$ dry mole fraction of 2.5 ppm (Fig. A.8b).

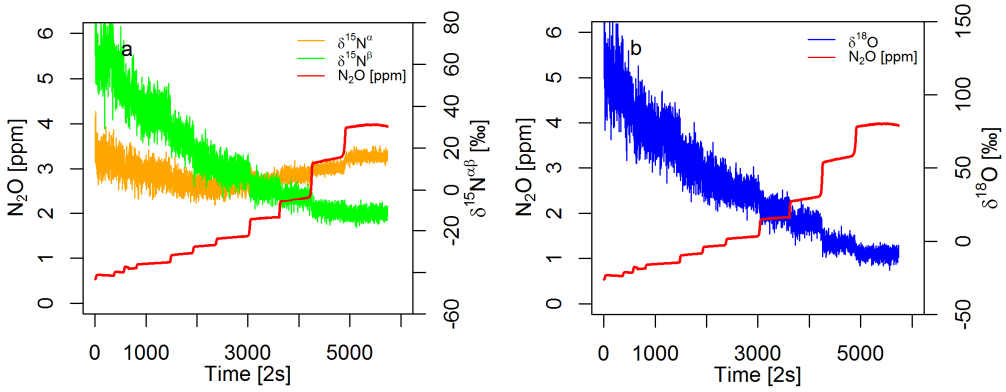


Figure A.8: Experimental results of test-1; a) $N_2O$ and $\delta^{15}N^{\alpha\beta}$ vs. time, b) $N_2O$ and $\delta^{18}O_{N2O}$ vs. time

Whereas a constant depletion was seen in $\delta^{15}N^{\beta}$ (~16‰ per 1 ppm) and $\delta^{18}O_{N2O}$ (~25‰ per 1 ppm), $\delta^{15}N^{\alpha}$ showed a non-constant pattern (Fig. A.8a). Isotopic values of $\delta^{15}N^{\alpha}$ first depleted about 20‰ up to a $N_2O$ level of ~1.5 ppm, and then enriched stepwise at higher $N_2O$ mole fractions (~7‰ per 1 ppm).

Results of test-2 showed that isotopic values of $\delta^{15}N^{\beta}$ and $\delta^{18}O_{N2O}$ are in average on a more constant level with increasing $N_2O$ dry mole fraction (Fig. A.9). However, variations of all delta values within the single $N_2O$ mole fraction were larger compared to test-1 and standard deviations improved stepwise for each step of $N_2O$ dilution up to 1.5 ppm (Tab. A).

Values of $\delta^{15}N^{\alpha}$ showed different trends in both experiments. Whereas in test-1 the depletion and enrichment of $\delta^{15}N^{\alpha}$ isotopes started and ended at the same isotopic concentration level (~20‰), results of test-2 showed a decrease of ~10‰ (up to a $N_2O$ mole fraction of 1.5ppm), which was followed by a stepwise increase from -25‰ to +27‰ $\delta^{15}N^{\alpha}$ (1.5 ppm to 6 ppm).

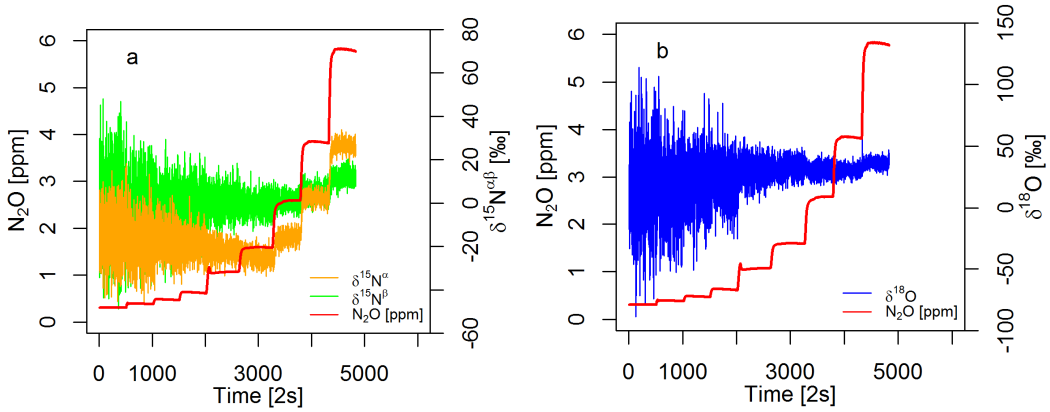


Figure A.9: Experimental results of test-2; a) $N_2O$ and $\delta^{15}N^{\alpha\beta}$ vs. time, b) $N_2O$ and $\delta^{18}O_{N2O}$ vs. time

Table A: Standard deviations (n=250) of $N_2O$ mole fractions of test-2

| $N_2O$ [ppm] | $\delta^{15}N^{\alpha}$ [‰] | $\delta^{15}N^{\beta}$ [‰] | $\delta^{18}O$ [‰] |
|---|---|---|---|
| **0.3** | ± 11 | ± 17 | ± 33 |
| **0.4** | ± 10 | ± 13 | ± 25 |
| **0.5** | ± 7 | ± 10.5 | ± 20 |
| **0.6** | ± 6 | ± 9 | ± 16 |
| **1.0** | ± 3.5 | ± 5 | ± 10 |
| **1.5 to 6.0** | ± 2.5 | ± 3 | ± 5 |

During both dilution experiments, $\delta^{15}N^{\beta}$ and $\delta^{18}O_{N2O}$ showed the same pattern and thus were obviously linked to each other (Fig. A.8 and Fig. A.9). Hence, $\delta^{15}N^{\beta}$ and $\delta^{18}O_{N2O}$ cross-plots were done to check for significance of linkage.

Results confirm a very strong linkage in both experiments (Fig. A.10), but also a high improvement ($R^2$ = 0.01) of their independency at test-2 (Fig. A.10.b). With over 4800 degrees of freedom, the significance in test-2 could almost be neglected, because such a high number of measurement points could also force a mathematical correlation which might be indicated by the very low values of $R^2$.

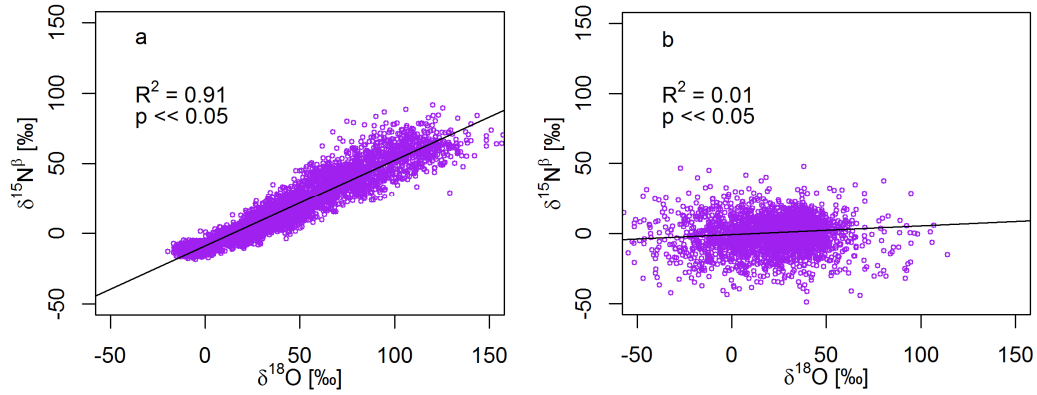


Figure A.10: Comparison of $\delta^{15}N^{\beta}$ vs. $\delta^{18}O$ and its significant relationship between test-1 (a) & test-2 (b)

## A.5. Water increase with increasing $N_2O$ mole fraction

The following results are from the data of the previous experiments of section A.4.2. - the $N_2O$ dilution tests in a bottle.

As formerly estimated in the Tedlar® bag experiment, a large increase of water vapor with increasing $N_2O$ dry mole fraction was also detected during the bottle-dilution experiments. By comparing test-1 with test-2 (Fig. A.11), the dependency of $H_2O$ vapor increase on increasing $N_2O$ mole fractions deteriorated in contrast to isotopomer measurement improvements.

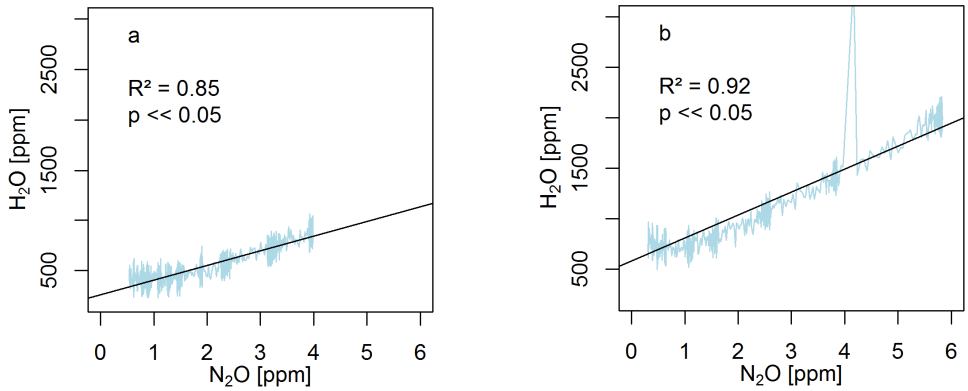


Figure A.11: Dependency of $H_2O$ vapor on increasing $N_2O$ concentration during test-1 (a) & test-2 (b)

As seen in figure A.12, a close relationship between $H_2O$ vapor and isotope values of $\delta^{18}O_{N2O}$ is still visible in test-2. Even if the effect of $\delta^{18}O_{N2O}$ on $N_2O$ was reduced, the influence on $H_2O$ vapor was still given, also seen in the simultaneous peaks of $H_2O$ vapor and $\delta^{18}O_{N2O}$ at a $N_2O$ mole fraction of ~4 ppm (and also seen in $H_2O$ vapor at Fig, A11.b).

No reason could be estimated for the sudden appearance of the large $H_2O$ and $\delta^{18}O_{N2O}$ peaks, because a constant mixing of the two gases (ZA and UHP) could be verified.

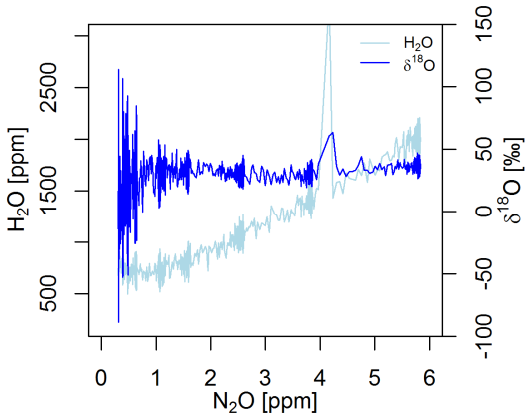


Figure A.12: Similar pattern of $H_2O$ vapor and $\delta^{18}O_{N2O}$ with increasing $N_2O$ in test-2

One potential reason for the dependency of $H_2O$ vapor and $\delta^{18}O_{N2O}$ could be derived from the absorption spectrum during measurements. As the screenshot shows (Fig. A.13), peaks of $H_2O$ vapor and $\delta^{18}O_{N2O}$ were not properly separated. Due to a shift seen in the $\delta^{18}O_{N2O}$ peak in the absorption spectrum, evidence of an alteration of $\delta^{18}O_{N2O}$ is provided with increasing water vapor.

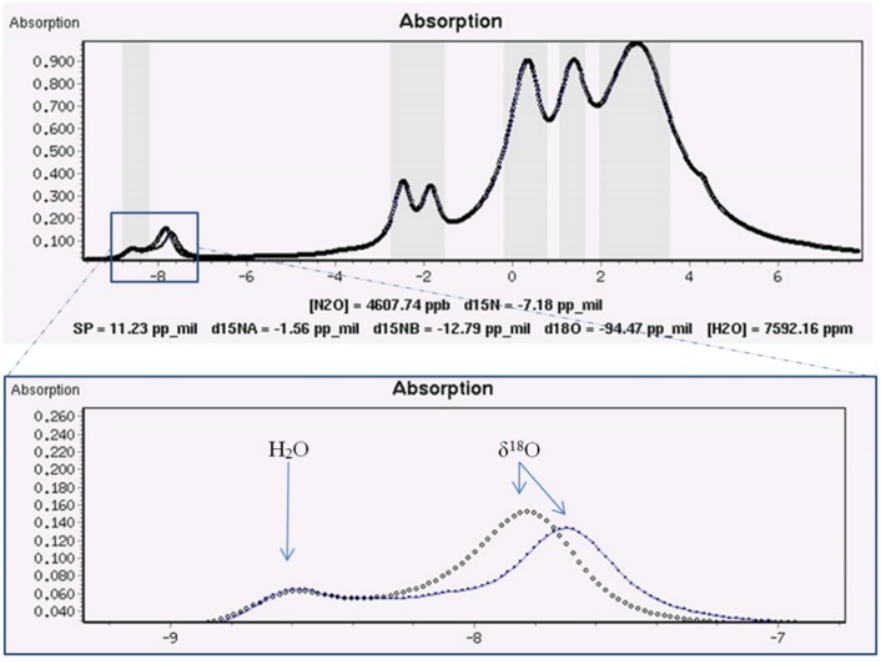


Figure A.13: Screenshots of the absorption spectrum during high $N_2O$ dry mole fraction measurements (~4600 ppb). Top graph: the whole spectrum as explained in Fig. A.1, bottom graph: Zoom of absorption spectrum of $H_2O$ vapor peak and $\delta^{18}O_{N2O}$ peak– black dotted line: optical absorption spectrum of $N_2O$ isotopomers, blue line: peak fit resulting from signal analysis

Summarized, the increase of $N_2O$ concentration triggered a chain of causation: the $N_2O$ dry mole fraction increase forced an increase in $H_2O$ vapor, the increase of $H_2O$ vapor led to an alteration of the $\delta^{18}O_{N2O}$ isotope absorption spectrum and hence, to an alteration of measured $\delta^{18}O_{N2O}$ values which results in this context in a similar pattern as $H_2O$ vapor.

## A.6. **Internal alteration of pressure: A loop-experiment**

In all the experiments described above, an open experimental setup was used where the inflowing sample gas was released through the outflow port into the surrounding air after passing the detector cell.

Additionally, the possibility of loop-measurements is given, where the sample gas is analyzed in a closed circuit. This method is useful, e.g. for $N_2O$-producing-bacteria incubation experiments. In this case the circulation of the sample gas ensures a constant pressure in the incubation, and $N_2O$ concentration increase due to biological $N_2O$ production can be obtained directly.

To check for pressure changes during loop measurements, inflow and outflow ports of the analyzer were connected with a tube (Viton®, inner diameter: 4 mm, length: 50 cm).

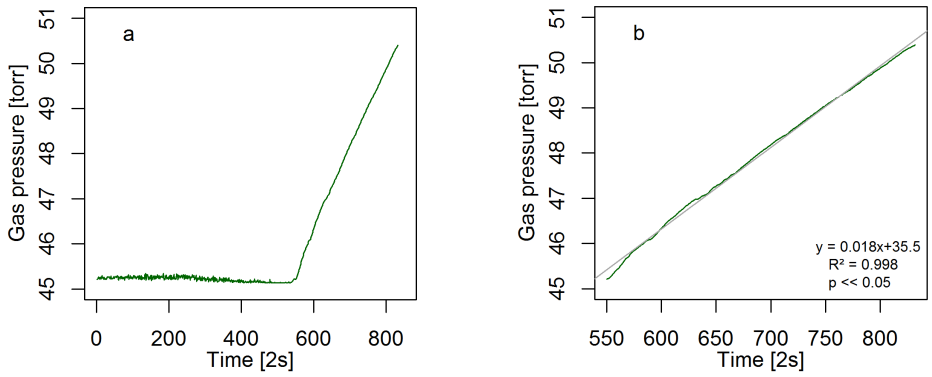


Figure A.14: Increase of gas over time: a) all data points including the assumption of 'buffer volume', b) starting point 550 - beginning of pressure increase (grey: regression line)

Results of the loop-experiment indicated a leak inside the operational system of the analyzer. As seen in figure A.14a, an increase of pressure could be estimated which appeared suddenly after a time point of 550 [measurement rate 0.5 Hz = 2 s]. A possible reason for the late pressure increase might be that the gas volume inside the Viton® tube

(~250 ml) serves as a buffer and could compensate the leaking gas for a while. Once the buffer is exhausted, a steeply pressure increase would be detectable. By taking only the increased interval, a pressure increase with a rate of 0.009 torr per second was calculated (Fig. A.14b).

As assumed before, a reason for the pressure increase must be a loss of sampling gas inside the analyzer. The loss indicated an appearance of slightly over pressure during operation of instrumental measurements which should be intended by LGR, otherwise leakage of ambient air could not be excluded.

A closer look at the instrument's internal structure showed that all tubes are made of PTFE (Polytetrafluorethylene) which is not 100% gas tight (Fig. A.15). To guarantee 100% tightness in the instrument, steal capillaries should be installed. But an exchange of the PTFE tubes with capillaries is not trivial due to forcing an alteration of the internal construction of the analyzer, and thus, should be done by LGR and not by the costumer.

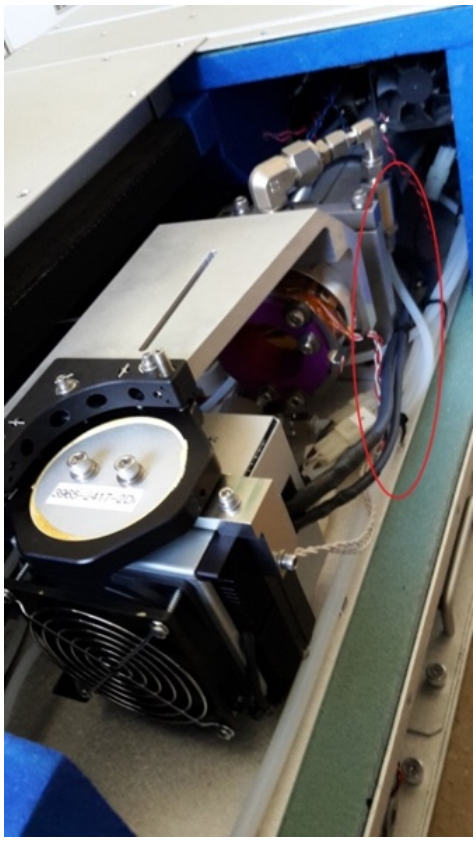

Figure A.15: Inside the $N_2O$-isotope-analyzer of LGR – the red circle marks one of the PTFE tubes (Picture: Lisa Brase®)

## A.7. Summary of laboratory experiments with the $N_2O$-isotope-analyzer & future outlook

To summarize the outcome of the pre-experiments:

An installation of the analyzer for reliable isotope measurements was not possible during the given time.

A better stability for isotope values was reached after several internal calibrations done by support of LGR, e.g. for $\delta^{18}O_{N2O}$, but this led to further complications: We observed a decline of stable isotope measurements in the upper $N_2O$ dry mole fraction range, and a larger variation of standard deviation during isotopomer measurements at lower dry mole fractions of $N_2O$ (300 ppb to 1.5 ppm).

Additionally, there is an urgent need to solve $H_2O$ vapor dependency on $N_2O$ mole fraction which still forces an alteration of the $\delta^{18}O_{N2O}$ spectrum, even if water vapor does not exceed 20,000 ppm. Thus, for higher water contents, a water trap is needed to keep water vapor on a low level smaller than 5000 ppm.

Experiments with a Nafion® tube water trap indicated significant alterations in $\delta^{18}O_{N2O}$ values. However, as results of the $N_2O$ - $H_2O$ fraction increase experiment showed, it cannot be excluded by now if this alteration of $\delta^{18}O_{N2O}$ values was forced due to the link between $\delta^{18}O_{N2O}$ and water vapor, or if it was a 'real' fractionation induced by the Nafion® tube. Both possibilities should be kept in mind and tested again by repeating the experiment after the problem of $H_2O$ vapor dependency on $N_2O$ mole fraction has been solved.

A stepwise dilution experiment of daily measurement repetition to check for variabilities between the days could also not be performed after the latest dilution test (test-2) and should be a mandatory outlook for future work, once the analyzer could be calibrated correctly to isotopomers values of $N_2O$.

The loop experiment showed another interesting part for future work of trouble shooting work: creating a gastight construction of the $N_2O$-analyzer by changing the PTFE tubes with steel capillaries to exclude a loss of measured sample gas and avoid pressure increase inside the instrument.

## B. Additional figures - not used in this thesis

In this thesis, additional measurements during transect and tidal sampling were performed, but not used in the single chapters (3 and 4).

The measured values were plotted as seen in the following figures:

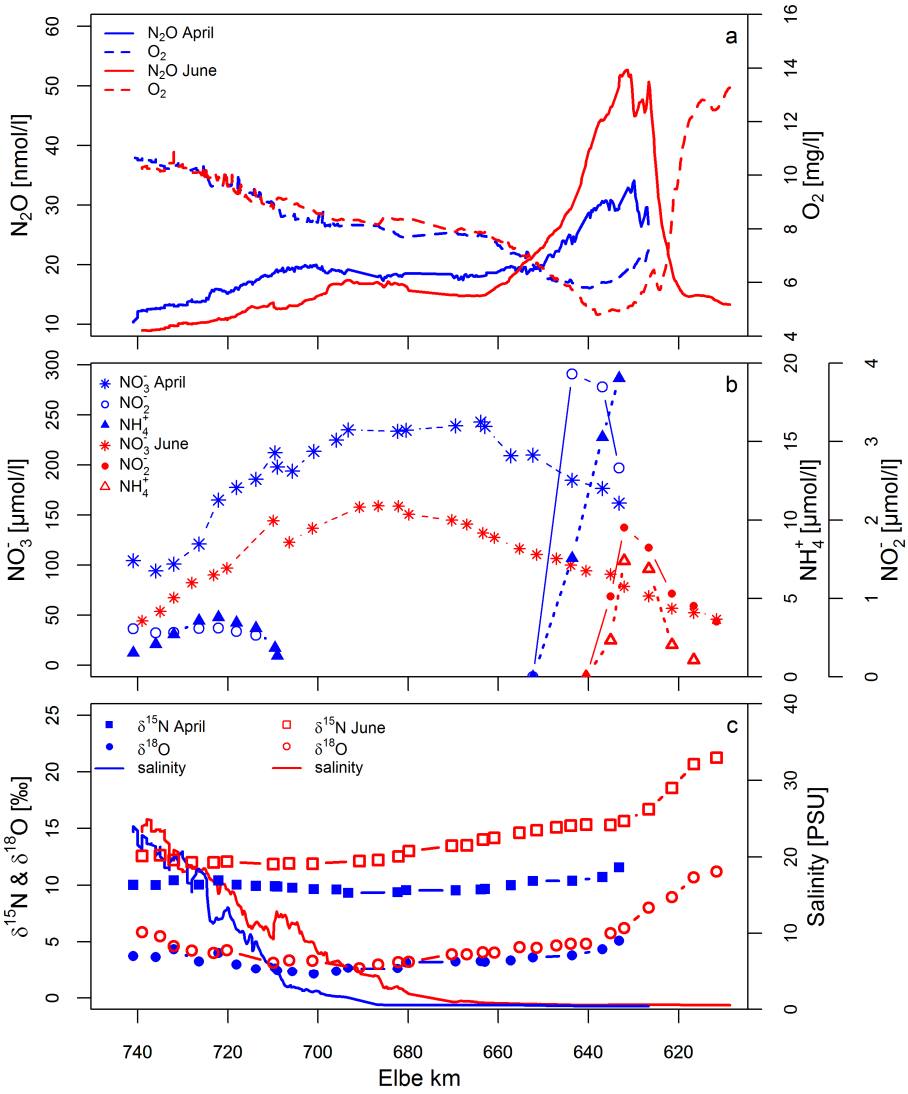


Figure B.1: Transect measurements in April '15 (blue) and June '15 (red) - Elbe km 609 to 745: a) continuous measurements of $N_2O$ and $O_2$ concentration, b) DIN concentration of distinct samples ($NO_3^-$, $NH_4^+$, $NO_2^-$), c) Isotopic ratio of $\delta^{15}N_{NO3}$ and $\delta^{18}O_{NO3}$ along the transect

(This figure was published on a poster at EGU 2016)

Supplementary data according to Figure B.1c:

| Month | Latitude | Longitude | $\delta^{15}N_{NO3-}$ [‰] | Std.-dev. $\delta^{15}N_{NO3-}$ [‰] | $\delta^{18}O_{NO3-}$ [‰] | Std.-dev. $\delta^{18}O_{NO3-}$ [‰] |
|---|---|---|---|---|---|---|
| ***April*** | 53.96429 | 8.528573 | 10.0 | 0.1 | 3.8 | 0.1 |
| | 53.95365 | 8.602160 | 10.0 | 0.1 | 3.7 | 0.1 |
| | 53.92592 | 8.656825 | 10.4 | 0.5 | 4.3 | 1.2 |
| | 53.88729 | 8.697132 | 10.0 | 0.1 | 3.3 | 0.0 |
| | 53.85542 | 8.743629 | 10.4 | 0.6 | 4.0 | 1.4 |
| | 53.83660 | 8.804277 | 10.0 | 0.2 | 3.0 | 0.3 |
| | 53.83775 | 8.873690 | 9.9 | 0.1 | 2.6 | 0.0 |
| | 53.84335 | 8.939693 | 9.9 | 0.0 | 2.6 | 0.1 |
| | 53.84379 | 8.949021 | 9.9 | 0.1 | 2.4 | 0.1 |
| | 53.85028 | 8.999209 | 9.8 | 0.0 | 2.3 | 0.0 |
| | 53.86647 | 9.066623 | 9.6 | 0.1 | 2.1 | 0.2 |
| | 53.87763 | 9.139404 | 9.6 | 0.0 | 2.4 | 0.0 |
| | 53.8783 | 9.178949 | 9.3 | 0.0 | 2.6 | 0.2 |
| | 53.84219 | 9.328455 | 9.4 | 0.0 | 2.6 | 0.1 |
| | 53.82977 | 9.348468 | 9.6 | 0.3 | 3.2 | 0.6 |
| | 53.74252 | 9.424526 | 9.6 | 0.2 | 3.3 | 0.4 |
| | 53.70674 | 9.483226 | 9.6 | 0.2 | 3.3 | 0.5 |
| | 53.69929 | 9.490077 | 9.7 | 0.2 | 3.2 | 0.3 |
| | 53.64954 | 9.515655 | 10.0 | 0.2 | 3.3 | 0.4 |
| | 53.61422 | 9.558226 | 10.4 | 0.1 | 3.6 | 0.4 |
| | 53.56708 | 9.663842 | 10.4 | 0.1 | 3.8 | 0.2 |
| | 53.55947 | 9.763868 | 10.7 | 0.2 | 4.3 | 0.1 |
| | 53.55005 | 9.817544 | 11.6 | 0.1 | 5.1 | 0.1 |

| | | | | | | |
|---|---|---|---|---|---|---|
| ***June*** | 53.96069 | 8.562820 | 12.6 | 0.3 | 5.8 | 0.4 |
| | 53.94701 | 8.617343 | 12.6 | 0.3 | 5.5 | 0.8 |
| | 53.92442 | 8.654799 | 12.2 | 0.3 | 4.6 | 0.4 |
| | 53.89580 | 8.686550 | 12.0 | 0.2 | 4.2 | 0.2 |
| | 53.86182 | 8.729598 | 12.0 | 0.3 | 4.0 | 0.5 |
| | 53.84334 | 8.768433 | 12.1 | 0.1 | 4.2 | 0.2 |
| | 53.84190 | 8.934398 | 11.9 | 0.2 | 3.1 | 0.1 |
| | 53.84956 | 8.988376 | 11.9 | 0.1 | 3.3 | 0.4 |
| | 53.86588 | 9.062577 | 11.9 | 0.1 | 3.3 | 0.3 |
| | 53.87646 | 9.216995 | 12.1 | 0.2 | 2.7 | 0.3 |
| | 53.86479 | 9.276196 | 12.2 | 0.2 | 3.0 | 0.3 |
| | 53.84006 | 9.329625 | 12.5 | 0.2 | 3.2 | 0.3 |
| | 53.82453 | 9.352356 | 13.0 | 0.1 | 3.2 | 0.3 |
| | 53.74993 | 9.420117 | 13.5 | 0.1 | 3.9 | 0.1 |
| | 53.72688 | 9.450417 | 13.5 | 0.2 | 3.9 | 0.1 |
| | 53.70197 | 9.485129 | 14.0 | 0.1 | 4.1 | 0.0 |
| | 53.68190 | 9.499766 | 14.2 | 0.1 | 4.0 | 0.2 |
| | 53.63406 | 9.525500 | 14.6 | 0.0 | 4.5 | 0.1 |
| | 53.60975 | 9.567905 | 14.8 | 0.1 | 4.5 | 0.0 |
| | 53.58293 | 9.616375 | 15.1 | 0.0 | 4.7 | 0.1 |
| | 53.56796 | 9.658249 | 15.3 | 0.0 | 4.8 | 0.2 |
| | 53.56432 | 9.710192 | 15.3 | 0.0 | 4.8 | 0.2 |
| | 53.55552 | 9.789849 | 15.3 | 0.0 | 5.7 | 0.1 |
| | 53.54775 | 9.833284 | 15.7 | 0.0 | 6.2 | 0.1 |
| | 53.54062 | 9.914884 | 16.7 | 0.0 | 8.0 | 0.0 |

| | | | | | | |
|---|---|---|---|---|---|---|
| | 53.53762 | 9.989455 | 18.6 | 0.1 | 8.9 | 0.1 |
| | 53.52009 | 10.05503 | 20.7 | 0.0 | 10.7 | 0.0 |
| | 53.4781 | 10.06073 | 21.2 | 0.1 | 11.2 | 0.2 |

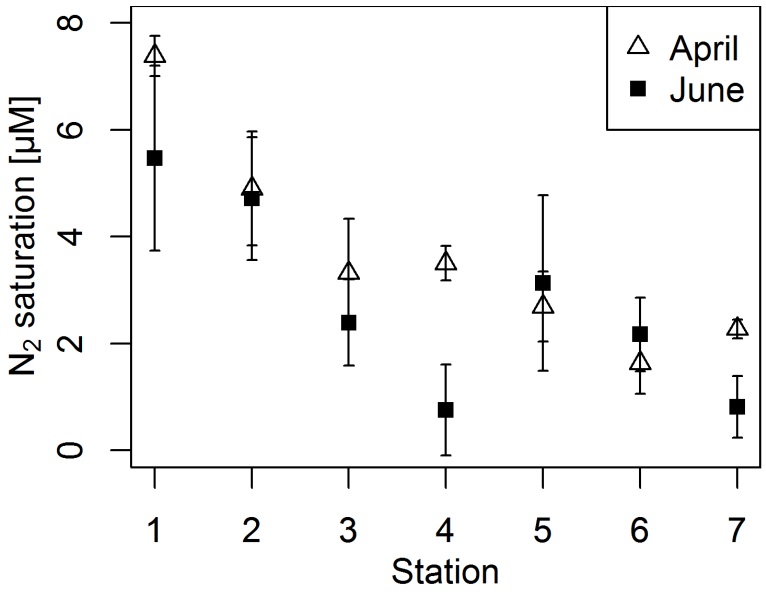


Figure B.2: $N_2$ oversaturation along the Elbe estuary at different stations (Elbe km - St. 1: 633, St. 2: 643, St. 3: 663, St. 4: 680, St. 5: 690, St. 6: 709, St. 7: 741)

Supplementary data according to Figure B.2:

| Month | Station | Latitude | Longitude | $N_2$ saturation [µM] | Std.-dev. $N_2$ saturation [µM] |
|---|---|---|---|---|---|
| ***April*** | 1 | 53.550054 | 9.817544 | 7.4 | 0.4 |
| | 2 | 53.567080 | 9.663842 | 4.9 | 1.1 |
| | 3 | 53.699285 | 9.490077 | 3.3 | 1.0 |
| | 4 | 53.829773 | 9.348468 | 3.5 | 0.3 |
| | 5 | 53.878300 | 9.178949 | 2.7 | 0.7 |
| | 6 | 53.843788 | 8.949021 | 1.6 | 0.6 |
| | 7 | 53.964292 | 8.528573 | 2.3 | 0.2 |
| | | | | | |
| ***June*** | 1 | 53.555517 | 9.789849 | 5.5 | 1.7 |
| | 2 | 53.567961 | 9.658249 | 4.7 | 1.1 |
| | 3 | 53.701972 | 9.485129 | 2.4 | 0.8 |
| | 4 | 53.824531 | 9.352356 | 0.8 | 0.8 |
| | 5 | 53.876455 | 9.216995 | 3.1 | 1.6 |
| | 6 | 53.841904 | 8.934398 | 2.2 | 0.7 |
| | 7 | 53.960689 | 8.56282 | 0.8 | 0.6 |

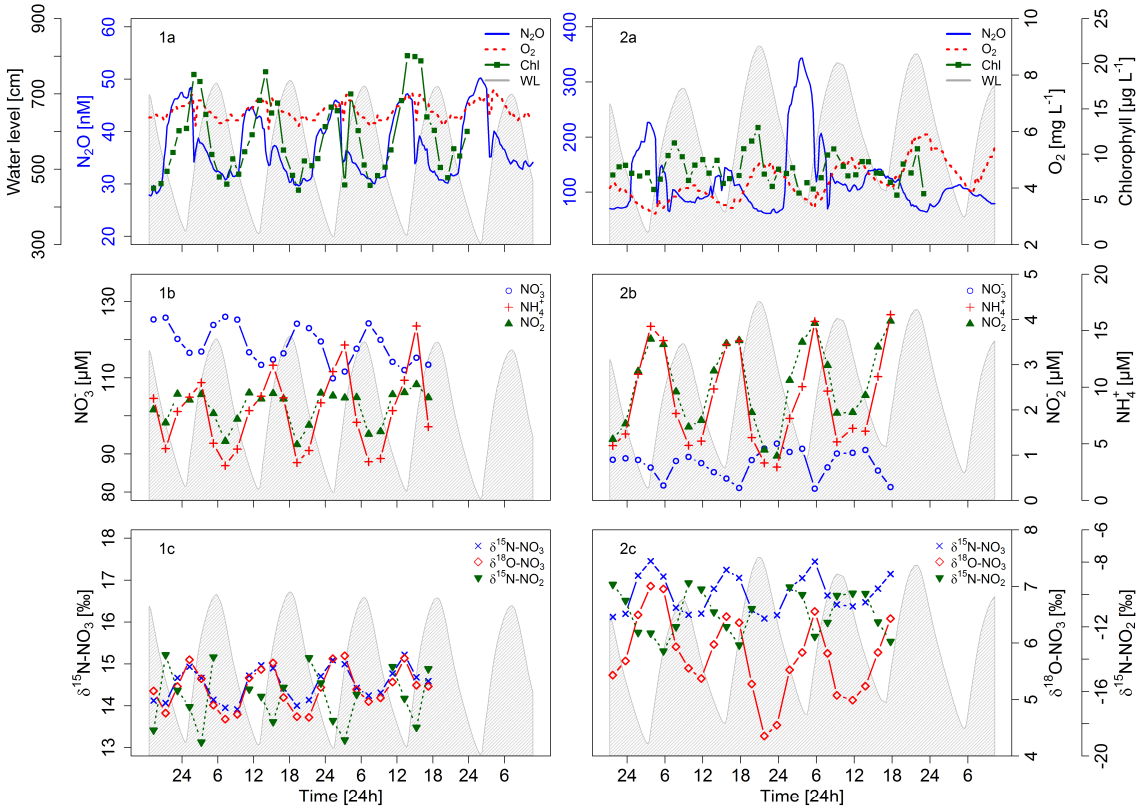


Figure B.3: Tidal dependent measurements in May (1) and July (2) (water level is indicated by the grey line): (a) $N_2O$ (blue line, note: different scale), $O_2$ (red dotted line) and chlorophyll concentration (green □), (b) dissolved inorganic nutrients ($NO_3^-$ - blue o, $NH_4^+$ - red +, $NO_2^-$ - green ▲) and (c) stable isotopes of $NO_3^-$ ($\delta^{15}N$ and $\delta^{18}O$ – blue x and red ◊), $NO_2$- ($\delta^{15}N$ – green ▼)

Supplementary data according to Figure B.3b:

| Month | Date Time | $NO_3^-$ [µM] | Std.-dev. $NO_3^-$ [µM] | $NO_2^-$ [µM] | Std.-dev. $NO_2^-$ [µM] | $NH_4^+$ [µM] | Std.-dev. $NH_4^+$ [µM] |
|---|---|---|---|---|---|---|---|
| ***May*** | 2015-05-19 19:10:00 | 125.3 | 1.2 | 2.0 | 0.4 | 9.0 | 1.2 |
| | 2015-05-19 21:10:00 | 125.8 | 3.1 | 1.7 | 0.0 | 4.6 | 0.1 |
| | 2015-05-19 23:10:00 | 120.2 | 3.5 | 2.4 | 0.1 | 7.9 | 0.2 |
| | 2015-05-20 01:10:00 | 116.5 | 2.6 | 2.2 | 0.1 | 9.1 | 0.1 |
| | 2015-05-20 03:10:00 | 116.9 | 2.9 | 2.3 | 0.0 | 10.4 | 0.1 |
| | 2015-05-20 05:10:00 | 123.9 | 3.6 | 1.9 | 0.0 | 5.0 | 0.0 |
| | 2015-05-20 07:10:00 | 126.0 | 4.4 | 1.3 | 0.0 | 3.1 | 0.1 |
| | 2015-05-20 09:10:00 | 125.3 | 2.8 | 1.8 | 0.2 | 4.5 | 0.4 |
| | 2015-05-20 11:10:00 | 116.7 | 4.4 | 2.4 | 0.5 | 7.9 | 1.5 |
| | 2015-05-20 13:10:00 | 113.4 | 3.4 | 2.2 | 0.1 | 9.2 | 0.8 |
| | 2015-05-20 15:10:00 | 114.8 | 2.3 | 2.4 | 0.3 | 11.9 | 2.0 |
| | 2015-05-20 16:55:00 | 116.4 | 4.2 | 2.2 | 0.2 | 9.1 | 1.0 |
| | 2015-05-20 19:10:00 | 124.2 | 4.4 | 1.2 | 0.2 | 3.3 | 0.3 |
| | 2015-05-20 21:10:00 | 123.0 | 4.0 | 1.7 | 0.1 | 4.4 | 0.1 |
| | 2015-05-20 23:10:00 | 119.5 | 2.0 | 2.4 | 0.3 | 8.6 | 0.7 |

| | | | | | | | |
|---|---|---|---|---|---|---|---|
| | 2015-05-21 01:10:00 | 109.8 | 5.6 | 2.3 | 0.1 | 11.4 | 0.1 |
| | 2015-05-21 03:10:00 | 111.6 | 2.9 | 2.3 | 0.2 | 13.7 | 0.7 |
| | 2015-05-21 05:10:00 | 117.6 | 3.8 | 2.3 | 0.3 | 6.9 | 0.3 |
| | 2015-05-21 07:10:00 | 124.3 | 4.4 | 1.5 | 0.0 | 3.4 | 0.0 |
| | 2015-05-21 09:10:00 | 119.9 | 6.2 | 1.5 | 0.1 | 3.7 | 0.1 |
| | 2015-05-21 11:10:00 | 114.2 | 4.8 | 2.3 | 0.2 | 7.9 | 0.2 |
| | 2015-05-21 13:10:00 | 112.0 | 3.1 | 2.4 | 0.2 | 10.6 | 1.2 |
| | 2015-05-21 15:10:00 | 115.3 | 3.9 | 2.6 | 0.2 | 15.4 | 1.7 |
| | 2015-05-21 17:10:00 | 113.4 | 5.8 | 2.3 | 0.2 | 6.5 | 0.2 |
| | | | | | | | |
| ***July*** | 2015-07-07 21:46:00 | 88.4 | 1.4 | 1.4 | 0.0 | 4.8 | 0.2 |
| | 2015-07-07 23:46:00 | 88.8 | 0.3 | 1.7 | 0.0 | 5.9 | 0.0 |
| | 2015-07-08 01:46:00 | 88.4 | 0.3 | 2.9 | 0.0 | 11.2 | 0.1 |
| | 2015-07-08 03:46:00 | 86.4 | 0.6 | 3.6 | 0.0 | 15.4 | 0.2 |
| | 2015-07-08 05:46:00 | 81.7 | 1.0 | 3.4 | 0.0 | 14.1 | 0.3 |
| | 2015-07-08 07:46:00 | 88.1 | 0.4 | 2.4 | 0.0 | 7.7 | 0.1 |
| | 2015-07-08 09:46:00 | 89.2 | 1.4 | 1.6 | 0.0 | 4.9 | 0.1 |
| | 2015-07-08 11:46:00 | 87.6 | 0.3 | 1.8 | 0.0 | 5.2 | 0.0 |

| | | | | | | | |
|---|---|---|---|---|---|---|---|
| | 2015-07-08 13:46:00 | 85.2 | 0.1 | 2.9 | 0.0 | 9.8 | 0.1 |
| | 2015-07-08 15:46:00 | 83.5 | 0.2 | 3.5 | 0.0 | 13.8 | 0.1 |
| | 2015-07-08 17:46:00 | 81.1 | 0.2 | 3.5 | 0.0 | 14.1 | 0.0 |
| | 2015-07-08 19:46:00 | 88.4 | 2.1 | 1.9 | 0.0 | 5.6 | 0.2 |
| | 2015-07-08 21:46:00 | 91.4 | 1.5 | 1.1 | 0.0 | 3.3 | 0.0 |
| | 0015-07-08 23:46:00 | 92.7 | 0.3 | 1.0 | 0.0 | 3.0 | 0.0 |
| | 2015-07-09 01:46:00 | 90.5 | 1.5 | 2.7 | 0.0 | 7.2 | 0.1 |
| | 2015-07-09 03:46:00 | 91.4 | 0.9 | 3.5 | 0.0 | 10.0 | 0.0 |
| | 2015-07-09 05:46:00 | 80.9 | 0.8 | 3.9 | 0.0 | 15.8 | 0.3 |
| | 2015-07-09 07:46:00 | 86.5 | 0.1 | 3.0 | 0.0 | 9.7 | 0.1 |
| | 2015-07-09 09:16:00 | 90.1 | 0.6 | 1.9 | 0.0 | 5.2 | 0.1 |
| | 2015-07-09 11:46:00 | 90.3 | 0.4 | 1.9 | 0.0 | 6.4 | 1.1 |
| | 2015-07-09 13:46:00 | 91.0 | 0.6 | 2.3 | 0.0 | 6.1 | 0.0 |
| | 2015-07-09 15:46:00 | 85.6 | 0.5 | 3.4 | 0.0 | 11.0 | 0.2 |
| | 2015-07-09 17:46:00 | 81.3 | 1.5 | 4.0 | 0.0 | 16.4 | 0.1 |

Supplementary data according to Figure B.3c:

| Month | Date Time | $\delta^{15}N_{NO3-}$ [‰] | Std.-dev. $\delta^{15}N_{NO3-}$ [‰] | $\delta^{18}O_{NO3-}$ [‰] | Std.-dev. $\delta^{18}O_{NO3-}$ [‰] | $\delta^{15}N_{NO2-}$ [‰] | Std.-dev. $\delta^{15}N_{NO2-}$ [‰] |
|---|---|---|---|---|---|---|---|
| ***May*** | 2015-05-19 19:10:00 | 14.1 | 0.0 | 5.2 | 0.1 | -18.4 | 0.2 |
| | 2015-05-19 21:10:00 | 14.1 | 0.0 | 4.8 | 0.1 | -13.7 | 0.3 |
| | 2015-05-19 23:10:00 | 14.7 | 0.0 | 5.2 | 0.0 | -15.9 | 0.0 |
| | 2015-05-20 01:10:00 | 14.9 | 0.1 | 5.7 | 0.3 | -16.9 | 0.3 |
| | 2015-05-20 03:10:00 | 14.7 | 0.0 | 5.4 | 0.1 | -19.1 | 0.3 |
| | 2015-05-20 05:10:00 | 14.1 | 0.1 | 4.9 | 0.1 | -13.9 | 0.6 |
| | 2015-05-20 07:10:00 | 14.0 | 0.0 | 4.7 | 0.0 | n.a. | n.a. |
| | 2015-05-20 09:10:00 | 13.9 | 0.1 | 4.7 | 0.2 | n.a. | n.a. |
| | 2015-05-20 11:10:00 | 14.7 | 0.1 | 5.4 | 0.0 | -15.9 | 0.1 |
| | 2015-05-20 13:10:00 | 15.0 | 0.0 | 5.5 | 0.1 | -16.3 | 0.3 |
| | 2015-05-20 15:10:00 | 14.9 | 0.2 | 5.6 | 0.1 | -17.9 | 0.0 |
| | 2015-05-20 16:55:00 | 14.4 | 0.1 | 5.0 | 0.2 | -15.7 | 0.2 |
| | 2015-05-20 19:10:00 | 14.0 | 0.1 | 4.7 | 0.2 | n.a. | n.a. |
| | 2015-05-20 21:10:00 | 14.1 | 0.1 | 4.7 | 0.2 | -13.9 | 0.2 |
| | 2015-05-20 23:10:00 | 14.7 | 0.1 | 5.2 | 0.0 | -15.5 | 0.3 |

| | | | | | | | |
|---|---|---|---|---|---|---|---|
| | 2015-05-21 01:10:00 | 15.1 | 0.1 | 5.7 | 0.1 | -17.8 | 0.1 |
| | 2015-05-21 03:10:00 | 15.0 | 0.0 | 5.8 | 0.1 | -19.0 | 0.2 |
| | 2015-05-21 05:10:00 | 14.4 | 0.0 | 5.2 | 0.5 | -16.2 | 0.2 |
| | 2015-05-21 07:10:00 | 14.2 | 0.1 | 5.0 | 0.2 | n.a. | n.a. |
| | 2015-05-21 09:10:00 | 14.3 | 0.1 | 5.0 | 0.2 | n.a. | n.a. |
| | 2015-05-21 11:10:00 | 14.8 | 0.0 | 5.3 | 0.1 | -14.5 | 0.2 |
| | 2015-05-21 13:10:00 | 15.2 | 0.0 | 5.7 | 0.5 | -16.4 | 0.1 |
| | 2015-05-21 15:10:00 | 14.7 | 0.1 | 5.3 | 0.3 | -18.2 | 0.6 |
| | 2015-05-21 17:10:00 | 14.6 | 0.1 | 5.2 | 0.1 | -14.6 | 0.2 |
| | | | | | | | |
| ***July*** | 2015-07-07 21:46:00 | 16.1 | 0.0 | 5.4 | 0.1 | -9.4 | 0.2 |
| | 2015-07-07 23:46:00 | 16.2 | 0.0 | 5.7 | 0.1 | -10.4 | 0.4 |
| | 2015-07-08 01:46:00 | 17.1 | 0.1 | 6.5 | 0.0 | -12.4 | 0.2 |
| | 2015-07-08 03:46:00 | 17.5 | 0.0 | 7.0 | 0.0 | -12.4 | 0.1 |
| | 2015-07-08 05:46:00 | 17.1 | 0.1 | 7.0 | 0.1 | -13.5 | 0.0 |
| | 2015-07-08 07:46:00 | 16.3 | 0.0 | 5.9 | 0.1 | -12.0 | 0.2 |
| | 2015-07-08 09:46:00 | 16.2 | 0.0 | 5.6 | 0.1 | -9.3 | 0.2 |
| | 2015-07-08 11:46:00 | 16.2 | 0.0 | 5.4 | 0.1 | -9.7 | 0.3 |

| | | | | | | | |
|---|---|---|---|---|---|---|---|
| | 2015-07-08 13:46:00 | 16.8 | 0.0 | 6.0 | 0.0 | -11.1 | 0.0 |
| | 2015-07-08 15:46:00 | 17.2 | 0.0 | 6.5 | 0.1 | -12.0 | 0.0 |
| | 2015-07-08 17:46:00 | 17.1 | 0.0 | 6.4 | 0.1 | -13.1 | 0.2 |
| | 2015-07-08 19:46:00 | 16.3 | 0.0 | 5.3 | 0.1 | -10.9 | 0.2 |
| | 2015-07-08 21:46:00 | 16.1 | n.a. | 4.4 | n.a. | n.a. | n.a. |
| | 2015-07-08 23:46:00 | 16.2 | 0.0 | 4.5 | 0.0 | n.a. | n.a. |
| | 2015-07-09 01:46:00 | 16.8 | 0.0 | 5.5 | 0.2 | -9.5 | 0.2 |
| | 2015-07-09 03:46:00 | 17.0 | 0.0 | 5.8 | 0.2 | -10.0 | 0.4 |
| | 2015-07-09 05:46:00 | 17.4 | 0.1 | 6.6 | 0.1 | -12.6 | 0.4 |
| | 2015-07-09 07:46:00 | 16.6 | 0.0 | 5.8 | 0.2 | -11.7 | 0.3 |
| | 2015-07-09 09:16:00 | 16.4 | 0.0 | 5.1 | 0.2 | -10.1 | 0.1 |
| | 2015-07-09 11:46:00 | 16.4 | 0.1 | 5.0 | 0.0 | -9.9 | 0.1 |
| | 2015-07-09 13:46:00 | 16.5 | 0.1 | 5.2 | 0.0 | -9.9 | 0.0 |
| | 2015-07-09 15:46:00 | 16.8 | 0.1 | 5.8 | 0.2 | -11.7 | 0.0 |
| | 2015-07-09 17:46:00 | 17.1 | 0.07 | 6.4 | 0.09 | -12.9 | 0.04 |

## List of publications

A list of publications is given below. My own contribution is specified in cases of co-authorship.

- ***High resolution measurements of nitrous oxide ($N_2O$) in the Elbe estuary***

Brase, L., Bange H.W., Lendt R., Sanders T., & Dähnke K.

DOI: 10.3389/fmars.2017.00162

Published in: Frontiers in Marine Science (2017)

- ***High frequency measurements of reach scale nitrogen uptake in a fourth order river with contrasting hydromorphology and variable water chemistry (Weiße Elster, Germany)***

Kunz, J. V., Hensley, R., Brase, L., Borchardt, D., & Rode, M.

Published in: Water Resources Research (13 January 2017)

DOI: 10.1002/2016WR019355

My contribution: analyzing and interpretation of dual stable isotopes of $NO_3^-$ and critical discussion

- ***Quantifying the role of nitrification, N-retention and elimination along an anthropogenic gradient in a small river***

Brase L., Sanders T., & Dähnke K.

Submitted to Isotopes in Environmental and Health studies (2017)

## Acknowledgements

I would like to thank all people without whom this Ph.D. project would not have been possible:

First of all I would like to thank Dr. Kirstin Dähnke for the exemplary supervision of my Ph.D. project, her very constructive comments and fruitful discussions during the last four years.

I thank Prof. Dr. Kay-Christian Emeis for the helpful suggestions regarding my work and for his support at HZG.

I am grateful to all HZG colleagues: In particular Juliane Jacob and Jördis Petersen for the nice conversations and constructive talks - also outside the HZG. Markus Ankele, Céline Naderipour and Verena Küppers for any kind of technical (and non-technical) support.

Many thanks to Dr. Tina Sanders for proofreading parts of my thesis and the helpful discussions, especially during Kirstin's maternity leave.

I also would like to thank Prof. Dr. Hermann W. Bange from the GEOMAR for fruitful discussions regarding $N_2O$ processes.

The whole team of the Ludwig Prandtl on board and onshore, Alexander Bratek and Andreas Neumann are grateful acknowledged for their help at the research cruises.

Special thanks to Dr. Ralf Lendt from the University of Hamburg for supporting me in so many ways: technical support, research cruises, proofreading part of my thesis and fruitful discussions - not only about $N_2O$.

Susanne, Anja and Finbarr – thank you for last minute proofreading and English corrections.

Last but not least, I want to thank all my friends for their support and patience, my wonderful parents and my lovely sister Tina for always being there for me!

## Eidesstattliche Erklärung

Hiermit erkläre ich an Eides statt, dass ich die vorliegende Dissertationsschrift selbst verfasst und keine anderen als die angegebenen Quellen und Hilfsmittel benutzt habe.

Hamburg, den

_____

(Lisa Brase)